

JEMS

JOURNAL OF ETA MARITIME SCIENCE



www.jemsjournal.org



Volume: **11** Issue: **3**
September **2023**

E-ISSN: 2148-9386



Editorial Board

On Behalf of UCTEA The Chamber of Marine Engineers

Yaşar CANCA
UCTEA Chamber of Marine Engineers,
Chairman of the Board

EDITOR-IN-CHIEF

Prof. Dr. Selçuk NAS
Dokuz Eylül University Maritime Faculty,
Department of Maritime Education and
Training, İzmir/Türkiye

DEPUTY EDITOR

Asst. Prof. Dr. Remzi FİŞKIN
Ordu University Faculty of Marine Sciences,
Department of Marine Transportation
Engineering, Ordu/Türkiye

Section Editors

Marine Transportation Engineering

Prof. Dr. Ender ASYALI
Maine Maritime Academy, Marine Transportation
Operations, Castine Maine/United States

Prof. Dr. Özkan UĞURLU
Ordu University Faculty of Marine Science,
Department of Maritime Transportation and
Management Engineering, Ordu/Türkiye

Prof. Dr. Selçuk ÇEBİ
Yıldız Technical University Faculty of Mechanical
Engineering, Department of Industrial Engineering,
İstanbul/Türkiye

Prof. Dr. Emre AKYÜZ
İstanbul Technical University Maritime Faculty,
Department of Maritime Transportation and
Management, İstanbul/Türkiye

Assoc. Prof. Dr. Momoko KITADA
World Maritime University, Department of Maritime
Education and Training, Malmö/Sweden

Marine Engineering

Assoc. Prof. Dr. Alper KILIÇ
Bandırma Onyedi Eylül University Maritime Faculty,
Department of Marine Business Management and
Ship Machines Operational Engineering, Balıkesir/
Türkiye

Assoc. Prof. Dr. Görkem KÖKKÜLÜNK
Yıldız Technical University Faculty of Naval
Architecture and Maritime, Department of Marine
Engineering, İstanbul/Türkiye

Asst. Prof. Dr. Fırat BOLAT
İstanbul Technical University Maritime Faculty,
Department of Marine Engineering, İstanbul/Türkiye

Dr. Jing YU
Dalian Maritime University Maritime Faculty
Engineering, Dalian/China

Dr. José A. OROSA
University of A Coruña, Department of Navigation
Science and Marine Engineering, Galicia/Spain

Maritime Business Administration

Prof. Dr. Soner ESMER
Kocaeli University Faculty of Maritime, Kocaeli,
Türkiye

Assoc. Prof. Dr. Çimen KARATAŞ ÇETİN
Dokuz Eylül University Maritime Faculty,
Department of Maritime Business Administration,
İzmir/Türkiye

Naval Architecture

Prof. Dr. Ahmet TAŞDEMİR
Piri Reis University Maritime Faculty, Department
of Marine Engineering, İstanbul, Türkiye

Prof. Dr. Ercan KÖSE
Karadeniz Technical University Faculty of Marine
Science, Department of Shipbuilding and Marine
Engineering, Trabzon/Türkiye

Assoc. Prof. Dimitrios KONOVESSIS
Singapore Institute of Technology, Department
Naval Architecture, Marine Engineering and
Offshore Engineering, Singapore

Dr. Rafet Emek KURT
University of Strathclyde Faculty of Engineering,
Department of Naval Architecture Ocean and
Marine Engineering, Glasgow/United Kingdom

Dr. Sefer Anıl GÜNBEYAZ
University of Strathclyde Faculty of Engineering,
Department of Naval Architecture, Ocean and
Marine Engineering, Glasgow/United Kingdom

Asst. Prof. Gökhan BUDAK
İzmir Katip Çelebi University, Department of
Shipbuilding and Ocean Engineering, İzmir, Türkiye

Coastal and Port Engineering

Assoc. Prof. Dr. Kubilay CİHAN
Kırıkkale University Faculty of Engineering and
Architecture, Department of Hydraulics, Kırıkkale/
Türkiye

Logistic and Supply Chain Management

Assoc. Prof. Dr. Ceren ALTUNTAŞ VURAL
Chalmers University of Technology, Department of
Technology Management and Economics, Division
of Service Management and Logistics, Göteborg/
Sweden

Marine Tourism

PhD Eng. Aleksandra LAPKO
Maritime University of Szczecin, Faculty of
Economics and Transport Engineering, Szczecin/
Poland

Editorial Board

Prof. Dr. Ersan BAŞAR
Karadeniz Technical University, Sürmene Faculty
of Marine Sciences, Department of Maritime
Transportation and Management Engineering,
Trabzon/Türkiye

Prof. Dr. Masao FURUSHO
Director of the National Institute of Technology,
Oshima Maritime College, Japan

Prof. Dr. Metin ÇELİK
İstanbul Technical University Maritime Faculty,
Department of Marine Machinery Management
Engineering, İstanbul/Türkiye

Prof. Dr. Nikitas NIKITAKOS
University of the Aegean School of Business,
Department of Shipping Trade and Transport,
Mytilene/Greece

Assoc. Prof. Dr. Ghiorghe BATRINCA
Maritime University of Constanta Faculty of
Navigation and Naval Transport, Department of
Economic Engineering in Transports, Constanta/
Romania

Assoc. Prof. Dr. Marcella Castells-SANABRA
Polytechnic University of Catalonia, Barcelona
School of Nautical Studies, Department of Nautical
Science and Engineering, Barcelona/Spain

Assoc. Prof. Radu HANZU-PAZARA
Constanta Maritime University, Vice-Rector,
Constanta/Romania

Dr. Angelica M BAYLON
Maritime Academy of Asia and the Pacific (MAAP),
Central Luzon/Philippines

Dr. Iraklis LAZAKIS
University of Strathclyde Faculty of Engineering,
Department of Naval Architecture, Ocean and
Marine Engineering, Glasgow/United Kingdom



Editorial Board

Guest Editors

Prof. Dr. Ethem DUYGULU

Dokuz Eylül University Faculty of Economics and Administrative Sciences, İzmir/Türkiye

Prof. Dr. Lucjan GUCMA

Maritime University of Szczecin, Department of Marine Traffic Engineering, Szczecin/Poland

Assoc. Prof. Charif MABROUKI

Hassan 1st University Faculty of Science and Technology, Settat/Morocco

Assoc. Prof. Violeta ROSO

Chalmers University of Technology, Department of Technology Management and Economic, Gothenburg/Sweden

Dr. Neslihan PAKER

İzmir Kavram Vocational School, İzmir/Türkiye

Associate Editors

Asst. Prof Dr. Emin Deniz ÖZKAN

Dokuz Eylül University Maritime Faculty, Department of Marine Transportation Engineering, İzmir/Türkiye

Res. Asst. Dr. Ömer ARSLAN

Dokuz Eylül University Maritime Faculty, Department of Marine Transportation Engineering, İzmir/Türkiye

Dr. Pelin ERDEM

University of Strathclyde Faculty of Engineering, Department of Naval Architecture, Ocean and Marine Engineering, Glasgow/United Kingdom

Res. Asst. Burak KUNDAKÇI

İskenderun Technical University Faculty of Barbaros Hayrettin Naval Architecture and Maritime, Department of Marine Transportation Engineering, Hatay/Türkiye

Res. Asst. Coşkan SEVGİLİ

Zonguldak Bülent Ecevit University Maritime Faculty, Department of Marine Transportation Management Engineering, Zonguldak/Türkiye

Res. Asst. Elif ARSLAN

Dokuz Eylül University Maritime Faculty, Department of Marine Transportation Engineering, İzmir/Türkiye

Dr. Gizem KAYIŞOĞLU

İstanbul Technical University Maritime Faculty, Department of Marine Transportation Engineering, İstanbul/Türkiye

Res. Asst. Merve GÜL ÇIVGIN

İstanbul Technical University Maritime Faculty, Marine Engineering Department, İstanbul/Türkiye

Advisory Board

Prof. Dr. Ali Muzaffer FEYZİOĞLU

Karadeniz Technical University Sürmene Faculty of Marine Sciences, Department of Marine Sciences and Technology Engineering, Trabzon/Türkiye

Prof. Dr. Şermin AÇIK ÇINAR

Dokuz Eylül University Maritime Faculty, Department of Maritime Business Management, İzmir/Türkiye

Prof. Dr. Özcan ARSLAN

İstanbul Technical University Maritime Faculty, Marine Transportation Engineering, İstanbul/Türkiye

Prof. Dr. Ferhat KALAYCI

Recep Tayyip Erdoğan University The Faculty of Fisheries and Aquatic Sciences, Rize/Türkiye

Prof. Dr. Özkan UĞURLU

Ordu University Faculty of Marine Science, Department of Maritime Transportation and Management Engineering, Ordu/Türkiye

Prof. Dr. Mehmet BİLGİN

İstanbul University Faculty of Engineering, Department of Chemical Engineering, İstanbul/Türkiye

Prof. Osman TURAN

University of Strathclyde Faculty of Engineering, Department of Naval Architecture Ocean and Marine Engineering, Glasgow/United Kingdom

Journal Info

► Please refer to the journal's webpage (www.jemsjournal.org) for "About Us", "Aim and Scope", "Guide for Authors" and "Ethical Policy".

JEMS is currently indexed in Web of Science Emerging Sources Citation Index (ESCI), Tubitak Ulakbim Science Database, Transport Research International Documentation (TRID), Directory of Open Access Journals (DOAJ), EBSCO, J-Gate, Scopus and CNKI.

Owner UCTEA The Chamber of Marine Engineers

Address: Sahrayıcedit Mah. Halk Sk. Golden Plaza No: 29 C Blok K:3 D:6 Kadıköy/İstanbul - Türkiye

Web: gemimo.org **E-mail:** bilgi@gemimo.org **Phone:** +90 216 747 15 51

Fax: +90 216 747 34 35

Publisher Galenos Publishing House

Address: Molla Gürani Mah. Kaçamak Sk. No: 21/1 34093 İstanbul, Türkiye

Phone: +90 (530) 177 30 97 **E-mail:** info@galenos.com.tr **Web:** www.galenos.com.tr



JEMS apply the Creative Commons Attribution NonCommercial 4.0 International Licence to all manuscripts to be published.

E-ISSN: 2148-9386

Online Publication Date:

September 2023

Journal website:

www.jemsjournal.org

Submit Article:

jag.journalagent.com/jems

► **Cover Photo:**

2023/ Volume 11 / Issue 3

Capt. Ümit Kaplan



ED	Editorial	136
AR	Numerical Investigation of the Maneuvering Forces of Different DARPA Suboff Configurations for Static Drift Condition	137
	Hasan Öztürk, Kadir Beytullah Gündüz, Yasemin Arıkan Özden	
AR	Fear of COVID-19 in Seafarers: Association with Psychological Distress	148
	Arda Toygar, Umut Yıldırım	
AR	The Selection of Ocean Container Carrier: An Analytic Network Process (ANP) Approach	159
	Ayfer Ergin, Güler Alkan	
AR	Multi-Criteria Analysis of Capesize Bulk Carrier Design Optimization Model	168
	Cansu Aksu, Ramazan Yaman	
AR	Neuroscience Approach to Situational Awareness: A Research on Marine Navigation	186
	Serkan Kahraman, Durmuş Ali Deveci, İbrahim Öztura, Dilara Mermi Dibek	
AR	Estimation of Human Errors During Cargo Unloading Operations on Bulk Carriers Using SLIM and Interval Type 2 Fuzzy Sets	198
	Ahmet Lutfi Tunçel, Pelin Erdem, Osman Turan	
AR	Application of Relaxation Times Distribution of Dielectric Permittivity for Marine Engine Oils Analysis	209
	Nikolay Sinyavsky, Oksana Synashenko, Natalia Kostrikova	
PI	Autonomous Network System with Specialized and Integrated Multi-Sensor Technology for Dynamic Monitoring of Marine Pollution (SMARTPOL)	217
	Nurten Vardar, Bülent Bayram, Amit Mishra, Mihai Palade, Bekir Şener, Ines Boujmil, Jeremy Scerri, Andre Attard, İskender Demir	

● Selçuk Nas

Selçuk Nas, Dokuz Eylül University Maritime Faculty, Department of Maritime Education and Training, İzmir, Türkiye

Dear Readers,

I am pleased to introduce JEMS 11 (3) to our valuable followers. In this issue, there are valuable and intriguing studies. No doubt that these studies will contribute to the maritime field. Hereby, I would like to express our gratitude to the authors, who sent their valuable studies for publication in this issue, our reviewers, editorial board, section editors, and the publisher, who provided quality publications by diligently following our publication policies.

I would like to announce that, the next year, 2024, “The 5th Global Maritime Conference (GMC’24)” will be organized with the partnership of the Turkish Chamber of Marine Engineers (TMMOB) and Istanbul Technical University (Turkey) on 21-22 May 2024. GMC is an international conference, demonstrating the capabilities and importance of academic research power in developing solutions to face immediate challenges and achieving ambitious environmental targets in maritime industry.

Hope to see all stakeholders at the GMC’24,

Best regards,

Prof. Dr. Selçuk NAS

Editor in Chief



Address for Correspondence: Selçuk Nas, Dokuz Eylül University Maritime Faculty, Department of Maritime Education and Training, İzmir, Türkiye

E-mail: snas@deu.edu.tr

ORCID ID: orcid.org/0000-0001-5053-4594

Numerical Investigation of the Maneuvering Forces of Different DARPA Suboff Configurations for Static Drift Condition

Hasan Öztürk, Kadir Beytullah Gündüz, Yasemin Arıkan Özden

Yıldız Technical University Faculty of Naval Architecture and Maritime, Department of Naval Architecture and Marine Engineering, İstanbul, Türkiye

Abstract

In this study, the maneuvering forces and moments of the DARPA Suboff submarine model were determined under static drift condition using computational fluid dynamics (CFD) methods. Two different configurations of the submarine model namely; the AFF-3 configuration, which consists of bare hull and four stern rudders, and the fully appended configuration AFF-8, which is formed from bare hull, sail, and four stern rudders, have been used. Initially, for the AFF-3 configuration, a mesh independence study has been conducted. Three different cases; coarse, medium and fine meshes are investigated at small angles (0-2-4-6 degrees). After that the results have been verified, the medium mesh structure has been selected and the analyzes have been continued for larger angles (from 00 to 180 degrees). The accuracy of the obtained results was assessed by comparing them with non-dimensional experimental results. The comparison between the CFD results and the experimental results demonstrated a high level of agreement, indicating the effectiveness and accuracy of the CFD methods used in this study. After the validation studies, the maneuvering forces and moments of the AFF-8 fully appended configuration were calculated for which no prior experimental data existed in the literature. To achieve this, steady-state CFD simulations were performed using the commercial software ANSYS Fluent, and the results were presented for the same flow angles.

Keywords: Submarine, Maneuvering forces, Static drift, DARPA Suboff, CFD

1. Introduction

Submarines can be designed for military, research, equipment installation, and maintenance purposes by considering many parameters during the design process. Besides many specifications of a ship, it is of great importance to evaluate its maneuvering characteristics. In the past, many studies have been conducted to estimate the maneuvering characteristics of ships and submarines with good precision. To determine the maneuvering performance of vessels, four different methods are generally used in the literature. Empirical and semi-empirical methods are generally used in the early design stages to determine the hydrodynamic properties of the vehicle. Its advantages are that necessary changes can be made quickly and at low cost. With the use of experimental methods generally the most reliable results are obtained since non-linear effects are included in the problem by their nature. With numerical

methods, characteristics such as force, velocity, pressure, and turbulence can be obtained faster and cheaper than experimental methods and also in areas where it would be difficult to collect experimental data. System diagnostic methods based on statistical theory have become increasingly popular in recent years because they offer the possibility of fast results [1].

In 1989, Groves et al. [2] described the DARPA SUBOFF submarine model as a recommended submarine hull form for benchmark tests. In 1990, Roddy [3] conducted towing tank experiments to investigate stability and control characteristics. In this study, experimental results belonging to different configurations of DARPA SUBOFF are presented [3]. Detailed flow measurements are published by Huang and Liu [4] based on measurements in a wind tunnel. DARPA SUBOFF submarine models are extensively used in submarine research studies. Generally among



Address for Correspondence: Yasemin Arıkan Özden, Yıldız Technical University Faculty of Naval Architecture and Maritime, Department of Naval Architecture and Marine Engineering, İstanbul, Türkiye

E-mail: yarikan@yildiz.edu.tr

ORCID ID: orcid.org/0000-0001-9909-0859

Received: 24.11.2022

Last Revision Received: 09.05.2023

Accepted: 05.06.2023

To cite this article: H. Öztürk, K. B. Gündüz, and Y. Arıkan Özden. "Numerical Investigation of the Maneuvering Forces of Different DARPA Suboff Configurations for Static Drift Condition." *Journal of ETA Maritime Science*, vol. 11(3), pp. 137-147, 2023.

©Copyright 2023 by the Journal of ETA Maritime Science published by UCTEA Chamber of Marine Engineers

the benchmark submarines, the main reason for using the DARPA Suboff generic model is the optimized and streamlined hull form. It is also interesting to use DARPA Suboff geometry because of the many studies that can be found in the open literature. The use of the bare hull (AFF-1) and the fully appended configuration (AFF-8) are also recommended to the researchers by the ITTC-Maneuvering Committee, 2014 [5].

Toxopeus and Vaz [6] previously studied the flow at different drift angles around the bare hull of the DARPA SUBOFF configuration. They used their own code and completed the verification and validation study. In their study, different turbulence models were used and results were presented [6]. Vaz et al. [7] conducted another study to calculate the maneuvering forces of DARPA SUBOFF using CFD. This time, they used two viscous-flow solvers and focused on the accurate prediction of the maneuvering forces and moments of the DARPA SUBOFF AFF-1 and AFF-8 configurations for 0° and 18° drift angles. They investigated the influence of different turbulence models. The results obtained using Reynolds-Averaged-Navier-Stokes (RANS) approach are compared with the theoretically more realistic Delayed-Detached-Eddy-Simulation (DDES) results. They also investigated the influence of the appendages on the forces and flow fields [7]. In a collaborative CFD exercise, the Submarine Hydrodynamics Working Group, which consists of different institutions, performed calculations on the bare hull of the DARPA SUBOFF submarine to investigate the capability of RANS viscous flow solvers to predict the flow field around the hull and the forces and moments for several steady turns. The study was conducted using several different viscous flow solvers, turbulence models, and grid types. The study improved the knowledge and understanding of underwater vehicle hydrodynamics. They performed verification and validation of the solutions and in several cases the results were validated at acceptable levels (below 10%). They also stated that modeling errors are present in the cases for which validation was not achieved and these can be attributed to the turbulence model [8]. In their study, Pan et al. [9] tried to predict submarine hydrodynamic coefficients by numerical simulations. They have carried out steady and unsteady RANS simulations. They made the simulation of the oblique towing tank experiment and the planar motion mechanism (PMM) experiment performed on the SUBOFF submarine model. They explored the possibility of developing a numerical method to evaluate the maneuvering characteristics of a submarine, especially at an earlier stage of the design cycle. Consequently, the studies were verified with the experimental data, and a good agreement between each other has been seen. They also have stated that PMM experiment may be the most effective

way; however, it requires special facilities and equipment and is both time-consuming and costly, and not economical at the preliminary design stage [9].

Ray and Sen [10] estimated the hydrodynamic coefficients using the System Identification (SI) technique of the Extended Kalman Filter for a submarine from its full-scale maneuvering sea trials data. Data from sea trials with two submarines were used to identify the hydrodynamic coefficients. The authors provide advice for problems related to the robustness of SI techniques applied to the identification of hydrodynamic parameters from noisy full-scale data [10]. Jiang et al. [11] performed a study on the prediction of straight-line hydrodynamic coefficients for a portable autonomous underwater vehicle using empirical methods and computational fluid dynamics (CFD). They compared empirical and CFD results with experimental results obtained from wind tunnel tests. They showed trends in the variation of forces and moments and that they can be captured well by CFD [11].

Shadlaghani and Mansoorzadeh [12] investigated the advantage of steady test simulations relative to unsteady experiments, especially PMM tests, for computing velocity-based hydrodynamic coefficients. Steady maneuvers including towing with drift and attack angles together with rotating arm tests were simulated to calculate the linear damping coefficients of DARPA Suboff. The obtained results were compared with available unsteady experimental results of the SUBOFF submarine. It was also stated that the expensive and complicated unsteady simulations of PMM maneuvers can be replaced by simple steady-state simulations by towing and rotating the model [12]. Lin et al. [13] established an efficient experimental procedure to analyze the maneuvering derivatives of a half-scale submerged body of DARPA SUBOFF in the horizontal plane for four different configurations, including bare hull, bare hull with sail, bare hull with rudders, and bare hull with all appendages. They conducted PMM experiments in the towing tank of National Cheng Kung University. The results obtained for evaluating the feasibility of the test method and verifying the results compared with the results of previous experiments performed by DTRC [13]. They also improved the design of the flange connecting the load cell with the stainless strut to reduce the installation time in the PMM tests. The results about the uncertainty of the test results are presented [13]. Atik [14] investigated a suitable solution mesh and turbulence model for the DARPA SUBOFF submarine AFF-1 hull form by performing static drift test simulations. She compared the obtained results with experimental results conducted by DTRC/SHD. She stated that all turbulence models gave close results at small angles, small differences were seen between the models

as the angles increased, and the Shear Stress Transport (SST) $k-\omega$ turbulence model gave the closest results, while after 8 degrees of static drift, there was an average of 10% difference between numerical and experimental results [14].

Kahramanoglu [15] examined the scale effects on the horizontal maneuvering derivatives for three different scales for the fully appended DARPA Suboff submarine. To achieve this, a numerical viscous solver was used to model the PMM. Pure sway and pure yaw calculations for the model scale of the DARPA Suboff were performed numerically. After the verification assessment of the numerical results, the sway forces and yaw moments are obtained for different scenarios and the linear horizontal maneuvering derivatives are obtained for different scales. The comparison revealed that the sway forces obtained from pure yaw analyzes exhibited significant sensitivity to changes in scale, whereas the sway forces obtained from pure sway analyzes were relatively insensitive. The results also indicated that neither pure sway nor pure yaw analyzes showed a significant sensitivity to changes in scale for the yaw moment values, as reported by the author [15].

This study focused on conducting maneuvering analyzes of the AFF-3 and AFF-8 configurations using CFD simulations. Specifically, the analyzes were carried out for drift angles ranging from 0 to 18 degrees at a speed of 6.5 knots. The obtained results were brought to the non-dimensional values to compare with the experimental results presented by Liu and Huang [16]. After validation of the results of the AFF-3 configuration, the same calculations are applied to the AFF-8 fully appended configuration. Due to the DARPA Suboff submarine's symmetry about the y-axis, the calculations were performed solely for the PS. The primary objective of this study is to examine the forces and moments in the static drift condition of the AFF-8 configuration, which has no available experimental data in the literature.

2. Methodology

To be able to make a better prediction about the hydrodynamic forces and moments, the six degrees of freedom maneuvering motion is decoupled into the horizontal and the vertical motions; thus, the problem can be simplified into a set of linear equations. Therefore, the estimation of the hydrodynamic coefficients of these motion equations is a key step in predicting the motion of the submarine.

2.1. Maneuvering Equations

The generalized 6-DoF rigid-body equations of motion in a body-fixed, non-inertial frame of reference XYZ that is moving relative to an Earth-fixed, inertial reference frame $X_0 Y_0 Z_0$ can be derived as follows [17]:

$$m[\dot{u} - vr + \omega q - x_G(q^2 + r^2) + y_G(pq - \dot{r}) + z_G(pr + \dot{q})] = X \quad (1)$$

$$m[\dot{v} - \omega p + ur - y_G(r^2 + p^2) + z_G(qr - \dot{p}) + x_G(qp + \dot{r})] = Y \quad (2)$$

$$m[\dot{w} - uq + vp - z_G(p^2 + q^2) + x_G(rp - \dot{q}) + y_G(rq + \dot{p})] = Z \quad (3)$$

$$I_x \dot{p} + (I_z - I_y)qr - (\dot{r} + pq)I_{xz} + (r^2 - q^2)I_{yz} + (pr - \dot{q})I_{xy} \quad (4)$$

$$+ m[y_G(\dot{w} - uq + vp) - z_G(\dot{v} - \omega p + ur)] = K$$

$$I_y \dot{q} + (I_x - I_z)rp - (\dot{p} + qr)I_{xy} + (p^2 - r^2)I_{zx} + (qp - \dot{r})I_{yz} \quad (5)$$

$$+ m[z_G(\dot{u} - vr + \omega q) - x_G(\dot{w} - uq + vp)] = M$$

$$I_z \dot{r} + (I_y - I_x)pq - (\dot{q} + rp)I_{yz} + (q^2 - p^2)I_{xy} + (rq - \dot{p})I_{zx} \quad (6)$$

$$+ m[x_G(\dot{v} - \omega p + ur) - y_G(\dot{u} - vr + \omega q)] = N$$

Equations 1, 2, and 3 represent the translational motions; surge-x, sway-y, and heave-z, and 4, 5 and 6 represent the rotational motions; roll- ϕ , pitch- θ and yaw- ψ , respectively. These given 6-DoF equations of motion represent the forces and moments; X, Y, Z which are the external forces acting on the submarine and K, M, N are the external moments, respectively. In maneuvering studies two coordinate systems are used; an inertial coordinate system (or fixed on earth $x_0 y_0 z_0$) and a moving coordinate system (or fixed on body $x-y-z$). Also, m describes the mass of the vessel and I_x, I_y, I_z are the moments of inertia of the vessel for each axis. In the equations the points (x_G, y_G, z_G) define the center of gravity of the submarine. In this study, the coordinate system is used so that the longitudinal axis of the submarine is in the x-axis and the bow is in the positive x direction, the y-axis is positioned to determine the starboard (SB) and PS of the submarine, and the z-axis is positioned vertically upwards to the submarine (Figure 1). The position of the center of moment used in moment calculations on the z-axis is determined according to the center of gravity of the model at $0.4621 * Lo_a$ distance from the stern.

$$\left\{ \begin{array}{l} \dot{x} = u \quad \rightarrow \text{surge velocity} \\ \dot{y} = v \quad \rightarrow \text{sway velocity} \\ \dot{z} = w \quad \rightarrow \text{heave velocity} \end{array} \right\} \xrightarrow{\frac{d}{dt}} \left\{ \begin{array}{l} \ddot{x} = \dot{u} \quad \rightarrow \text{surge acceleration} \\ \ddot{y} = \dot{v} \quad \rightarrow \text{sway acceleration} \\ \ddot{z} = \dot{w} \quad \rightarrow \text{heave acceleration} \end{array} \right\}$$

The rotational velocities and accelerations are given below for each axis:

$$\left\{ \begin{array}{l} \dot{\phi} = p \quad \rightarrow \text{roll rate} \\ \dot{\theta} = q \quad \rightarrow \text{pitch rate} \\ \dot{\psi} = r \quad \rightarrow \text{yaw rate} \end{array} \right\} \xrightarrow{\frac{d}{dt}} \left\{ \begin{array}{l} \ddot{\phi} = \dot{p} \quad \rightarrow \text{roll acceleration} \\ \ddot{\theta} = \dot{q} \quad \rightarrow \text{pitch acceleration} \\ \ddot{\psi} = \dot{r} \quad \rightarrow \text{yaw acceleration} \end{array} \right\}$$

For submarines and ships, forces and moments acting on the hull are in the horizontal plane. In this case, the heave, pitch, and roll motions are neglected; in other words, these values become $\omega = p = q = \dot{\omega} = \dot{p} = \dot{q} = 0$. In the XZ plane $y_G = 0$ because of the symmetry of the submarine. If we apply these simplifications to the equations of motion,

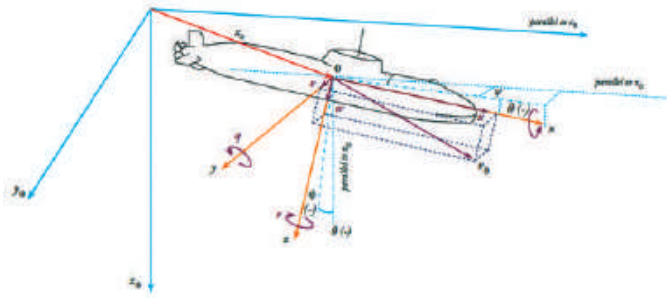


Figure 1. Fixed and moving reference frames of a submarine [18]

the aforementioned equations become as shown in the Equations (7), (8) and (9) respectively for surge, sway, and yaw. If we look at past studies to better understand the maneuvering ability of vessels, some studies can be found. One of the most preferred studies belongs to Abkowitz [19], who proposed a model based on solving the equations of motion for the hydrodynamic forces (X , Y) and moment (N) acting on the hull by considering the ship as a whole, and based on the expansion of hydrodynamic forces (X , Y) and moment (N) to the third-order Taylor series [19]. Yoon [20] studied Abkowitz's [19] maneuvering model in his PhD thesis and obtained hydrodynamic derivatives of the surface combatant model DTMB5415 by conducting PMM tests.

$$m(\dot{u} - vr - x_g r^2) = X \quad (7)$$

$$[[\text{OMML-EQ-3}]] \quad (8)$$

$$I_z \dot{r} + m x_g (\dot{v} + ur) = N \quad (9)$$

Velocity coordinates are $V = (u, v, w)$. Here, u defines the velocity on the x -axis and v defines the velocity on the y -axis. U and V velocities occur because of the β static drift angle. All integral forces and moments on the hull are based on a right-handed axis system that corresponds to the positive directions normally applied in maneuvering operations. This means that the X force directs Y to the SB and Z downwards. To be able to compare with the experimental results obtained values should be nondimensionalized. It should also be known that the hydrodynamic derivatives used in ship-maneuvering studies are commonly known as maneuvering coefficients.

2.2. The RANS Equations

RANS equations are employed to numerically solve the flow around the DARPA Suboff configurations. The governing equations are the continuity equation and the momentum equation. The continuity equation in cartesian coordinates can be given as (Equation 10):

$$\frac{\partial U_i}{\partial x_i} = 0 \quad (10)$$

The momentum equation can be written as in equation 11:

$$\frac{\partial U_i}{\partial t} + \frac{\partial (U_i U_j)}{\partial x_j} = -\frac{1}{\rho} \frac{\partial P}{\partial x_i} + \frac{\partial}{\partial x_j} \left[\nu \left(\frac{\partial U_i}{\partial x_j} + \frac{\partial U_j}{\partial x_i} \right) \right] - \frac{\partial \overline{u'_i u'_j}}{\partial x_j} \quad (11)$$

Where U_i and U_j are the mean velocity and the turbulence components, p is the mean pressure, ρ is the density, and ν is the molecular kinematic viscosity of the fluid. Since all analyses were performed at steady state for this study, the initial term was not taken into account. The k - ω turbulence model is applied in order to simulate the turbulent flow around the submarine. Because submarines are submerged bodies, there are no free surface effects. During the analyses, the Reynolds stress tensor was calculated according to the following equation.

$$\overline{u'_i u'_j} = -\nu_t \left(\frac{\partial U_i}{\partial x_j} + \frac{\partial U_j}{\partial x_i} \right) + \frac{2}{3} \delta_{ij} k \quad (12)$$

Here ν_t is the eddy viscosity and it must be modeled in order to take into account the turbulence contribution of the motion equation. It is known that various turbulence models are developed for this purpose.

2.3. Presentation of Forces and Moments

In order to be able to convert the obtained forces and moments to non-dimensional values, the following equations (Equations 13-14) are used according to the proposal of SNAME 1950 [21]. The resistive forces in the X , Y , and Z axis are non-dimensionalized by using the following formula.

$$X', Y', Z' = \frac{X, Y, Z}{\frac{1}{2} \rho V_0^2 L_{pp}^2} \quad (13)$$

K , M , N are the moments that occur around the X , Y , Z axis, respectively. To make non-dimensionalisation of these moments, the following formula is used.

$$K', M', N' = \frac{K, M, N}{\frac{1}{2} \rho V_0^2 L_{pp}^3} \quad (14)$$

The non-dimensionalisation of the maneuvering forces and moments is carried out according to Equations 13 and 14. The obtained numerical results were compared with the experimental values of the DARPA Suboff experiments [16].

3. Geometry of Bodies

The DARPA Submarine Technology Program provides resources to help develop submarines. Various experiments were carried out using the submarine model defined as the DARPA Suboff. The purpose of these experiments is to contribute to the development of submarines produced today and to be produced in the future. The SUBOFF project provides data for the CFD community to compare numerical data. Within the scope of the results given by this project, analyzes were performed on AFF-3 (Body and control surfaces) and AFF-8 (Fully appended) configurations.

The DARPA SUBOFF is a generic submarine model geometry with a length of 4.356 m and a maximum diameter of 0.508 m. According to the arrangement of the sails, rudders, and ring wings, there are different configurations of the submarine model. The stability and control characteristics of the DARPA SUBOFF model were determined experimentally for five different configurations of the DARPA Suboff submarine model in the horizontal plane and for one configuration in the vertical plane [3]. The AFF-8 configuration consists of a sail located at the top dead center of the hull starting at $x=0.92$ m from the bow and ending at $x=1.29$ m. The AFF-3 configuration has no sail. In both configurations, the cross-shaped rudders and hydroplanes are located at $x=4$ m from the bow. The hull and appendage arrangement of the AFF-3 and AFF-8 configurations are shown in Figure 2 and the main particulars are given in Table 1 [2].

4. Mesh Independence Study

In the present study, three different mesh sizes were used in the mesh independence study. Firstly, CFD analyzes were carried out for DARPA Suboff AFF-3 configuration. This configuration is formed from the bare hull and rudder fins. The CFD calculations were performed using a commercial finite volume method with the commercial code ANSYS Fluent. Steady-state RANS simulations were conducted for all calculations. The mesh generation was carried out using both structured and unstructured mesh techniques

in Pointwise. The submarine model was investigated in a spherical computational domain with a radius of approximately eight times its own length. The total grid number is nearly 16×10^6 elements (Figure 3). T-REX elements were used to provide the non-dimensional wall distance $y^+ \approx 50$. A mesh independence study was conducted to select an adequate grid size with three different mesh densities: coarse, medium, and fine (Figure 4). Generally, in the mesh independence study, the growing factor is used as the mesh refinement factor. Thus, the total cell numbers that make up the entire calculation area can be changed. According to the ITTC Guidelines, this growing factor should be between $\sqrt{2}$ and 2. Also, ITTC have stated that refinement ratio $r=2$ may often be too large, instead of this as an alternative refinement ratio may be $r=\sqrt{2}$ [22]. The equations are discretized using a limited volume approach with cell-centered collographic variables. In the analysis of submarine models, as a solver, the ANSYS-Fluent program based on Reynolds-Averaged-Navier-Stokes Equations, which works with the principle of the finite volume method have been used.

A spherical domain was chosen as the outer domain and its radius was determined to be eight submarine lengths. After the meshing process was completed, the surfaces were defined and CFD simulations were initiated. Since it is known that submarine models will be subject to turbulent flow, the realizable k-omega turbulence model was chosen. The reason for choosing this turbulence model is that the objects analyzed in naval engineering problems have a

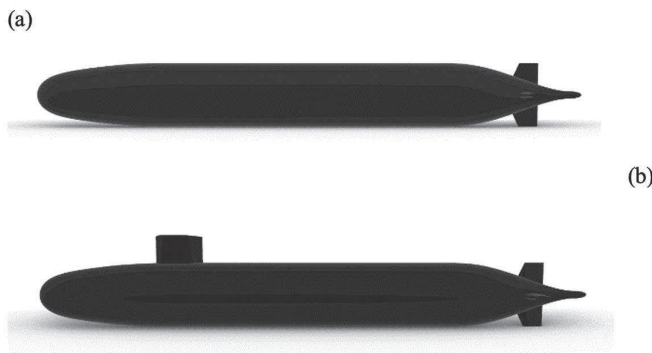


Figure 2. Geometry of DARPA Suboff AFF-3 (a) and AFF-8 (b)

Table 1. Main particulars of the DARPA Suboff AFF-3 and AFF-8 models [2]

	Symbol	Magnitude (AFF-3)	Magnitude (AFF-8)
Length overall	L_{OA}	4.356	4.356
Length between perpendiculars	L_{BP}	4.261	4.261
Maximum hull radius	R_{MAX}	0,254	0.254
Centre of buoyancy (aft of nose)	LCB	$0.4625 L_{OA}$	$0.4621 L_{OA}$
Volume of displacement		0.701	0.718
Wetted surface area	S_{WA}	6.188	6.338

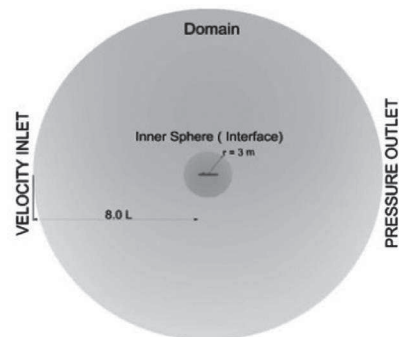


Figure 3. Computational domain and boundary conditions

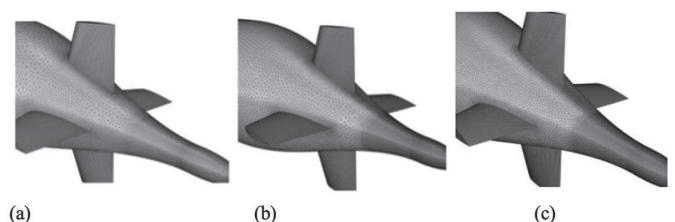


Figure 4. Structures of Coarse (a), Medium (b) and Fine (c)

relatively delicate structure, and this turbulence model is a good representation of the turbulent flow around such objects.

Boundary conditions can be analyzed in three parts.

- Inlet: It is determined as a speed input where the flow enters and moves forward.
- Output (Outlet): It is determined as the pressure output. By accepting the pressure value at the outlet as zero, it provides the energy conservation equation.
- Model (Wall): The Suboff model is defined as wall, so the flow cannot pass through it, and velocity and pressure changes can be observed here.

In the first part of the validation, the forces and moments for the static drift condition of the AFF-3 configuration were obtained for the model velocity $V=3.3436$ m/s at inflow angles changing at two-degree intervals from 0 to 6 degrees for each mesh density. Then, the CFD results were converted to non-dimensional values to be able to compare with experimental results. Medium mesh density was selected for further analysis. The analysis for larger angles were continued (at two-degree intervals from 0° to 18°) and the obtained values were compared by non-dimensional values and shown that they agree well with the experimental data.

The solution scheme is selected as Semi Implicit Methods for Pressure Linked Equations-SIMPLE and the gradient

discretization is Green-Gauss node based. In the study as turbulence model SST $k-\omega$ turbulence model was selected. The spatial discretization for the pressure gradient and momentum gradient is the second order, and for the turbulent kinetic energy and specific dissipation rate, it is selected as quick. Incoming flow is defined as the velocity inlet and the outflow is defined as the pressure outlet. The turbulence intensity and viscosity ratio were selected in the boundary conditions as 2 and 5. In this process, to get better results two spheres have been used around the submarine model, where the inner domain is defined as non-slip wall and the outer spherical domain is defined as symmetry.

Table 2 shows the first validation part of the present study. As can be seen, the computational results are in very good agreement with the experimental results. Considering these results, the medium grid size was chosen to be used for further analysis. The numerical analyzes were conducted using $k-\omega$ SST turbulence model throughout all analyses. Figures 5-7 show the comparison of the CFD results with the experimental results for the AFF-3 configuration for the longitudinal force X' , transverse force Y' and yawing moment N' values, respectively. The results for three different mesh densities are presented.

5. Obtaining the Maneuvering Forces and Moments for Larger Drift Angles for AFF-3 and

Table 2. Results of the maneuvering forces and moments of the AFF-3 configuration for different mesh densities

$\beta=0$ degree		CFD results			% Errors (acc. to experiment results)		
Grid size	Cell Number	X (N)	Y (N)	N (Nm)	(X')	(Y')	(N')
Fine	26034561	112.1016	0.0988	0.1154	1.8578	-	-
Medium	16146445	112.3571	0.0664	0.1113	1.6341	-	-
Coarse	9256715	113.1616	0.3080	0.4964	0.9298	-	-
$\beta=2$ degree		CFD results			% Errors (acc. to experiment results)		
Grid size	Cell Number	X (N)	Y (N)	N (Nm)	(X')	(Y')	(N')
Fine	26034561	111.2394	36.2315	164.2729	2.9568	6.7429	-0.1455
Medium	16146445	111.3642	34.9620	164.2448	2.8480	10.0107	-0.1284
Coarse	9256715	112.0950	34.2674	163.0828	2.2105	11.7984	0.5800
$\beta=4$ degree		CFD results			% Errors (acc. to experiment results)		
Grid size	Cell Number	X (N)	Y (N)	N (Nm)	(X')	(Y')	(N')
Fine	26034561	110.8821	81.6928	322.7482	3.5244	2.8037	5.4054
Medium	16146445	111.0518	80.2730	323.7442	3.3767	4.4930	5.1135
Coarse	9256715	111.5469	79.0410	321.7783	2.9460	5.9588	5.6897
$\beta=6$ degree		CFD results			% Errors (acc. to experiment results)		
Grid size	Cell Number	X (N)	Y (N)	N (Nm)	(X')	(Y')	(N')
Fine	26034561	110.0291	138.0959	464.8401	3.3723	5.3701	2.6802
Medium	16146445	110.2680	137.3063	466.0138	3.1624	5.9112	2.4344
Coarse	9256715	110.9607	136.2890	464.9756	2.5541	6.6083	2.6518

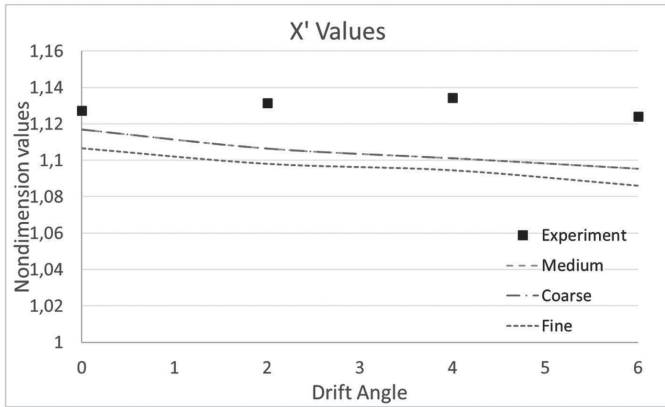


Figure 5. Longitudinal Force X' for drift angle from 0 to 6 degrees for AFF-3 configuration

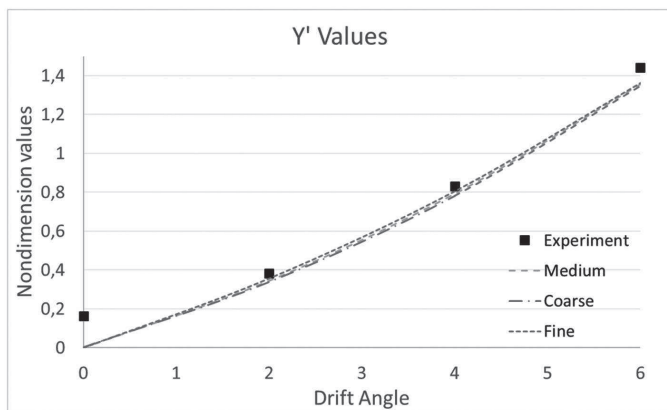


Figure 6. Transverse Force Y' for drift angle from 0 to 6 degrees for AFF-3 configuration

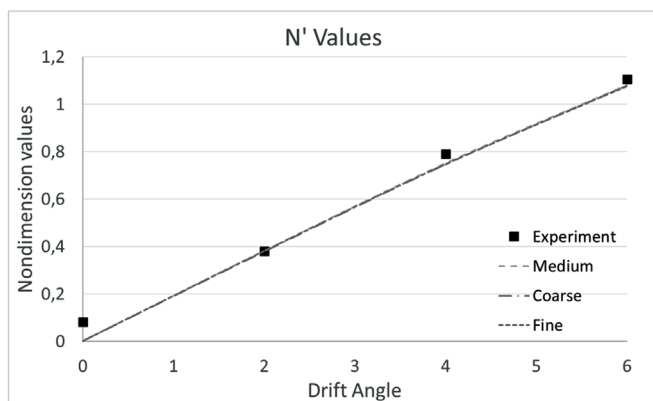


Figure 7. Yawing Moment N' for drift angle from 0 to 6 degrees for AFF-3 configuration

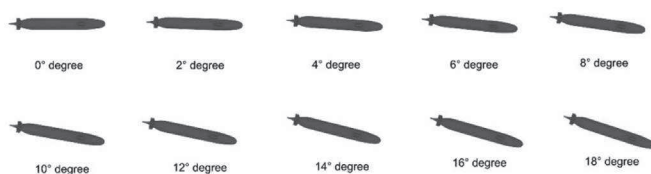


Figure 8. The position of AFF-3 configuration at different drift angles

AFF-8 Configuration

After selecting the medium grid size, numerical analyzes were performed at two-degree intervals from 0° to 18° for the AFF-3 configuration (Figure 8). The obtained hydrodynamic forces and moments were converted to non-dimensional values according to equations 10 and 11 as recommended by SNAME, 1950. Following, similar analyses were conducted for the fully appended AFF-8 configuration, which includes bare hull, sail, and four rudders. However, the AFF-8 configuration is extensively used in CFD validation studies and no experimental data is available for the static drift condition; therefore, it is not possible to make a comparison with experimental results. For the static drift condition, a numerical result found only for 18° was used for comparison [6].

The obtained values for the AFF-3 configuration from 0 to 18 degrees are compared with experimental data and are shown in Figures 9-11 and the calculation results obtained are given in Table 3.

From the figures it is seen that the results are in good

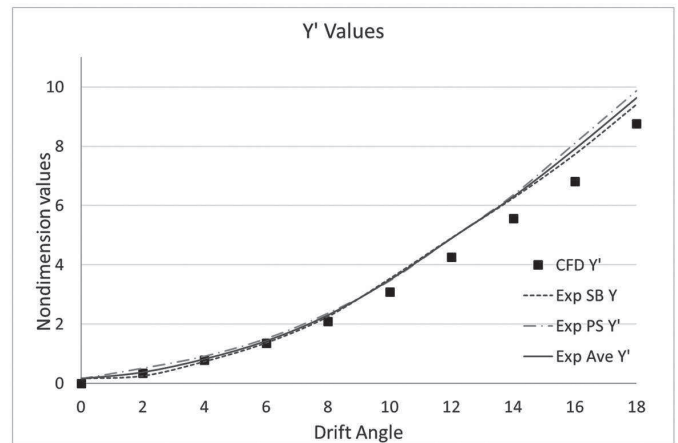


Figure 9. Longitudinal Force X' for drift angle from 0 to 18 degrees for AFF-3 configuration

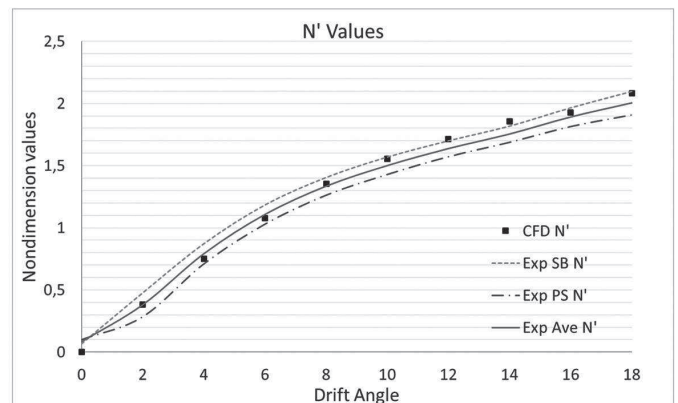


Figure 10. Transverse Force Y' for drift angle from 0 to 18 degrees for AFF-3 configuration

agreement with the experimental results. The experimental results are given for the incoming flow coming from both sides, namely the SB and PS. These two experimental results can be interpreted as the uncertainty of the experiments. It is seen that the CFD results are in the vicinity of the two experimental results. The deviation rates comparing the values obtained from CFD and experimental results are shown in Table 4.

After the studies for the AFF-3 configuration, analyses were run for the AFF-8 configuration using the same mesh structure and boundary conditions. The analysis results obtained by CFD are shown in Table 5. The CFD results obtained for 18 degrees are compared with the results obtained by Toxopeus et al. [7] and it is seen that the results are in good agreement. Toxopeus et al. [8] presented the longitudinal force X' as 0.85, transverse force Y' as 11.866, and the yawing moment N' as 2.973 for the static drift angle 18 degrees. The benchmark graphics are shown in Figures 12-14.

After the validation studies, the results for both configurations are compared. From Figure 15 to Figure 17, the results for the AFF-3 and AFF-8 configurations are given for the longitudinal force X' , transverse force Y' and yawing moment N' for the drift angles from 0 to 18 degrees in comparison. The AFF-3 configuration is formed from bare hull and four stern rudders. In addition, the AFF-8 configuration has a sail in the location at the top dead center of the hull starting from the bow at $x=0.92$ m and ending at $x=1.29$ m. The difference between the two configurations can be interpreted as the effect of the sail on the forces and moments. In the longitudinal force, an irregularity is seen for the drift angles 9-18 degrees. An increase in the transverse forces and yawing moments are seen compared with the AFF-3 configuration. Approximately at 17 degrees drift angle, the values reach their maximum value.

6. Conclusion

In the present study, forces and moments in the horizontal plane are investigated numerically for the model geometry of a benchmark submarine, DARPA Suboff AFF-3, and AFF-8 configuration using a viscous solver based on the finite volume method. First, the validation of the CFD calculations was carried out for small drift angles (from 0 to 6 degree), for the AFF-3 configuration, for which experimental data are available in the literature. To find the optimum grid size, a mesh independence study was done for three different cases; coarse, medium and fine cases at small angles (0-2-4-6 degrees) on the AFF-3 configuration and continued by selecting the medium mesh structure. Hence, the other analyzes are continued at two-degree intervals for larger angles (from 0° to 18° degrees). The results were verified and validated with available experimental data. The results of this analysis were converted into non-dimensional values and a good agreement was observed with the experimental data.

After the validation study, the analyzes of the DARPA Suboff AFF-8 configuration were carried out at two-degree

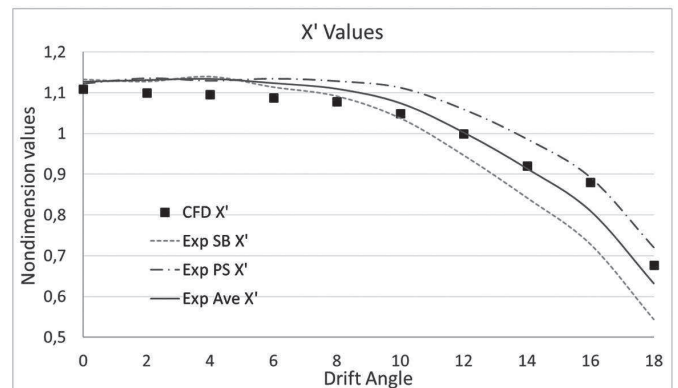


Figure 11. Yawing Moment N' for drift angle from 0 to 18 degrees for AFF-3 configuration

Table 3. Result of AFF-3

Drift angle	X (N)	X' ($\times 10^{-3}$)	Y (N)	Y' ($\times 10^{-3}$)	N (Nm)	N' ($\times 10^{-3}$)
0	112.3570	-1.1090	-0.0664	-0.000655	0.1113	0.0002578
2	111.3641	-1.0992	-34.9619	-0.345109	164.2448	0.3804878
4	111.0517	-1.0961	-80.2729	-0.792373	323.7442	0.7499826
6	110.2680	-1.0884	-137.3062	-1.355348	466.0138	1.0795630
8	109.2802	-1.0787	-212.1415	-2.094047	585.3134	1.3559312
10	106.2250	-1.0485	-312.6999	-3.086657	672.1073	1.5569972
12	101.2737	-0.9996	-431.0689	-4.255077	740.1920	1.7147214
14	93.2992	-0.9209	-564.1457	-5.568676	801.4047	1.8565262
16	89.12992	-0.8798	-691.3075	-6.823889	831.3774	1.9259606
18	68.5620	-0.6767	-887.8658	-8.764114	899.7069	2.0842521

intervals from 0 degree to 18 degrees with the resultant speed of 3,3436 m/s. However, it should be noted that unlike other configurations, there is no available experimental data for the static drift condition of the DARPA Suboff AFF-8 configuration. Thus, a comparison with experimental results was not possible for the static drift condition of the AFF-8 configuration. Only a numerical study on the results of the AFF-8 configuration for static drift at 18 degrees is available for comparison. It has been demonstrated that the CFD results obtained for a drift angle of 18 degrees exhibit good agreement with the results presented by Vaz et al. [7], which is the only source available for comparison with AFF-8 configuration.

As a result, the forces and moments generated under static drift conditions at different angles, which were previously not available in the literature, have been added to the literature and presented in this study. The study reveals that flow separation becomes significant at large angles, and with the increasing drift angle, the forces in the X direction decrease, the forces in the Y direction increase, and the moment around the Z axis increases. The difference

between the AFF-3 and AFF-8 configurations is the sail added on the top of the submarine geometry. The increase in the transverse forces and yawing moment for the AFF-8 configuration shows the effect of the sail on the static drift performance of the submarine. In future work, analyzes

Table 4. The deviation of the AFF-3 CFD results from experimental results

Drift angle	% Deviation (X')	% Deviation (Y')	% Deviation (N')
2	2.8480	10.0106	-0.1283
4	3.376	4.4929	5.1135
6	3.1623	5.9112	2.4344
8	2.8194	9.3486	-1.6821
10	2.4607	11.7467	-3.8690
12	0.3317	13.1882	-4.8118
14	-0.7170	11.6153	-5.9056
16	-8.5436	13.7744	-1.9026
18	-7.0001	9.1000	-4.0565

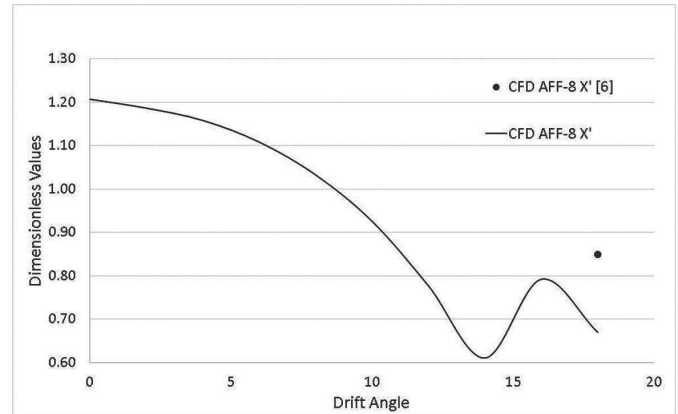


Figure 12. Longitudinal Force X' for drift angle from 0 to 18 degrees for AFF-8 configuration

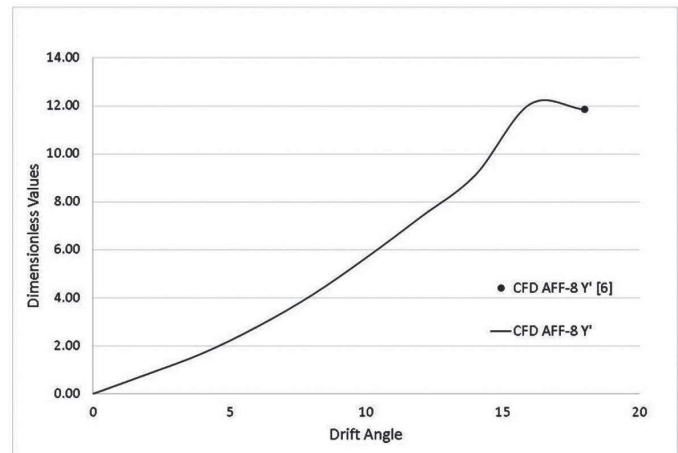


Figure 13. Transverse Force Y' for drift angle from 0 to 18 degrees for AFF-8 configuration

Table 5. Forces and moments obtained by CFD for the AFF-8 configuration

Drift angle	X (N)	X' (x10 ⁻³)	Y	Y' (x10 ⁻³)	N	N' (x10 ⁻³)
0	122,2605	-1,20683	-0,07076	-0,00069	0,36253	0,00084
2	120,1928	-1,18642	-83,65574	-0,82576	196,39776	0,45497
4	117,3173	-1,15803	-170,72788	-1,68525	413,57488	0,95808
6	112,2693	-1,10821	-282,83820	-2,79189	605,27235	1,40216
8	104,6136	-1,03264	-415,85953	-4,10494	780,27290	1,80757
10	93,7995	-0,92589	-574,71143	-5,67297	933,66604	2,16292
12	78,7258	-0,77710	-746,74898	-7,37115	1065,71360	2,46882
14	61,8646	-0,61066	-924,11950	-9,12197	1174,60530	2,72107
16	80,2412	-0,79206	-1223,29300	-12,07511	1298,31590	3,00766
18	67,8632	-0,66987	-1200,20900	-11,84725	1259,51750	2,91778

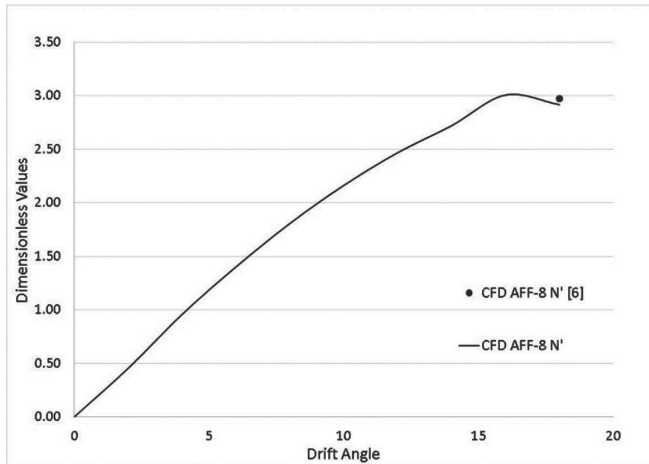


Figure 14. Yawing Moment N' for AFF-3 and AFF-8 configurations

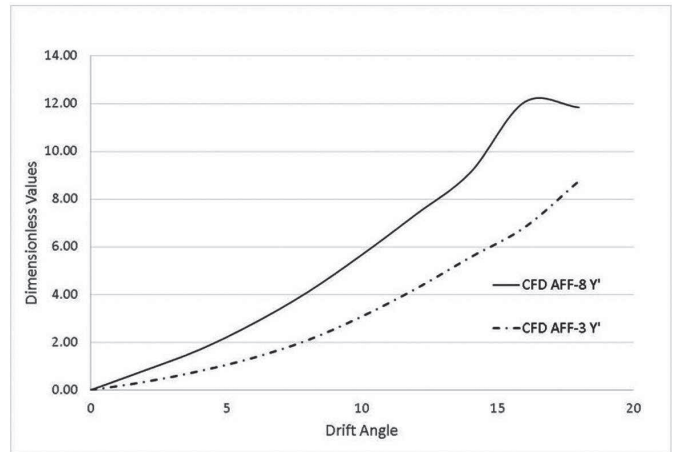


Figure 16. Transverse Force Y' for AFF-3 and AFF-8 configurations

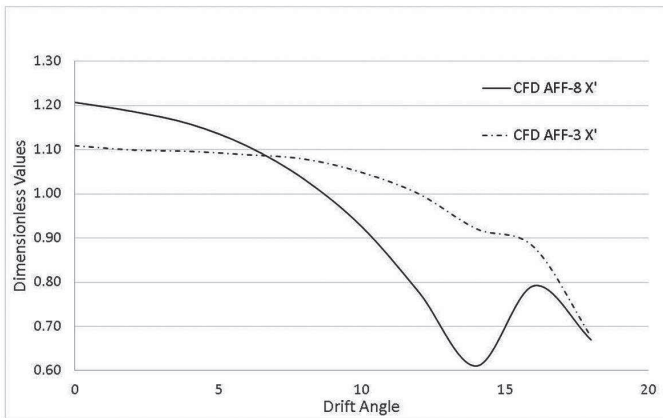


Figure 15. Longitudinal Force X' for AFF-3 and AFF-8 configurations

will be performed with the self-propelled AFF-3 and self-propelled AFF-8 configurations on horizontal planes to see the change of forces and moments in static drift conditions.

Peer-review: Externally peer-reviewed.

Authorship Contributions

Concept design: H. Öztürk, K. B. Gündüz, Y. Arıkan Özden, Data Collection or Processing: H. Öztürk, K. B. Gündüz, Y. Arıkan Özden, Analysis or Interpretation: H. Öztürk, K. B. Gündüz, Y. Arıkan Özden, Literature Review: H. Öztürk, K. B. Gündüz, Y. Arıkan Özden, Writing, Reviewing and Editing: H. Öztürk, K. B. Gündüz, Y. Arıkan Özden.

Funding: The author(s) received no financial support for the research, authorship, and/or publication of this article.

References

- [1] Ö. F. Sukas, Ö. K. Kınacı, and Ş. Bal, "Gemilerin manevra performans tahminleri için genel bir değerlendirme -I", *Gemi ve Deniz Teknolojisi*, vol. 23, pp.37-75, 2017.
- [2] N. Groves, T. Huang, and M. Chang, "Geometric characteristics of DARPA SUBOFF models (DTRC Model Nos. 5470 and 5471)", 1989.

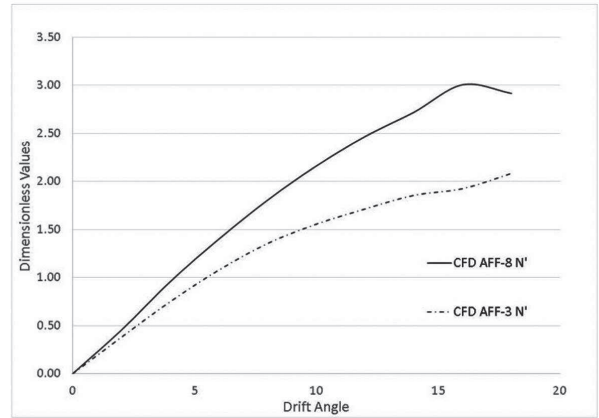


Figure 17. Yawing Moment N' for AFF-3 and AFF-8 configurations

- [3] R. Roddy, "Investigation of the stability and control characteristics of several configurations of the DARPA SUBOFF model (DTRC Model 5470) from captive- model experiments", 1990.
- [4] T. Huang, and H. Liu, "Measurements of flows over an axisymmetric body with various appendages in a wind tunnel: the DARPA SUBOFF experimental program", 1994.
- [5] "ITTC Manoeuvring Committee. (2014). Final report and recommendations to the 27th ITTC. Proceedings of the 27th International Towing Tank Conference, Copenhagen, Denmark."
- [6] S. Toxopeus, and G. Vaz, "Calculation of current or manoeuvring forces using a viscous-flow solver". *International Conference on Offshore Mechanics and Arctic Engineering*, vol. 43451, pp. 717-728, 2009.
- [7] G. Vaz, S. Toxopeus, and S. Holmes, "Calculation of manoeuvring forces on submarines using two viscous-flow solvers", *International Conference on Offshore Mechanics and Arctic Engineering*, vol. 49149, pp. 621-633, Dec 2010.
- [8] S. Toxopeus, et al. "Collaborative CFD exercise for a submarine in a steady turn", *International Conference on Offshore Mechanics and Arctic Engineering*, vol. 44922, pp. 761-772, Aug 2012.
- [9] Y. C. Pan, H. X. Zhang, and Q. D. Zhou, "Numerical prediction of submarine hydrodynamic coefficients using CFD simulation", *Journal of Hydrodynamics*, vol. 24, pp. 840-847, Dec 2012.

- [10] A. Ray, and D. Sen, "Identification of submarine hydrodynamic coefficients from sea trials using extended kalman filter", *10th International Conference on Hydrodynamics*, St. Petersburg, Russia, 2012.
- [11] J. Jiang, Y. Shi, and G. Pan, "Computation of hydrodynamic coefficients of portable autonomous underwater vehicle", *Apcom Iscm*, pp. 1-6, 2013.
- [12] A. Shadlaghani, and S. Mansoorzadeh, "Calculation of linear damping coefficients by numerical simulation of steady state experiments", *Journal of Applied Fluid Mechanics*, vol. 9, pp. 653-660, Feb 2016.
- [13] Y. H. Lin, S. H. Tseng, and Y. H. Chen, "The experimental study on maneuvering derivatives of a submerged body SUBOFF by implementing the Planar Motion Mechanism tests", *Ocean Engineering*, vol. 170, pp. 120-135, Dec 2018.
- [14] H. Atik, "Türbülans modellerinin DARPA SUBOFF statik sürükleme testi üzerinden incelenmesi", *Gazi Üniversitesi Mühendislik-Mimarlık Fakültesi Dergisi*, vol 3, pp. 1509-1522, 2021.
- [15] E. Kahramanoglu, "Numerical investigation of the scale effect on the horizontal maneuvering derivatives of an underwater vehicle", *Ocean Engineering*, vol. 272, pp 113883, Mar 2023.
- [16] H.L. Liu, and T.T. Huang, "Summary of DARPA suboff experimental program data," 1998.
- [17] T. I. Fossen, "Guidance and control of ocean vehicles. Wiley," 1994.
- [18] J. D. Mora Paz, and O. D. Tascón Muñoz, "Multiobjective optimization of a submarine hull design", *Ciencia y Tecnología de Buques*, vol. 7, pp. 27-42, 2014.
- [19] M. A. Abkowitz, "Lectures on ship hydrodynamics - Steering and maneuvering", *Hydro & Aerodynamic Laboratory*, 1964.
- [20] H. Yoon, "Phase-averaged stereo-PIV flow field and force/moment/motion measurements for surface combatant in PMM maneuvers" *The University of Iowa*, 2009.
- [21] T. Sname, "Nomenclature for treating the motion of a submerged body through a fluid" *Technical and Research Bulletin*, pp. 1950.
- [22] ITTC Resistance Committee, "Uncertainty analysis in CFD Verification and validation methodology and procedures", *ITTC - Recomm Proced. Guidel*, pp. 1-13, 2017.

Fear of COVID-19 in Seafarers: Association with Psychological Distress

© Arda Toygar¹, © Umut Yıldırım²

¹Artvin Çoruh University, Maritime and Port Management Program, Artvin, Türkiye

²Karadeniz Technical University, Department of Maritime Transportation and Management Engineering, Trabzon, Türkiye

Abstract

Since its inception, the coronavirus pandemic has caused serious social, economic, and health problems around the world. Seafarers have been identified as key workers in mitigating the negative impact of the coronavirus on global trade and ensuring the delivery of medical and hygiene supplies to regions in need. However, the complete closure policies implemented by certain countries have led to prolonged periods on board for seafarers with expired contracts and economic hardship for those unable to join new assignments. Seafarers who spend long periods on board a ship must deal with issues that may affect their psychological state. Therefore, it is important to identify the factors that cause seafarers to experience psychological distress and to develop relevant strategies to address them. The aim of this study was to determine the association between seafarers' fear of coronavirus disease-2019 (COVID-19) and psychological distress including symptoms of anxiety, depression, and stress. The questionnaire used the fear of COVID-19 Scale and the expression, Anxiety and Stress Scale), which have strong psychometric properties. Data were collected from 425 qualified seafarers working on international merchant ships and analyzed by structural equation modeling using AMOS-24. The results indicate that seafarers' fear of COVID-19 is positively associated with symptoms of anxiety and stress but not with depression. Maritime companies, sectoral organizations, and policymakers should collaborate to reduce these associations among seafarers. A unified management approach improved access to health services, and regular mental health assessments can be effective solutions.

Keywords: DASS-21, FCV-19S, Stress, Anxiety, Depression

1. Introduction

From the past to the present, every crisis has tested the mechanisms of all systems, exposed their weaknesses, and forced those involved to develop and create new strategies [1]. In considering the major breaks and transformations in history, the most important underlying reasons for these can be said to be the great depressions and crises experienced by all humanity. Innovations concerning solutions for overcoming challenging times have affected all societies, albeit in different ways and have given them experiences of change and transformation. The coronavirus disease-2019 (COVID-19) pandemic, which has affected almost every country, both economically and sociologically, is one such crisis [2]. This epidemic disease has also affected the global economy and brought the activities of many

sectors to a standstill due to the serious damages it has caused. After the coronavirus was declared an epidemic disease, widespread quarantine and restriction policies have been implemented all over the world and countries have subsequently adopted a complete closure approach [3]. This development has resulted in the deterioration of global-scale production, distribution, and consumption activities and has resulted in decreased international trade opportunities and volumes. Volumetric decreases in global trade due to the pandemic have also caused some problems with regard to maritime transport. Maritime transport is the most widely used transportation method in today's global trade structure, with more than 80% of volume-based trade being performed by this method [4,5]. Because of this high rate of trade, maritime transport creates employment for



Address for Correspondence: Umut Yıldırım, Karadeniz Technical University, Department of Maritime Transportation and Management Engineering, Trabzon, Türkiye
E-mail: uyildirim@ktu.edu.tr
ORCID ID: orcid.org/0000-0002-3991-5457

Received: 31.03.2023
Last Revision Received: 19.06.2023
Accepted: 20.06.2023

To cite this article: A. Toygar, and U. Yıldırım. "Fear of COVID-19 in Seafarers: Association with Psychological Distress." *Journal of ETA Maritime Science*, vol. 11(3), pp. 148-158, 2023.

©Copyright 2023 by the Journal of ETA Maritime Science published by UCTEA Chamber of Marine Engineers

many seafarers. In fact, about 1.9 million seafarers work on international trade ships [6].

Coronavirus pandemic negatively affects people's physical and psychological state [7,8]. One of the common reactions to epidemics is fear [9]. Fear related to coronavirus has caused several people around the world to experience mental health issues [10]. Additionally, because of this fear, individuals can make illogical decisions and have ambiguous thoughts [9]. Lee [11] has determined that individuals who have anxiety symptoms due to fear of COVID-19 are more anxious than those without such fears, and that these individuals are more likely to be suicidal. Coronavirus pandemic not only affects people's living standards on land but also directly affects the lives of seafarers. During the most intense periods of the COVID-19 pandemic, most countries did not allow seafarers to set foot on land to slow the spread of coronavirus. Some charter companies also added a "no crew change" clause to their charter parties [12]. In this process, over 400,000 seafarers could not leave their ships and had to live in a closed environment for prolonged periods [13]; some seafarers were even required to live on their ship for periods of up to 18 months [14]. Seafarers who were unable to return to their countries were required to stay on out-of-contract ships and were unable to sign new contracts; some of these individuals were not paid during their prolonged stay on board their respective vessels [12].

Several variables such as physical working conditions, natural environmental factors and health crises affect seafarers' health [15,16]. Although there have been several studies on the psychological state of seafarers, particularly during coronavirus pandemics [17-20], the association between coronavirus pandemics and the psychological state of seafarers remains unclear [21]. Further studies are needed to address this uncertainty [22]. Although there are studies using structural equation modeling (SEM) no study has been conducted using a measurement tool with a consistency and validity analysis of fear of coronavirus on seafarers' psychological state. Therefore, it will be necessary to investigate the issue comprehensively using different methodologies, and the issue should be evaluated within a scientific framework to develop scientifically based solutions. The novelty of this study is highlighted in three contexts, namely the measurement tools, the research method, and the sample group. First, seafarers' fear of COVID-19 was assessed using the Fear of COVID-19 Scale (FCV-19S), which has robust psychometric properties [7]. This scale has been used extensively in various studies of psychological aspects, including anxiety, stress, and depression, and has been successfully adapted to several languages [7,23]. Second, SEM, a rigorous statistical technique, was used to examine the relationship between

seafarers' fear of COVID-19 and their levels of anxiety, stress, and depression. SEM allows simultaneous examination of both structural and measurement models, providing a robust framework for exploring the causal associations and directional effects among research variables. By employing SEM, this study takes advantage of its strong theoretical foundation, allowing for the exploration of unidirectional or bidirectional effects within the research framework [24]. Third, symptoms of depression, anxiety, and stress are common among people living in isolated environments [25]. During the process of working on ships, seafarers live an isolated life away from their social environment. In this context, the participants in this study are seafarers. They all have a certificate from the Standards of Training, Certification and Watchkeeping for Seafarers (STCW). Therefore, they can work on all merchant ships, including the largest and those on unlimited or international voyages. In other words, the participants constituting the sample group of this study are qualified seafarers who are actively working on merchant ships and whose qualifications and certificates meet the requirements of the flag state in accordance with the provisions of the STCW Convention. This study examined the association between seafarers' fear of COVID-19 and psychological distress, including symptoms of anxiety, depression, and stress. This is an original study, as no study has yet been conducted on the association between fear of coronavirus and psychological status in seafarers using a powerful measurement tool and statistical technique. The results of this study will contribute to the improvement of the maritime literature and the development of scientifically based solutions by maritime authorities.

2. Theoretical Basis and Research Hypotheses

2.1. Fear of Coronavirus Pandemic

Some studies have examined the impact of fear of coronavirus disease on the psychological state of individuals. Most of these suggest that fear of coronavirus disease is positively associated with symptoms of anxiety, stress and depression [10,26,27]. In addition, Şimşir et al. [23] found that fear of coronavirus was associated with symptoms of anxiety and stress. Similar to the experience of people working on land, coronavirus disease has caused physical and psychological problems for seafarers [16]. In fact, seafarers may experience much higher levels of mental health problems compared with other occupations [28]. Some of these problems can be explained by the difficult working conditions associated with seafaring. Seafarers work in two main areas of the ship, the deck and the engine, in harsh conditions where they are constantly moving and exposed to vibration and static electricity. Seafarers working in the engine room are exposed to a noisy, dirty, fuel-smelling,

high temperature and indoor environment, while those working on deck clean hatches, tanks and bilges in enclosed spaces or are exposed to the sun, dust and humidity for long periods of time [29-32]. There are studies in the literature examining seafarers' challenges during COVID-19. Zhao et al. [33] analyzed Chinese seafarers' fatigue during COVID-19. They found that seafarers were more fatigued during COVID-19 than before. The study identified several causes of fatigue, including seafarers' fear of infection, wearing of protective equipment, workload, denial of shore leave, and extension of contract duration. Kaptan and Olgun Kaptan's [34] qualitative research aimed at exploring the challenge mariners experienced during the COVID-19 outbreak and to identify possible solutions. These results show that COVID-19 has a negative impact on seafarers, with a higher incidence of infectious diseases because of their shared accommodation and quality of health services. Furthermore, Onakpojeruo et al. [35] investigated the effect of COVID-19 quarantine measures on seafarers' mental health and its influence on human error occurrence. The results indicate that with significant deviations of more than 55% in the mooring operation scenario, the quarantine measures had an unfavorable effect on seafarers' psychological well-being. The qualitative study by Timilsina and Baygi [36] identified seafarers' perceptions of the COVID-19 guidelines in relation to their health and well-being. The majority of participating seafarers reported that the guidelines could reduce stress and anxiety, while others expressed that they may not have a significant impact. Another result of the study was that seafarers who had completed their contracts were experiencing delays in returning to their home countries. Considering the aforementioned studies, the hypothesis proposed in the present study was to test the associations between fear of coronavirus and psychological distress including symptoms of anxiety, stress, and depression.

2.2. Anxiety

Pandemic diseases may cause some individuals to live with the fear of death under quarantine, and this can harm their mental health, leading to anxiety, depression, and stress [37]. Prolonged work periods experienced by seafarers on ships and the associated poor living conditions in limited, closed and/or isolated areas increase the pressure and mental fatigue on this population [38]. In addition, family pressure for seafarers to return home during the coronavirus disease, intense concern about the health status of relatives, and limited access to health services on board ships can be listed as other factors that increase mental fatigue among seafarers [39]. There are studies that found that the depression and anxiety levels of seafarers increased during coronavirus infection [19]. Lei et al. [40] determined that of those individuals who were exposed

to quarantine restrictions and who had to lead a closed and isolated life during the coronavirus disease, 12.9% experienced anxiety symptoms and 22.4% experienced symptoms of depression. Baygi et al. [22] found that 12.4% of seafarers had anxiety, 14.1% had depression, and 37.3% were experiencing stress. Considering all these studies, the hypothesis proposed in this study to test the association between the fear of coronavirus and symptoms of anxiety in seafarers is as follows:

H_1 : Fear of coronavirus among seafarers is positively associated with symptoms of anxiety.

2.3. Stress

It is normal for seafarers to experience more intense symptoms of stress than other individuals due to the harsh working conditions of maritime professions, the closed environments in which these individuals work, and the fact that they are required to work away from land for long periods. Having to work away from their families, not being able to stay away from their working area, even outside working hours, and the extra workloads can be cited as sources of stress in the maritime profession [41]. It is difficult for seafarers with mental health issues to be treated when at sea. Kinali et al. [29] conducted a study with 403 seafarers and determined that 33.2% had mental health issues and were not aware of health centers from which they could benefit regarding possible mental problems they might experience. Mental health problems of seafarers, which have been the subject of several studies, are exacerbated by high levels of physical and mental stress during coronavirus disease [42]. Symptoms of stress and related psychological disorders have caused the suicide rates of seafarers to be higher than other occupational groups [43]. Ali et al. [44] conducted a study to determine the stress structure in seafarers' job roles and to measure work-related stress. The results reveal the emergence of six different themes that encompass the effects of the COVID-19 pandemic. Furthermore, the results indicate that COVID-19 has had a negative impact on seafarers' careers and has led to the occurrence of various stress-related problems. Therefore, the possibility that the fear of coronavirus disease triggers suicidal ideation in individuals necessitates the development of relevant reliable measurement tools for the detection of this problem and performing tests accordingly [45]. Taking all these studies into account, the present study proposes the following hypotheses to test the association between coronavirus anxiety and stress:

H_2 : Fear of coronavirus among seafarers is positively associated with stress symptoms.

2.4. Depression

Fears of COVID-19 may cause adjustment disorders and increase the levels of depression in individuals [46]. During

the coronavirus disease, seafarers are faced with adverse situations that cause psychological distress, such as being abandoned, living an isolated life, and having to stay on the ship for prolonged periods [47]. Baygi et al. [22] have determined that seafarers who have to work on a ship for a long time are more likely to experience depressive symptoms. Slišković [18] argues that coronavirus disease adversely affects the psychological and physical health of seafarers working in an isolated and confined environment. Qin et al. [20] examined the changes in seafarers' depression symptoms during the coronavirus disease, collecting data from 441 seafarers, and found that seafarers had high levels of depression associated with the coronavirus pandemic. Pesel et al. [48] analyzed the physical and psychological states of seafarers during coronavirus disease and revealed that 50% did not feel safe, 30% experienced insomnia, and 26% were unhappy and depressed. Jonglertmontree et al. [49] investigated depressive symptoms in seafarers during the COVID-19 period. The results showed that 19.5% of the participating seafarers had depressive symptoms. Based on these studies, this study hypothesizes the following association between the fear of coronavirus and depression among seafarers:

H_3 : Fear of coronavirus among seafarers is positively associated with the symptoms of depression.

3. Methods

3.1. Sample Group of the Research

The research population comprises seafarers working on international trade ships. Two important methods were considered in determining the sample size of the present study, the sampling group table developed by Sekaran and Bougie [50] and power analysis. It is estimated that about 1.9 million seafarers work on more than 74,000 merchant ships in the global maritime transport sector. Sekaran and Bougie [50] argued that the sample size to represent a population over 1 million should comprise at least 384 participants. In addition, the researchers determined the research sample group size of the study using the "G.Power 3.1.9.2" tool before data collection process. To correct the sample size to be representative of the research population, a power analysis was performed using a confidence level of 99%. Accordingly, the minimum sample size for the goodness of fit analysis could be 287 ($p: 0.01, 1-\beta$ err probe: 0.95, df: 5) [51]. Subsequently, the data collection process was started from the research population. The sample group of the study was interviewed between 10 July and 17 September 2022. The data were collected online because the seafarers who comprised the study sample were actively working on a ship. For the purpose of this study, a questionnaire was sent to 461 seafarers. However, thirty-six questionnaires were

found to be missing or incorrectly completed and were not included in the study. After the final evaluation, this study was conducted with data collected from 425 seafarers. Table 1 shows the sociodemographic characteristics of seafarers.

3.2. Measures

The data were collected from seafarers using two different scales: the "FCV-19S" and the "Depression, Anxiety and Stress Scale (DASS-21)". FCV-19S was developed by Ahorsu et al. [9] to evaluate the fear of coronavirus pandemic using a valid and reliable measurement tool. The Scale was adapted to Turkish by Satici et al. [7], who found the reliability coefficient of the scale to be $\alpha=0.82$. The authors also performed validity and reliability analyzes for the Scale and provided the structural validity of the scale [Goodness-of-fit index (GFI), NFI, Comparative fit index (CFI) ≥ 0.90 , and Standardized Root Mean Square Residual (SRMR) ≤ 0.08]. DASS-21 was preferred to test the psychological state of seafarers. The original version of this scale comprises 42 items but was shortened by Henry and Crawford [52]; the revised version comprises 21 items. The scale has three subscales with each containing seven items: anxiety, stress, and depression. The scale was adapted to Turkish by Yilmaz et al. [53], who found

Table 1. Sociodemographic characteristics of seafarers

Variable	Sub-variable	Frequency (n)	%
The term of contract	1-3 months	144	33.9
	4-6 months	186	43.8
	7-9 months	62	14.6
	10-12 months	33	7.8
	Total	425	100.0
Voyage area	Port voyage	24	5.6
	Cabotage	68	16
	Coastal voyage	63	14.8
	Unlimited or international voyage	270	63.5
	Total	425	100.0
Duty on the ship	Master	59	13.9
	Officer (deck and engineer)	165	38.8
	Rating and catering	33	7.8
	Cadet (deck and engineer)	168	39.5
	Total	425	100.0
Ship type	Dry cargo ship/bulk carrier	137	32.2
	Tanker	147	34.6
	Container ship	50	11.8
	Ro-Ro	56	13.2
	Other	35	8.2
	Total	425	100.0

the reliability coefficient of the Scale and its subscales to be 0.755-0.822. The subscales also had structural validity [$\chi^2/df \leq 3$, GFI and Adjusted goodness-of-fit ≤ 1 , and Root mean square error of approximation (RMSEA) ≤ 0.06].

4. Results

In this study, confirmatory factor analysis (CFA) was conducted as a precursor to SEM analysis. This step was taken for two crucial reasons. First, the sample group in this study differed from those in previous studies, which necessitated the selection of the most suitable scale for the research objectives. Second, it is important to verify the measurement model through CFA before assessing the suitability of the proposed SEM model [54]. SEM is an important analysis that

has become increasingly common in recent studies. SEM focuses on analyzing the effects or associations between independent and dependent variables [7,55,56]. In this study, which included four variables, the AMOS-24 program was used to validate the research model. Data collected from 425 seafarers were entered into the program, and CFA was performed by establishing covariances between variables. The model fit values are χ^2/df : 2.927, RMSEA: 0.067, CFI: 0.921, GFI: 0.849, Incremental Fit Index: 0.921 and SRMR: 0.064, which are compatible with those accepted in the literature [57-60]. Table 2 presents the standardized regression weights of the items in the measurement model and regression weights, standard error, and significance

Table 2. Standardized item loadings, AVE, CR, Alpha values

Dimension	Factor	β	S.E.	p	Cronbach's α	CR	AVE
Anxiety	Anx1	0.654	-	***	0.889	0.89	0.54
	Anx2	0.752	0.076	***			
	Anx3	0.754	0.075	***			
	Anx4	0.775	0.071	***			
	Anx5	0.742	0.077	***			
	Anx6	0.751	0.079	***			
	Anx7	0.709	0.077	***			
Depression	Dep1	0.808	-	***	0.913	0.91	0.60
	Dep2	0.798	0.054	***			
	Dep3	0.782	0.053	***			
	Dep4	0.735	0.055	***			
	Dep5	0.830	0.052	***			
	Dep6	0.772	0.061	***			
	Dep7	0.671	0.06	***			
Stress	Str1	0.773	-	***	0.905	0.91	0.58
	Str2	0.814	0.06	***			
	Str3	0.844	0.057	***			
	Str4	0.715	0.056	***			
	Str5	0.781	0.059	***			
	Str6	0.704	0.067	***			
	Str7	0.701	0.058	***			
FCV-19S	Fcv1	0.787	-	***	0.926	0.92	0.63
	Fcv2	0.839	0.048	***			
	Fcv3	0.714	0.057	***			
	Fcv4	0.866	0.06	***			
	Fcv5	0.855	0.057	***			
	Fcv6	0.701	0.053	***			
	Fcv7	0.761	0.058	***			

***p<0.001.

AVE: Average variance extracted, CR: Composite reliability, S.E.: Standard error, α : Cronbach alfa coefficient, β : Standardized regression weight, p: Probability value

level of the composite reliability (CR) and average variance extracted (AVE) values.

The standardized regression item weights of the latent variables ranged between 0.654-0.754 for anxiety, 0.671-0.830 for depression, 0.701-0.844 for stress, and 0.701-0.866 for FCV-19S, and all path coefficients were found to be significant ($p < 0.01$). The fact that standardized factor loadings are greater than 0.60 and less than 0.90 indicates the absence of correlation problem. Convergent validity, divergent validity, and Cronbach's α were emphasized for the reliability values of the measurement model. In this context, the AVE and CR values were examined after the first order CFA. The generally accepted values in the literature for ensuring scale validity are >0.70 for CR and >0.50 for AVE [58,61]. These values were determined using the "Stats Tools Package" developed by Gaskin [62]. The results of this study indicate that both AVE and CR values of all dimensions are greater than the determined values, providing convergent and divergent validity for the measurement model (AVE: 0.54-0.63; CR: 0.89-0.92). In addition, the Cronbach's α value of the dimensions should be greater than 0.70 to ensure scale reliability [63]. The results of the analysis show that the Cronbach's α values of all dimensions in the study are well above the value accepted in the literature (FCV-19S: 0.926; Anxiety: 0.889; Depression: 0.913; Stress: 0.905). These values suggest that the measurement structure comprising four latent variables and 28 items were confirmed and the data collected from the seafarers were compatible with the scales.

Table 3 presents information on the path coefficients of the structural model and the regression coefficients of the latent variables on the observed variables. It also presents the results of standardized regression weights and hypothesis tests, which are indicator values generated as a result of SEM. Considering the model fit values in the structural model, all values are within the limitations accepted in the literature and comply with the data collected from the study participants. Considering the path coefficients among the latent variables, the independent variable fear of coronavirus has a significant and positive association with the dependent variables' symptoms of anxiety (β : 0.475; $p < 0.001$) and stress (β : 0.392; $p < 0.001$). However, there is no significant

association between the fear of coronavirus and depression. In line with these results, two path coefficients have positive and significant values and one path coefficient does not.

5. Discussion

Coronavirus disease is an important contemporary development that threatens the mental and physical health of individuals and can cause them to be highly stressed. It is important to understand the changes in individuals' behaviors during coronavirus disease and to create a roadmap in this direction. The coronavirus pandemic has caused serious social, economic and health issues across the world since its beginning. Seafarers who provide the transportation of important human goods such as food, fuel, equipment and medical supplies come to the fore as key workers within this process [64,65]. There is a need to investigate the problems of seafarers through a powerful measurement tools and evaluate the results. This study investigated the association between the fear of coronavirus and the psychological states of seafarers. In this study, the psychological states of seafarers were tested in terms of symptoms of anxiety, depression, and stress. Validity and reliability analyses of the scales used in this study were performed and strong psychometric properties were proven by authors who developed and adapted the scales [7,9,52,53]. The results indicate that fear of coronavirus has a significant positive association with psychological distress, including symptoms of anxiety and stress, and suggest that fear of coronavirus disease has an aggravating effect in seafarers' psychological distress. The results of the study comply with those in the literature, suggesting that fear of coronavirus disease positive association with stress [7] and anxiety [9]. These also indicate compatibility with those of studies on the psychological health of seafarers during coronavirus [18,19]. In this process, several countries have imposed disembarkation bans on seafarers or crew when changing ports, causing severe pressure on seafarers [20]. Therefore, the results of this study coincide with those of one study in which mental problems of seafarers during the pandemic to be associated with pandemic precautions preventing them from setting foot in ports [22].

Table 3. Hypothesis test results

Structural Path			Hypothesis	β	S.E.	t	p	Supported or not
The fear of coronavirus	→	Anxiety	H_1	0.366	0.033	6.454	<0.001	Yes
The fear of coronavirus	→	Stress	H_2	0.139	0.039	2.608	0.009	Yes
The fear of coronavirus	→	Depression	H_3	0.083	0.037	1.562	0.118	No

$\chi^2 = 995.147$; $sd = 340$, χ^2/sd : 2.927; RMSEA: 0.067, SRMR: 0.064, IFI: 0.921, CFI: 0.921.
 β : Standardized regression weights, S.E.: Standard error, p: Probability value, t: Critic ratio

The results of the first hypothesis test indicate that fear of coronavirus has a significant positive association with symptoms of anxiety in seafarers, so H_1 is accepted. In addition, these also indicate that the fear of coronavirus causes psychological distress and is most associated with symptoms of anxiety. This result explains the limited access of seafarers to land. The implementation of various restrictions on seafarers during the pandemic, including the prohibition on leaving their ships, has resulted in their confinement in confined spaces without access to necessary physical and mental health care, exacerbating their existing health problems. In addition, the restriction of seafarers' access to shore has resulted in prolonged periods of isolation and loneliness, cutting them off from their social environment. During this process, increased psychological stress and anxiety about their future can be identified as factors contributing to this outcome. These results are consistent with the study indicating that seafarers experience increased levels of anxiety related to COVID-19 and that this contributes to an increased perception of COVID-19 burnout [66]. It is also consistent with the literature [22,40].

The results of the second hypothesis demonstrate that the fear of coronavirus disease has a significant positive association with symptoms of stress among seafarers; therefore, H_2 is accepted. This can be explained by the harsh working conditions and inadequate health services on ships. Although the fear of coronavirus disease has a negative impact on several occupational groups, workers in most occupations have access to health services for their health problems. This difference between seafaring and other professions may lead to symptoms of stress among seafarers. The results of the study are consistent with those in the literature suggesting that the physical and mental stress of seafarers increased during the coronavirus outbreak [42], and accordingly, it can be argued that long periods of quarantine would be stressful for individuals [67]. They are also consistent with the results of a study indicating that seafarers' concerns about the risk of contracting the novel coronavirus had a positive effect on their perceptions of work-related stress [66]. Another notable result of the study was that symptoms of stress were second only to symptoms of anxiety associated with the fear of coronavirus. These problems can also be reduced by ensuring compliance with working hours and rest periods on board ships (despite commercial pressures), joint decisions by maritime companies and authorities, improving health services, and creating social areas for activities on board. Furthermore, four-month contracts and action plans to facilitate the departure of seafarers whose contracts have expired can provide important solutions to mental health problems.

The results of the final hypothesis indicate that fear of coronavirus does not have a significant positive association with symptoms of depression in seafarers, leading to the rejection of hypothesis H_3 . These results differ from previous studies that suggested an association between fear of coronavirus disease and high levels of depression symptoms among seafarers [20] and that argued that half of the participating seafarers did not feel safe in their work environment during the pandemic and that a quarter of them experienced unhappiness and depression during their last contracts [48]. The restriction of seafarers from ships during the coronavirus outbreak provides important insights into the visibility of their mental health problems, including depression. The lack of communication with their social environment may also contribute to uncontrollable sadness. However, seafarers have the opportunity to alleviate their depression by going ashore in ports of call, where they can learn about different cultural values and meet their personal needs, thereby reducing their depression levels [29]. During the COVID-19 pandemic, the increased time spent in port or at anchor has facilitated seafarers' increased use of telecommunications to maintain communication with their families and social circles. In addition, factors such as the provision of agency support, addressing seafarers' nutritional needs, and allowing limited shore leave to mitigate the effects of COVID-19 may have hindered the establishment of a significant and positive association between seafarers' depression symptoms and their fear of COVID-19. In other words, the relaxation of COVID-19-related restrictions during the study period may explain the lack of a significant and positive association between fear of the pandemic and symptoms of depression among seafarers.

6. Study Limitations

There is a significant limitation in the data collection process of this study. Strict quarantine measures are still in place in different regions, and seafarers are not allowed access to land in these regions. Due to strict quarantine measures at the time of data collection from the sample group, ships could not be visited, and seafarers had to be contacted online via email or social media accounts. An examination of the mobile phone and internet habits of Turkish seafarers showed that rating seafarers were less likely to use smartphones, had lower internet access rates, and were less interested in academic studies compared with officer seafarers. As a result, it is much more difficult to reach rating seafarers and get them to respond to questionnaires than it is for officer seafarers. This limitation in the data collection process also affected the sampling method of the research. In this study, convenience sampling, which is a non-probability sampling method, was preferred.

In the contemporary world, where various challenges such as pandemics and conflicts occur simultaneously, safeguarding the mental and physical health of seafarers holds paramount importance. Although several factors may contribute to psychological distress among seafarers, this study focuses specifically on the fear of COVID-19. To further explore this association, it is recommended that future studies investigate the effects of seafarers' fear of COVID-19 and psychological distress on their levels of occupational burnout. Understanding the potential implications of this fear on seafarers' occupational deformation, emotional exhaustion, depersonalization, and occupational commitment will provide valuable insights for intervention strategies and support systems. By expanding the existing knowledge in this field, policymakers and maritime organizations can develop targeted initiatives to protect seafarers' well-being and enhance their overall occupational experience.

7. Conclusion

Seafarers spend most of their time on board during working and rest periods. Time spent ashore is limited and is only possible at loading and discharging ports. Quarantine and restriction policies have been reduced in many countries. However, in some countries in the Asia-Pacific region, these policies remain in place and seafarers are not allowed access to land. In other words, access to land is restricted for seafarers working on ships bound for ports in these countries. The implementation of COVID-19 policies in a region with a high volume of maritime transport is the main indicator that the problem is not only regional but also global. Therefore, the present study aimed to investigate the association between fear of coronavirus and symptoms of anxiety, depression, and stress in a sample of seafarers. The study results demonstrate a positive association between seafarers' fear of COVID-19 and psychological distress including symptoms of anxiety and stress. To mitigate the impact of this association, collaboration among maritime companies, sectoral organizations, and policymakers are crucial. The following suggestions reduce the existing symptoms of stress and anxiety among seafarers related to their fear of COVID-19:

1. Establish collaborative initiatives: Encourage maritime companies, sectoral organizations, and policymakers to collaborate on initiatives focused on seafarers' mental health and well-being, specifically addressing symptoms of stress and anxiety. Comprehensive strategies and programs can be developed through such a collaboration.
2. Adopt a consistent management approach: To ensure consistent access to the limited health services and resources available to seafarers, particularly in association

with stress and anxiety management, a standardized management approach should be implemented across the maritime industry. This may include the establishment of protocols and guidelines for the provision of health care and mental health support.

3. Conduct regular mental health assessments: Introduce periodic mental health assessments for seafarers at specified intervals, including assessments specifically aimed at identifying and addressing symptoms of stress and anxiety. Utilize therapy methods and screening tools to promptly detect and address mental health problems at an early stage. This proactive approach can help identify symptoms of stress and anxiety issues early and provide appropriate support and intervention.

4. Include mental health discussions in safety meetings: Incorporate discussions on mental health, including symptoms of stress and anxiety, in shipboard safety meetings. Provide a platform for seafarers to share their experiences, challenges, and concerns related to symptoms of stress and anxiety. This can foster a supportive environment, reduce stigma, and promote collective problem-solving in addressing these issues.

5. Provide training and awareness programs: Implement training programs to educate seafarers, coping strategies specifically tailored to address symptoms of stress and anxiety. Raising awareness can contribute to a more empathetic and supportive environment in which seafarers feel empowered to manage their symptoms of stress and anxiety effectively.

6. Establish onshore support networks: Develop shore-based support networks consisting of mental health professionals, counselors and peer support groups specifically focused on addressing seafarers' symptoms of stress and anxiety. These networks can provide accessible resources, counseling services, and a platform for seafarers to connect with others who understand the unique stressors and anxieties they face.

By implementing these suggestions, maritime companies, sectoral organizations, and policymakers can work collaboratively to address seafarers' symptoms of stress and anxiety and promote a healthier and more resilient workforce in the face of COVID-19 and beyond.

Peer-review: Internally and externally peer-reviewed.

Authorship Contributions

Concept design: A. Toygar, U. Yıldırım, Data Collection or Processing: A. Toygar, U. Yıldırım, Analysis or Interpretation: A. Toygar, U. Yıldırım, Literature Review: A. Toygar, Writing, Reviewing and Editing: A. Toygar, U. Yıldırım.

Funding: The author(s) received no financial support for the research, authorship, and/or publication of this article.

References

- [1] T. E. Notteboom, T. Pallis, and J. P. Rodrigue, "Disruptions and resilience in global container shipping and ports: the COVID-19 pandemic versus the 2008–2009 financial crisis," *Maritime Economics & Logistics*, vol. 23, pp. 1–32, Jan 2021.
- [2] A. Toygar, and U. Yildirim, "The changing structure of international trade: an evaluation of the liner shipping industry," in *New Normal and New Rules about International Trade, Economics and Marketing*, Peter Lang GmbH, pp. 103–112, 2021.
- [3] A. Toygar, U. Yildirim, and G. M. İnegöl, "Investigation of empty container shortage based on swara-aras methods in the COVID-19 era," *European Transport Research Review*, vol. 14, pp. 1–17, Mar 2022.
- [4] UNCTAD, "The review of maritime transport 2021," 2021. https://unctad.org/system/files/official-document/rmt2021_en_0.pdf
- [5] R. Yan, H. Mo, X. Guo, Y. Yang, and S. Wang, "Is port state control influenced by the COVID-19? evidence from inspection data," *Transport Policy*, vol. 123, pp. 82–103, Jul 2022.
- [6] ICS, "New bimco/ics seafarer workforce report warns of serious potential officer shortage," 2021. <https://www.ics-shipping.org/press-release/new-bimco-ics-seafarer-workforce-report-warns-of-serious-potential-officer-shortage/>
- [7] B. Satici, E. Gocet-Tekin, M. Deniz, and S. A. Satici, "Adaptation of the fear of COVID-19 scale: its association with psychological distress and life satisfaction in turkey," *International Journal of Mental Health and Addiction*, vol. 19, pp. 1980–1988, Dec 2021.
- [8] A. Luqman, and Q. Zhang, "Explore the mechanism for seafarers to reconnect with work after post-pandemic psychological distress (papist19): the moderating role of health-supporting climate," *Ocean & Coastal Management*, vol. 223, pp. 106153, 2022.
- [9] D. K. Ahorsu, C. Y. Lin, V. Imani, M. Saffari, M. D. Griffiths, and A. H. Pakpour, "The fear of COVID-19 scale: development and initial validation," *International Journal of Mental Health and Addiction*, vol. 20, pp. 1537–1545, Mar 2020.
- [10] M. S. Mahmud, M. U. Talukder, and S. M. Rahman, "Does 'fear of COVID-19' trigger future career anxiety? an empirical investigation considering depression from COVID-19 as a mediator," *International Journal of Social Psychiatry*, vol. 67, pp. 35–45, July 2020.
- [11] S. A. Lee, "Coronavirus anxiety scale: a brief mental health screener for COVID-19 related anxiety," *Death Studies*, vol. 44, pp. 393–401, 2020.
- [12] IMO, "Coronavirus (covid 19) "no crew change" clauses in charterparties," 2020. [https://www.wcdn.imo.org/localresources/en/MediaCentre/HotTopics/Documents/COVID CL 4204 adds/CL.4204-Add.36 no crew change clause.pdf](https://www.wcdn.imo.org/localresources/en/MediaCentre/HotTopics/Documents/COVID%20CL%204204%20add/CL.4204-Add.36%20no%20crew%20change%20clause.pdf)
- [13] S. Cotton, and B. Ahmed, "ITF and jng joint statement: on seafarers' rights and the present crew change crisis," 2020. <https://www.itfglobal.org/en/news/itf-and-jng-joint-statement-seafarers-rights-and-present-crew-change-crisis>
- [14] J. Hines, and J. Burt, "Seafarers forced to spend up to 18 months on ships, international transport workers' federation says," 2020. <https://www.abc.net.au/news/2020-10-20/seafarers-spend-18-months-without-leaving-cargo-ships/12780960>
- [15] C. Hetherington, R. Flin, and K. Mearns, "Safety in shipping: The human element," *Journal of Safety Research* vol. 37, pp. 401–411, Oct 2006.
- [16] X. Li, Y. Zhou, and K. F. Yuen, "A systematic review on seafarer health: conditions, antecedents and interventions," *Transport Policy*, vol. 122, pp. 11–25, June 2022.
- [17] M. Mittal, G. Battineni, L. M. Goyal, B. Chhetri, N. Oberoi, S. V. Chintalapudi, and F. Amenta, "Cloud-based framework to mitigate the impact of COVID-19 on seafarers' mental health," *International Maritime Health*, vol. 71, no. 3, pp. 213–214, Sep 2020.
- [18] A. Slišković, "Seafarers' well-being in the context of the COVID-19 pandemic: a qualitative study," *Work*, vol. 67, pp. 799–809, Dec 2020.
- [19] F. Baygi, A. Mohammadian Khonsari, N. Agoushi, A. Hassani Gelsefid, S. Mahdavi Gorabi, and M. Qorbani, "Prevalence and associated factors of psychosocial distress among seafarers during COVID-19 pandemic," *BMC Psychiatry*, vol. 21, pp. 1–8, Apr 2021.
- [20] W. Qin, L. Li, D. Zhu, C. Ju, P. Bi, and S. Li, "Prevalence and risk factors of depression symptoms among Chinese seafarers during the COVID-19 pandemic: a cross-sectional study," *BMJ Open*, vol. 11, pp. e048660, June 2021.
- [21] B. Pauksztat, M. R. Grech, and M. Kitada, "The impact of the COVID-19 pandemic on seafarers' mental health and chronic fatigue: beneficial effects of onboard peer support, external support and internet access," *Marine Policy*, vol. 137, pp. 104942, 2022.
- [22] F. Baygi, et al. "Post-traumatic stress disorder and mental health assessment of seafarers working on ocean-going vessels during the COVID-19 pandemic," *BMC Public Health*, vol. 22, pp. 242, Feb 2022.
- [23] Z. Şimşir, H. Koç, T. Seki, and M. D. Griffiths, "The relationship between fear of COVID-19 and mental health problems: a meta-analysis," *Death Studies*, vol. 46, pp. 515–523, 2022.
- [24] S. L. Hoe, "Issues and procedures in adopting structural equation modelling technique," *Journal of Applied Quantitative Methods*, vol. 3, pp. 76–83, July 2008.
- [25] M. M. Hossain, A. Sultana, and N. Purohit, "Mental health outcomes of quarantine and isolation for infection prevention: a systematic umbrella review of the global evidence," *Epidemiology and Health*, vol. 42, pp. 1–11, June 2020.
- [26] C. A. Harper, L. P. Satchell, D. Fido, and R. D. Litzman, "Functional fear predicts public health compliance in the COVID-19 pandemic," *International Journal of Mental Health and Addiction*, vol. 19, pp. 1875–1888, Apr 2021.
- [27] A. J. Rodríguez-Hidalgo, Y. Pantaleón, I. Dios, and D. Falla, "Fear of COVID-19, stress, and anxiety in university undergraduate students: a predictive model for depression," *Frontiers in Psychology*, vol. 11, pp. 591797, Nov 2020.
- [28] Z. Zhen, R. Wang, and W. Zhu, "A deep learning based method for intelligent detection of seafarers' mental health condition," *Scientific Reports*, vol. 12, pp. 1–11, 2022.

- [29] H. Kinalı, U. Yıldırım, and A. Toygar, "A quantitative study on the mental health of Turkish seafarers," *International Journal of Occupational Safety and Ergonomics*, pp. 1–26, Feb 2022.
- [30] U. Yıldırım, A. Toygar, and C. Çolakoğlu, "Compensation effect of wages on decent work: A study on seafarers attitudes," *Marine Policy*, vol. 143, pp. 105155, Sep 2022.
- [31] M. Danacı and U. Yıldırım, "comprehensive analysis of lifeboat accidents using the fuzzy delphi method," *Ocean Engineering*, vol. 278, pp. 114371, June 2023.
- [32] R. Cui, Z. Liu, X. Wang, Z. Yang, S. Fan and Y. Shu, "The impact of marine engine noise exposure on seafarer fatigue: a china case," *Ocean Engineering*, vol. 266, pp. 112943, Sep 2022.
- [33] Z. Zhao, L. Tang, and Y. Wu, "Fatigue during the COVID-19 pandemic: the experiences of chinese seafarers," *Marine Policy*, vol. 153, pp. 105643, July 2023.
- [34] M. Kaptan, and B. Olgun Kaptan, "The investigation of the effects of COVID-19 restrictions on seafarers," *Australian Journal of Maritime & Ocean Affairs*, vol. 15, pp. 25–37, Aug 2023.
- [35] D. Onakpojeruo, B. Jeong, and C. Park, "Mental wellbeing; human reliability assessment of seafarers during the COVID-19 era," *Journal of International Maritime Safety, Environmental Affairs, and Shipping*, vol. 7, pp. 2184604, Feb 2023.
- [36] A. Timilsina, and F. Baygi, "COVID-19 guidelines and its perceived effect on seafarers' health and wellbeing: a qualitative study," *PLoS One*, vol. 18, pp. e0284155, Apr 2023.
- [37] F. Khademi, S. Moayedi, and M. Golitaleb, "The COVID-19 pandemic and death anxiety in the elderly," *International Journal of Mental Health Nursing*, vol. 30, pp. 346–349, Feb 2020.
- [38] D. Shan, "Occupational health and safety challenges for maritime key workers in the global COVID-19 pandemic," *International Labour Review*, vol. 161, pp. 267–287, 2021.
- [39] S. Stannard, "COVID-19 in the maritime setting: the challenges, regulations and the international response," *The International Labour Review*, vol. 71, pp. 85–90, 2020.
- [40] L. Lei, X. Huang, S. Zhang, J. Yang, L. Yang, and M. Xu, "Comparison of prevalence and associated factors of anxiety and depression among people affected by versus people unaffected by quarantine during the COVID-19 epidemic in southwestern china," *Medical Science Monitor International Scientific Information*, vol. 26, pp. e924609- e924601, 2020.
- [41] A. Slišković, "Occupational stress in seafaring," in *Maritime Psychology: Research in Organizational and Health Behavior at Sea*, M. MacLachlan, Ed., New York: Springer International Publishing, 2017, pp. 99–126.
- [42] Y. Guo, R. Yan, Y. Wu, and H. Wang, "Ports opening for seafarer change during the COVID-19: Models and applications," *Sustainability*, vol. 14, pp. 2908, March 2022.
- [43] R. T. Iversen, "The mental health of seafarers," *International Maritime Health*, vol. 63, pp. 78–89, 2012.
- [44] S. N. M. Ali, et al. "A study of psychometric instruments and constructs of work-related stress among seafarers: a qualitative approach," *International Journal of Environmental Research and Public Health*, vol. 20, pp. 2866, 2023.
- [45] M. A. Mamun, and M. D. Griffiths, "First COVID-19 suicide case in bangladesh due to fear of COVID-19 and xenophobia: possible suicide prevention strategies," *Asian Journal of Psychiatry*, vol. 51, pp. 102073, 2020.
- [46] J. Zhang, W. Wu, X. Zhao, and W. Zhang, "Recommended psychological crisis intervention response to the 2019 novel coronavirus pneumonia outbreak in China: a model of West China Hospital," *Precision Clinical Medicine*, vol. 3, pp. 3–8, 2020.
- [47] U. J. Okeleke, "A study of the results of coronavirus (COVID-19) on the nigerian maritime workers," *AIJR Preprint Server*, vol. 176, pp. 1–8, 2020.
- [48] G. Pesel, M. L. Canals, M. Sandrin, and O. Jensen, "Wellbeing of a selection of seafarers in eastern adriatic sea during the COVID-19 pandemic 2020," *International Maritime Health*, vol. 71, pp. 184–190, Sep 2020.
- [49] I. Jonglertmontree, W. Kaewboonchoo, O. Morioka, and P. Boonyamalik, "Depressive symptoms among thai male seafarers during the COVID-19 pandemic: a cross-sectional study," *BMC Public Health*, vol. 23, pp. 475, Mar 2023.
- [50] U. Sekaran and R. Bougie, *Research Methods for Business: A Skill-Building Approach*, 7th Edition. West Sussex: Wiley & Sons, 2016. <https://www.wiley.com/en-us/Research+Methods+For+Business%3A+A+Skill+Building+Approach%2C+7th+Edition-p-9781119266846>
- [51] J. Cohen, *Statistical Power Analysis for the Behavioral Sciences*, 2nd ed. New York, 1988. <https://www.taylorfrancis.com/books/mono/10.4324/9780203771587/statistical-power-analysis-behavioral-sciences-jacob-cohen>.
- [52] J. D. Henry, and J. R. Crawford, "The short-form version of the depression anxiety stress scales (dass-21): construct validity and normative data in a large non-clinical sample," *British Psychological Society*, vol. 44, pp. 227–239, Jun 2005.
- [53] Ö. Yılmaz, H. Boz, and A. Arslan, "The validity and reliability of depression stress and anxiety scale (DASS21) Turkish short form" *Research of Financial Economic and Social Studies*, vol. 2, pp. 78–91, 2017.
- [54] T. A. Brown, "Confirmatory factor analysis for applied research". New York: Guilford Press, 2006. <https://psycnet.apa.org/record/2006-07729-000>
- [55] K. Kara, and S. Edinsel, "The mediating role of green product innovation (gpi) between green human resources management (ghrm) and green supply chain management (gscm): evidence from automotive industry companies in turkey," *Supply Chain Forum: An International Journal*, pp. 1–22, Mar 2022.
- [56] U. Yıldırım, A. Toygar, and A. L. Tunçel, "Effects of power distance on organizational commitment: a study on maritime faculty students," *Journal of ETA Maritime Science*, vol. 9, pp. 256–265, 2021.
- [57] P. M. Bentler, and D. G. Bonett, "Significance tests and goodness of fit in the analysis of covariance structures," *Psychological Bulletin*, vol. 88, pp. 588–606, 1980.
- [58] C. Fornell, and D. Larcker, "Evaluating structural equation models with unobservable variables and measurement error," *Journal of Marketing Research*, vol. 18, pp. 39–50, 1981.
- [59] H. Schermelleh-Engel, K. Moosbrugger, and H. Müller, "Evaluating the fit of structural equation models: tests of significance and descriptive goodness-of-fit measures," *Methods of Psychological Research*, vol. 8, pp. 23–74, May 2003.

- [60] R. B. Kline, *Principles and practice of structural equation modeling*, Third. New York: Guilford Publications, 2011. https://www.researchgate.net/profile/Cahyono-St/publication/361910413_Principles_and_Practice_of_Structural_Equation_Modeling/links/62cc4f0ed7bd92231faa4db1/Principles-and-Practice-of-Structural-Equation-Modeling.pdf
- [61] D. Gefen, D. Straub, and M. C. Boudreau, "Structural equation modeling and regression: guidelines for research practice," *Communications of the Association for Information Systems*, vol. 4, 2000.
- [62] J. Gaskin, "Multi-group effects gaskination's statwiki," 2012. http://statwiki.gaskination.com/index.php?title=Main_Page
- [63] J. C. Nunnally, *Psychometric Theory*, 2nd ed. New York: McGraw-Hill Book Company, 1978. [https://www.scirp.org/\(S\(i43dyn45teexjx455qlt3d2q\)\)/reference/ReferencesPapers.aspx?ReferenceID=1867797](https://www.scirp.org/(S(i43dyn45teexjx455qlt3d2q))/reference/ReferencesPapers.aspx?ReferenceID=1867797)
- [64] C. Doumbia-Henry, "Shipping and COVID-19: protecting seafarers as frontline workers," *WMU Journal of Maritime Affairs*, vol. 19, pp. 279–293, Sep 2020.
- [65] IMO, "Coronavirus (COVID-19)-designation of seafarers as key workers," 2021. https://wwwcdn.imo.org/localresources/en/MediaCentre/HotTopics/Documents/COVID_CL_4204_adds/Circular_Letter_No.4204-Add.35-Coronavirus%28Covid-19%29-Designation_Of_Seafarers_As_Key_Workers.pdf (accessed June 21, 2022).
- [66] A.T. Erdem and H. Tutar, "Impact of COVID-19 anxiety on work stress in seafarers: the mediating role of COVID-19 burnout and intention to quit," *International Maritime Health*, vol. 73, pp. 133-142, 2022.
- [67] S. K. Brooks, et al. "The psychological impact of quarantine and how to reduce it: rapid review of the evidence," *Lancet*, vol. 395, pp. 912–920, Mar 2020.

The Selection of Ocean Container Carrier: An Analytic Network Process (ANP) Approach

© Ayfer Ergin¹, © Güler Alkan²

¹Istanbul University-Cerrahpaşa Faculty of Engineering, Maritime Transportation Management Engineering, İstanbul, Türkiye

²Mersin University Faculty of Maritime, Department of Maritime Transportation and Management Engineering, Mersin, Türkiye

Abstract

Carrier selection is a complicated problem as it includes many quantitative and qualitative criteria. Due to the complexity of this issue, many criteria that influence decision making interact with each other, making it necessary to consider these interactions in order to make the best decision. The analytical network process (ANP) method enables us to solve the carrier selection problem of decision making more effectively and realistically. This study, which aims to contribute to the research field, employs the previously unused ANP method, which permits criteria interaction, and investigates the carrier selection problem in order to determine the similarities and differences between different industries' expectations of ocean container carriers. In this context, this study has been applied in three different industries: textiles, white goods, and chemicals. In this way, the study contributes to the literature on ocean container carriers. From the results, the most important criterion for the three shipper groups was found to be reliability. However, there were significant differences in the ranking of other criteria.

Keywords: Carrier, Shipper, Carrier selection criteria, Container transportation, Analytic network process

1. Introduction

In parallel with the expanding trade volume between countries with globalization, transportation is increasing day by day. Maritime transport is the backbone of international trade, accounting for more than 80% of the world's trade volume [1]. Container transportation, which is easily integrated with other transportation modes, is the fastest-growing component of maritime transportation. With this feature, it has increased more than two and a half times in the last 25 years and reached 151 million TEUs in 2019 [2,3]. In addition, during the coronavirus disease-2019 (COVID-19) pandemic, restrictions have been imposed on all transportation systems in the world at specific periods, except maritime transportation. Maritime transportation is a strategic mode of transportation with its sustainability in a crisis, as well as being cheaper and more environmentally friendly than other transportation systems. Container

freight rates have increased significantly due to the impact of the COVID-19 pandemic, congestion in the ports, and equipment availability problem. This situation has increased the interest of researchers in studies on container transportation.

Many global supply chains work with specialized carriers to improve the competitiveness of their logistic operations. Carrier selection is not easy as it is a strategic decision for the supply chain, and it constantly involves uncertainty and complexity [4]. In supply chain management, the purpose of carrier selection decisions is to minimize logistic costs as much as possible and to achieve high quality, high delivery performance. In this way, supply chains increase competitiveness by reducing total logistic costs in the purchasing and distribution processes. To achieve this, it is important for carriers to accurately determine the demands and needs of their supply chains. Although carrier selection



Address for Correspondence: Ayfer Ergin, İstanbul University-Cerrahpaşa Faculty of Engineering, Maritime Transportation Management Engineering, İstanbul, Türkiye
E-mail: ayfersan@iuc.edu.tr
ORCID ID: orcid.org/0000-0002-6276-4001

Received: 23.11.2022
Last Revision Received: 20.04.2023
Accepted: 06.07.2023

To cite this article: A. Ergin, and G. Alkan. "The Selection of Ocean Container Carrier: An Analytic Network Process (ANP) Approach." *Journal of ETA Maritime Science*, vol. 11(3), pp. 159-167, 2023.

studies have been carried out for the last fifty years, most of the studies have been conducted by considering the shippers' view in road transport [5-9]. Murphy and Hall [10] stated that there are significant ranking differences between motor carrier selection and ocean container carrier selection studies. This situation increases the necessity of performing more studies on maritime transport, which is the backbone of world trade. Studies have been conducted on the selection of ocean container carriers [11-15], and although there has been an increase in the number of studies, especially after 2010 [16-19], the expectations of shippers from carriers vary depending on the size of the shipper and the industry they are in. However, a limited number of studies have examined the differences in perspectives among large shippers. Brooks examined carrier selection criteria for North American and European large and small shippers. It was emphasized that there are significant differences in the expectations of large and small shippers from ocean container carriers [20]. The expectations of shippers for carriers differ from industry to industry. In this context, it is necessary to research the differences in perspectives among large shippers with high carrying capacity in the ocean carrier selection process. This study fills the gap in this field by investigating the expectations of large shippers operating in different industries in the Turkish market from their container carriers.

Bagchi [7] argued that an analytical hierarchy process (AHP), a multi-criteria decision-making method, is a good model for the carrier selection. In contrast, many criteria that influence decision making interact with each other in carrier selection problems, and it is necessary to consider these interactions to make the best decision. The AHP method proposed by Bagchi [7] for carrier selection does not allow interaction between criteria. On the other hand, the analytical network process (ANP) captures interdependencies among decision qualities [21]. With this structure, the ANP method enables decision-making problems to be analyzed more effectively and realistically [22]. It has been observed that ANP is used effectively in many areas such as the selection of logistics service providers [21], ERP software selection [23], and energy policy planning [24]. The ANP method, which allows the interaction of criteria, is proposed for the first time in ocean container carrier selection studies to enrich the relevant literature.

2. Literature Review

The carrier selection process has been explored for nearly 50 years; therefore, it is not new in the relevant literature. However, although more than 80% of world trade is carried out by maritime transport, the number of studies on this subject is limited. Collison the Pacific examined the ocean

carrier selection criteria for the Northwest-Central Alaska inland trade route. In the study, it was determined how the order of importance changed among different customer groups. The importance given to the criteria may vary according to the characteristics of the cargo and the needs of the shipper [11]. Kent and Stephen Parker [13] detected the three most important container carrier selection criteria for American shippers to be equipment availability, service frequency, and reliability. The leading criteria for Taiwanese shippers are accurate documentation, availability of cargo space, and reliability of sailing, respectively [14]. Kannan et al. [16] evaluated the ocean carrier selection criteria of Indian shippers using the AHP method. As a result of their analysis, the most important three criteria were low freight, pricing flexibility, flexibility, and equipment availability. Tasmanian shippers found the freight rate less significant according to the criteria of cargo security and safety and capacity availability [25]. Taiwanese shippers considered transport reliability, transit time, and timely delivery as the most important criteria in the selection of ocean container carriers [26]. Brooks [20], in her study in 1989, stated that the importance given to transit time and carrier reputation criteria has decreased compared to 5 years ago. D'agostini et al. [27] stated that the top ten container carriers have a market share of 85% and the strategic partnerships they have made among themselves have an impact on the shippers. In their study, they examined the expectations of Hong Kong shippers from ocean container carriers.

In the literature on carrier selection, studies have been carried out by considering the perspectives of the shipper, consignee, freight forwarder, and carrier. Although many studies consider the shipper's perspective, the number of studies focusing on large shippers is limited. Pearson and Semeijn [28] investigated whether carrier selection behaviors of shippers change according to their size on motor carriers. While the order of important criteria such as reliability, transit time, and freight was the same for both groups (large shipper, small shipper), there were differences in the ranking of less important criteria such as over/short/damage, carrier considerations, and forwarding services [28]. Lu [29] studied the expectations of Taiwanese large shippers. Cargo safety, cargo tracking, and inland transport were among the important criteria in the study. While the most important criterion for small shippers was freight, the most important criterion for American large shippers was equipment availability in the Brooks [20] study. The main reason why many studies have examined this issue in detail is that shippers' decision criteria have changed significantly over time. There are serious differences according to the importance given by the shippers to the carrier selection criteria, transportation mode, the shippers' region, export or

import trade, its size, and the industry it is in. Although the ANP method has not been used in ocean container carrier selection studies until now, studies have been conducted with this method in the transportation sector. Chen [30] used the ANP method to select airline service quality improvement criteria for the airline industry. Jharkharia and Shankar [21] have proposed the ANP model, which enables them to better understand complex problems for logistic service provider selection. Onut et al. [31] utilized the ANP method, which takes into account the interaction between the criteria, to evaluate container port selection.

3. ANP Model

Recently, a method widely used in decision-making problems is the Analytic hierarchy process (AHP), which was developed by Thomas L. Saaty and takes into account qualitative values and quantitative values [32,33]. AHP models decision-making problems in a top-down hierarchical structure [34]. At the top of the hierarchy is an objective, and under this objective, there are options at the bottom for the criteria, sub-criteria, and hierarchy, respectively. The criteria found at the same level within this hierarchical structure are independent of each other, and the impact of the criteria on each other in the decision-making process is not considered [35]. In contrast, many factors that influence real-world decision making interact with each other, and making the best decision requires recognition of these relationships. The method that uses the relations between factors in the process mentioned above and eliminates the necessity of modeling the problem in a

single direction is the ANP method developed by Saaty [34]. The ANP method models the decision-making problem by constructing a network structure that takes into account factors and internal dependencies during the modeling phase. With this feature, the ANP method permits us to solve the problems of decision making more effectively and realistically.

While AHP shows hierarchical relations with a unidirectional framework, ANP allows for more complex relationships between decision levels and features. In this way, it enables easy modeling of complicated issues that hierarchical structures cannot model [33]. The structural difference between a hierarchy and a network is shown in Figure 1 [36].

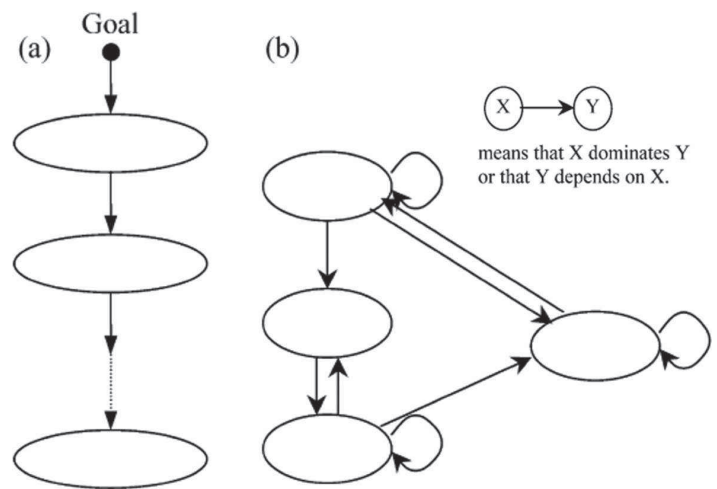


Figure 1. Structural difference between a hierarchy and a network

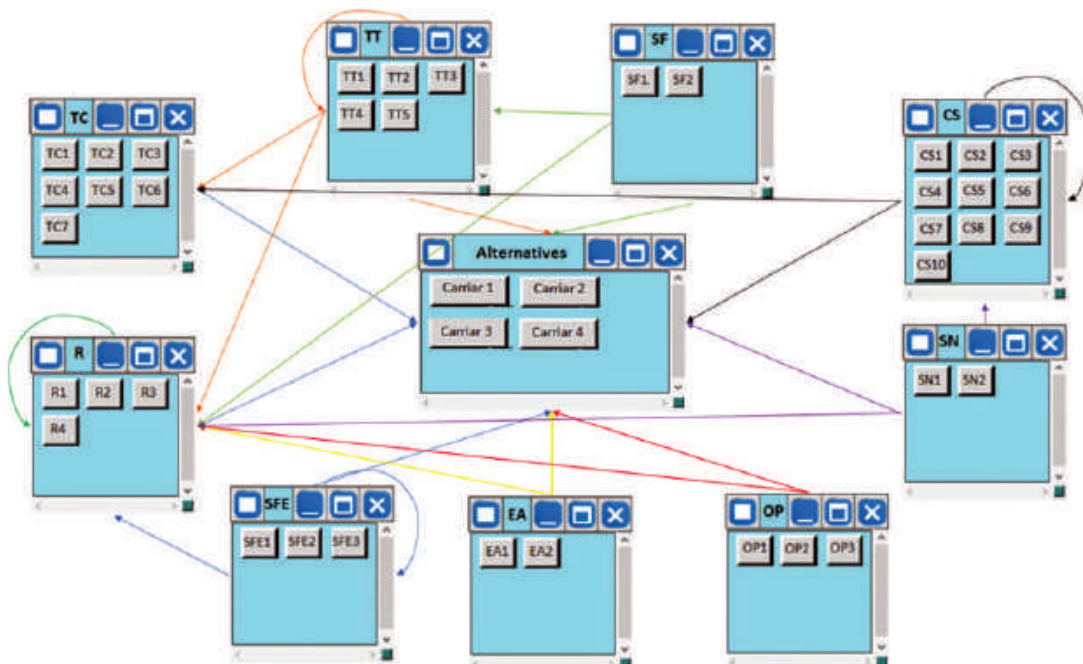


Figure 2. Network structure

real names of selected carriers have been not used to obey the fair competition rules.

5. Discussion

The ANP method was utilized to evaluate the differences and similarities between the three diverse large shippers’

expectations of ocean container carriers. After the main and sub-criteria to be used in the ocean container carrier selection model are determined as in Table 1, the interaction between the criteria should be determined. Besides the studies in the literature, the dependencies, relationships, and interactions between the criteria were revealed by referring to the opinions of experts working in shippers’ logistics departments and ocean container carriers. These interactions are shown in Table 2. The Super Decision program was used to decide the priorities of the criteria in the ocean container carrier selection study.

The network structure of the “container carrier firm selection” model, including the relationships between the criteria of the Super Decisions program, is shown in Figure 2. A comparison of the priority weights of the main criteria of three different large shipper groups (textiles, white goods, and chemicals) is shown in Table 3. As a result of evaluation with ANP, although its significance is changeable in different industries, the most notable main criterion for the ocean container carrier selection model has been reliability, while

Table 1. Ocean container carrier selection criteria

Main Criteria	Sub Criteria
Transportation cost (TC)	TC1 Freight
	TC2 Freight validity period
	TC3 Freight quote time
	TC4 Clarity and detail of freight
	TC5 Credit facility
	TC6 Inland cost
	TC7 Demurrage and detention tariff
Transit time (TT)	TT1 Direct shipping to destination port
	TT2 Short transit time
	TT3 Transit time reliability
	TT4 On-time notification for the customer
	TT5 Detention free days
Service frequency (SF)	SF1 Service frequency reliability
	SF2 Short service frequency
Customer satisfaction (CS)	CS1 Employees’ availability
	CS2 The competence of operation employees
	CS3 The competence of sales employees
	CS4 Shipment trace
	CS5 The accuracy of documentation
	CS6 Effect of ship age on insurance premiums
	CS7 Accurate and detailed invoice
	CS8 Carrier service quality
	CS9 Willingness to solve customers’ problems
	CS10 Behavior against complaints and suggestions
Reliability (R)	R1 Carrier’s brand-name
	R2 Carrier’s reputation
	R3 Damage cargo record
	R4 Lost and stolen cargo records
Special facilities and equipment (SFE)	SFE1 Special equipment availability
	SFE2 Special equipment cost
	SFE3 Special cargo transport ability
Equipment availability (EA)	EA1 The ease of booking
	EA2 Condition of equipment
Operation performance (OP)	OP1 Information flow rate between carrier and port
	OP2 Operation flexibility in making declarations
	OP3 The condition of container (CC)
Service network (SN)	SN1 Geographical coverage (GC)
	SN2 Willingness to solve customers’ problems from international offices

Table 2. Interaction between criteria

Affecting Criterion	Affected Criterion
TT1	TT2
TT3	R2
TT1	TT3
TT5	TC7
SF1	R2
SF2	TT2
CS1	CS8
CS2	CS5
CS2	CS7
CS2	CS8
CS3	TC3
CS3	TC4
CS3	CS8
CS4	CS8
CS5	CS8
CS7	CS8
CS9	CS8
CS10	CS8
R3	R2
R4	R2
SFE1	SFE3
EA2	R3
OP3	R3
SN1	R1
SN2	CS9

Table 3. The priority of main criteria between three large shipper groups

Main Criteria	Textiles/Rank	White Goods/Rank	Chemicals/Rank
TC	0.140 (4)	0.170 (3)	0.172 (3)
TT	0.215 (2)	0.135 (4)	0.136 (4)
SF	0.062 (5)	0.051 (6)	0.059 (5)
CS	0.158 (3)	0.206 (2)	0.212 (2)
R	0.255 (1)	0.259 (1)	0.252 (1)
SFE	0.015 (9)	0.024 (9)	0.030 (9)
EA	0.060 (6)	0.070 (5)	0.053 (6)
OP	0.056 (7)	0.040 (8)	0.035 (8)
SN	0.036 (8)	0.045 (7)	0.051 (7)
CR	0.042	0.027	0.023

special facilities and equipment were the least important criterion. The order of the other seven main criteria was also different for the three large shipper groups. Transportation cost has been the third most important criterion for the white goods and chemical industries and the fourth for the textile industry. Consistent with the study, in many articles, the importance given to service-based criteria was found to be more important than freight rate [13,14,25,43].

The importance of global weights and rankings of the sub-criteria for three large shipper groups is as in Table 4. Although the weights of importance differ for each of the three major shipper groups, the most prominent criterion was “carrier’s reputation”, while the most unimportant sub-criterion was the special equipment cost”. While freight was the third most important sub-criterion for the white goods and chemical industries, it was only the fifth most significant criterion for the shipper group in the textile industry. Freight, which was the most important criterion in previous carrier selection studies [12,16,44], was replaced by criteria such as reliability, customer satisfaction, and transit time. Freight has been the second most important criterion for Canadian and American shippers (Maloni et al. [17]). Similar to the study in Kent and Stephen Parker’s [13] study, freight was one of the most considerable criteria, if not the most important criterion, for American shippers. Likewise, freight was not the most considerable criterion for North American and European large shippers in Brooks’s [20] study. Since shippers in the white good industry mostly prefer their own transporters for domestic transportation, they find this criterion less notable than the other two industries. Consistent with the study, “inland cost” was not considered important in many studies [16,17].

For the textile industry, the second most important sub-criterion is transit time reliability. Again, the short transit time was the fourth most significant criterion for this industry.

Table 4. Overall priority of the sub-criteria between three large shipper groups

Sub-Criteria	Textiles/Rank	White Goods/Rank	Chemicals/Rank
TC1	0.060 (1)	0.070 (1)	0.072 (1)
TC2	0.008 (6)	0.030 (2)	0.015 (4)
TC3	0.014 (4)	0.007 (6)	0.014 (7)
TC4	0.021 (2)	0.022 (4)	0.020 (3)
TC5	0.016 (3)	0.012 (5)	0.015 (5)
TC6	0.013 (5)	0.004 (7)	0.014 (6)
TC7	0.008 (7)	0.024 (3)	0.021 (2)
CR	0.014	0.052	0.005
TT1	0.034 (3)	0.019 (3)	0.017 (3)
TT2	0.071 (2)	0.043 (2)	0.050 (2)
TT3	0.092 (1)	0.056 (1)	0.051 (1)
TT4	0.012 (4)	0.006 (5)	0.007 (5)
TT5	0.006 (5)	0.010 (4)	0.011 (4)
CR	0.064	0.028	0.004
SF1	0.042 (1)	0.040 (1)	0.035 (1)
SF2	0.020 (2)	0.011 (2)	0.024 (2)
CR	0.000	0.000	0.000
CS1	0.006 (7)	0.008 (7)	0.012 (5)
CS2	0.014 (3)	0.015 (5)	0.013 (4)
CS3	0.013 (4)	0.011 (6)	0.010 (7)
CS4	0.004 (9)	0.006 (8)	0.005 (9)
CS5	0.012 (5)	0.020 (3)	0.021 (3)
CS6	0.002 (10)	0.002 (10)	0.003 (10)
CS7	0.012 (5)	0.016 (4)	0.012 (5)
CS8	0.076 (1)	0.102 (1)	0.105 (1)
CS9	0.015 (2)	0.022 (2)	0.023 (2)
CS10	0.004 (8)	0.005 (9)	0.008 (8)
CR	0.038	0.023	0.007
R1	0.021 (4)	0.028 (4)	0.039 (2)
R2	0.167 (1)	0.157 (1)	0.141 (1)
R3	0.036 (2)	0.034 (3)	0.038 (3)
R4	0.030 (3)	0.039 (2)	0.034 (4)
CR	0.026	0.021	0.001
SFE1	0.003 (2)	0.009 (2)	0.009 (2)
SFE2	0.003 (3)	0.004 (3)	0.005 (3)
SFE3	0.009 (1)	0.012 (1)	0.015 (1)
CR	0.011	0.004	0.028
EA1	0.044 (1)	0.054 (1)	0.036 (1)
EA2	0.016 (2)	0.016 (2)	0.017 (2)
CR	0.000	0.000	0.000
OP1	0.010 (2)	0.013 (2)	0.007 (3)
OP2	0.009 (3)	0.012 (3)	0.008 (2)
OP3	0.037 (1)	0.015 (1)	0.019 (1)
CR	0.001	0.013	0.000
SN1	0.027 (1)	0.035 (1)	0.038 (1)
SN2	0.009 (2)	0.010 (2)	0.013 (2)
CR	0.000	0.000	0.000

Shippers in textile industry prefer container carriers with short transit times as an alternative to road and air transport modes. Although the weights of importance differ in the white goods and chemical industries, the fourth and fifth most important sub-criteria are transit time reliability and short transit time, respectively. Consistent with the study, American shippers [17] and Taiwanese shippers [14] found transit time reliability more remarkable than short transit time. Shipper groups did not see all the on-time notification for the customer criteria as effective. Service frequency reliability was a notable criterion in each of the three shipper groups. Short service frequency, which impacted transit time, was not seen as notable by the three shipper groups. This criterion was not remarkable for American shippers [17] and Taiwanese shippers [14] parallel to the study.

The impact of carrier service quality is the second position for the white goods and chemical industries and the third position for the textile industry. This criterion has been affected by criteria such as the availability of employees the competence of operations or sales employees and the accuracy of documentation. Large shippers stated that they had no problems with employee availability. Shippers and freight forwarders under a certain capacity have problems in this regard. Unlike the study, Kannan et al. [16] considered this criterion moderately significant. The three shipper groups that had no problem reaching the carrier also did not see the shipment tracking criterion as effective. Contrary to the study, Kent and Stephen Parker [13] found this criterion moderately important. The criteria of competence of operation and sales employees were found to be of moderate importance by three groups. Taiwanese shippers, especially the knowledge of sales personnel, are considered to be important criteria [14]. However, competence employees were among the top five most important criteria for Canadian and American shippers [17]. Influenced by criteria such as transit time reliability, service frequency reliability, damage cargo record, and lost and stolen cargo record, the carrier's reputation has been the most prominent criterion for each of the three shipper groups. Similarly, damage cargo records and lost and stolen cargo records were among the important criteria. This criterion was of moderate significance to American shippers in the study of Kent and Stephen Parker [13] and Maloni et al. [17]. One of the striking findings of the study is that special transportation facilities were determined as one of the least priority criteria since three shipper groups mostly carried out their transportation in standard containers. Consistent with this study, it was among the less important criteria in the carrier selection problem for American and Indian shippers [13,16]. Although the ease of booking criterion is not among the top five most important criteria for all

three shipper groups, it has remarkable significance. It was considered more essential, especially for the white good industry, which has a much larger cargo capacity than the other two industries. In the studies of Maloni et al. [17], this criterion was among the five most important criteria. For the textile industry, the condition of the container was more effective than in the other two industries. The container must be cleaned so that the sent textile products are not damaged. Maloni et al. [17], like the white goods and chemical industries, gave moderate importance to this criterion. Another notable finding is that the geographical coverage is remarkable for all three groups. This finding is supported by studies by Lu [14].

Table 5 shows the importance weights of the four alternative ocean container carriers. The results of this study indicated that carrier B was the most preferred company between Türkiye and the USA for container transport in maritime exportation, followed by carriers A, C, and D, respectively.

Table 5. Ocean container carrier priority weight between three large shipper groups

Ocean Container Carriers	Textiles/ Rank	White Goods/ Rank	Chemicals/ Rank
Carrier A	0.298 (2)	0.278 (2)	0.284 (2)
Carrier B	0.380 (1)	0.375 (1)	0.369 (1)
Carrier C	0.178 (3)	0.192 (3)	0.187 (3)
Carrier D	0.145 (4)	0.156 (4)	0.160 (4)

6. Conclusion

This study enriches the literature on ocean container carrier selection and provide comprehensive research on three large shipper groups. The study contributes to carrier selection literature by examining the textile industry, white goods industry, and chemicals industry, which all have a high export capacity in Türkiye. Many criteria that influence decision making interact with each other in carrier selection problems, and it is necessary to consider these interactions to make the best decision. To solve this problem, ANP method is extremely suitable. This study also brings innovation to the literature by using ANP, which permits criterion interaction in ocean container carrier selection studies for the first time. The results of ANP demonstrated that the range of importance given to the criteria among the three large shipper groups is not the same. Although the relative priority weights were different for each of the three industries, while the most important main criterion was reliability, the most important subcriterion was carrier reputation. The carrier reputation was the most significant subcriterion because it was influenced by important subcriterion such as transit time reliability, service frequency reliability, damaged cargo record, and lost and stolen cargo record. Unlike the textile

industry, the first four sub-criteria in the white goods and chemical industries are in the same rank. In the textile industry, transit time reliability and short transit time have been more important than in the other two industries. After the carrier's reputation and carrier service quality, freight is the third most important criterion for the white goods and chemistry industries, while it has been the fifth criterion in the textile industry. Such findings are critical to understanding ocean container carriers from supply chain expectations, as they can provide better service to companies in different industries and increase customer satisfaction and market share.

One of the remarkable results of the study is that none of the criteria such as special equipment availability, shipment tracing, and direct shipping to destination port, which require high investment costs by the carriers, are included in the top ten criteria and not considered significant by large shippers. In line with these results, carriers should use their resources to ensure a high level of satisfaction for the criteria of the highest importance.

In future studies, hybrid methods can be utilized by integrating different MCDM methods with ANP. In addition, the increasing importance of the environment in future research makes it necessary to include more environmental sustainability criteria in ocean carrier selection criteria. Most of the carrier selection literature has been done on container transportation. In the future, studies can be conducted on the selection of carriers for other maritime transportation segments such as tanker or dry cargo transportation.

Peer-review: Externally and internally peer-reviewed.

Authorship Contributions

Concept design: A. Ergin, G. Alkan, Data Collection or Processing: A. Ergin, Analysis or Interpretation: A. Ergin, Literature Review: A. Ergin, Writing, Reviewing and Editing: A. Ergin.

Funding: This study was supported by the project number 6261 of the İstanbul University Scientific Research Projects Executive Secretariat.

References

- [1] H. Yasa, M. F. Ergin, A. Ergin, and G. Alkan, "Importance of inert gases for chemical transportation," *Proceedings Book*, pp. 825, 2016.
- [2] A. Ergin, and M. F. Ergin, "The role of antifouling coating in the marine industry," *Research & Reviews in Engineering*, vol. 3, pp. 54-75, 2021.
- [3] UNCTAD, "Review of Maritime Transport 2021," United Nations Conference on Trade and Development, 2021.
- [4] D. Choudhary, and R. Shankar, "A goal programming model for joint decision making of inventory lot-size, supplier selection and carrier selection," *Computers & Industrial Engineering*, vol. 71, pp. 1-9, May 2014.
- [5] E. J. Bardi, "Carrier selection from one mode," *Transportation Journal*, vol. 13, pp. 23-29, 1973.
- [6] M. A. McGinnis, "Segmenting freight markets," *Transportation Journal*, vol. 18, pp. 58-68, 1978.
- [7] P. K. Bagchi, "Carrier selection: the analytic hierarchy process," *Logistics and Transportation Review*, vol. 25, pp. 63, Mar 1989.
- [8] M. A. McGinnis, "The relative importance of cost and service in freight transportation choice: before and after deregulation," *Transportation Journal*, vol. 30, pp. 12-19, 1990.
- [9] B. Davis-Sramek, J. L. Robinson, J. L. Darby, and R. W. Thomas, "Exploring the differential roles of environmental and social sustainability in carrier selection decisions," *International Journal of Production Economics*, vol. 227, pp. 1-9, Sep 2020.
- [10] P. R. Murphy, and P. K. Hall, "The relative importance of cost and service in freight transportation choice before and after deregulation: an update," *Transportation Journal*, vol. 35, pp. 30-38, 1995.
- [11] F. M. Collison, "Market segments for marine liner service," *Transportation Journal*, vol. 24, pp. 40-54, 1984.
- [12] M. R. Brooks, "Ocean carrier selection criteria in a new environment". *Centre for International Business Studies, Dalhousie University*, vol 26. pp. 339, Dec 1990.
- [13] J. L. Kent, and R. Stephen Parker, "International containership carrier selection criteria: shippers/carriers differences," *International Journal of Physical Distribution & Logistics Management*, vol. 29, pp. 398-408, Aug 1999.
- [14] C.-S. Lu, "An evaluation of service attributes in a partnering relationship between maritime firms and shippers in Taiwan," *Transportation Journal*, vol. 42, pp. 5-16, 2003.
- [15] P. C. Wong, H. Yan, and C. Bamford, "Evaluation of factors for carrier selection in the China Pearl River delta," *Maritime Policy & Management*, vol. 35, pp. 27-52, Feb 2008.
- [16] V. Kannan, S. K. Bose, and N. G. Kannan, "An evaluation of ocean container carrier selection criteria: an Indian shipper's perspective," *Management Research Review*, vol. 34, pp. 754-772, June 2011.
- [17] M. J. Maloni, D. M. Gligor, and I. N. Lagoudis, "Linking ocean container carrier capabilities to shipper-carrier relationships: a case study," *Maritime Policy & Management*, vol. 43, pp. 959-975, Apr 2016.
- [18] A. Ergin, "A fuzzy AHP approach to evaluating differences between ocean container carriers and their customers," *International Journal of Shipping and Transport Logistics*, vol. 13, pp. 402-421, Mar 2021.
- [19] A. Ergin, M. J. Feizollahi, and C. Kutlu, "Ocean container carrier selection using fuzzy TOPSIS method: customers' perspective," *Marine Technology Society Journal*, vol. 56, pp. 59-71, Jan-Feb 2022.
- [20] M. R. Brooks, "Understanding the ocean container market—a seven country study [1]," *Journal of the History of Economic Thought*, vol. 22, pp. 39-49, Jul 1995.
- [21] S. Jharkharia, and R. Shankar, "Selection of logistics service provider: An analytic network process (ANP) approach," *Omega*, vol. 35, pp. 274-289, June 2007.

- [22] E. Aksakal, and M. Dağdeviren, "ANP ve DEMATEL yöntemleri ile personel seçimi probleminde bütünlük bir yaklaşım," *Gazi Üniversitesi Mühendislik Mimarlık Fakültesi Dergisi*, vol. 25, pp. 905-913, 2010.
- [23] Z. Ayağ, and R. G. Özdemir, "An intelligent approach to ERP software selection through fuzzy ANP," *International Journal of Production Research*, vol. 45, pp. 2169-2194, June 2007.
- [24] B. C. Ervural, S. Zaim, O. F. Demirel, Z. Aydin, and D. Delen, "An ANP and fuzzy TOPSIS-based SWOT analysis for Turkey's energy planning," *Renewable and Sustainable Energy Reviews*, vol. 82, pp. 1538-1550, Feb 2018.
- [25] P. D. Fanam, and L. Ackerly, "Evaluating ocean carrier selection criteria: perspectives of Tasmanian shippers," *Journal of Shipping and Trade*, vol. 4, pp. 1-16, July 2019.
- [26] C.-L. Hsu, and T.-C. Ho, "Evaluating Key Factors of Container Shipping Lines from the Perspective of High-Tech Industry Shippers," *Journal of Marine Science and Technology*, vol. 29, pp. 3, 2021.
- [27] E. D'agostini, S. Jo, H.-S. Nam, and Y. S. Kim, "Q-method and its application in clustering Hong Kong shippers' selection criteria of ocean carriers," *Research in Transportation Business & Management*, vol. 44, pp. 100785, Sep 2022.
- [28] J. N. Pearson, and J. Semeijn, "Service priorities in small and large firms engaged in international logistics," *International Journal of Physical Distribution & Logistics Management*, vol. 29, pp. 181-192, Apr 1999.
- [29] C.-S. Lu, "Market segment evaluation and international distribution centers," *Transportation Research Part E: Logistics and Transportation Review*, vol. 39, pp. 49-60, Jan 2003.
- [30] I.-S. Chen, "A combined MCDM model based on DEMATEL and ANP for the selection of airline service quality improvement criteria: A study based on the Taiwanese airline industry," *Journal of Air Transport Management*, vol. 57, pp. 7-18, Oct 2016.
- [31] S. Onut, U. R. Tuzkaya, and E. Torun, "Selecting container port via a fuzzy ANP-based approach: A case study in the Marmara Region, Turkey," *Transport Policy*, vol. 18, pp. 182-193, Jan 2011.
- [32] Y. Wind, and T. L. Saaty, "Marketing applications of the analytic hierarchy process," *Management Science*, vol. 26, pp. 641-658, July 1980.
- [33] M. Dağdeviren, and E. Eraslan, "Priority determination in strategic energy policies in Turkey using analytic network process (ANP) with group decision making," *International Journal of Energy Research*, vol. 32, pp. 1047-1057, 2008.
- [34] T. L. Saaty, "Decision making with dependence and feedback: The analytic network process," *RWS Publ*, 1996.
- [35] N. Alptekin, "Analitik ağ süreci yaklaşımı ile Türkiye'de beyaz eşya sektörünün pazar payı tahmini," *Dogus University Journal*, vol 11. pp. 18-27, 2010.
- [36] E. E. Karsak, S. Sozer, and S. E. Alptekin, "Product planning in quality function deployment using a combined analytic network process and goal programming approach," *Computers & Industrial Engineering*, vol. 44, pp. 171-190, Jan 2003.
- [37] A. Ergin, "Container carrier firm selection in the supply chain management and its application in Turkey," *Phd, Istanbul University*, 2011.
- [38] V. Kannan, S. Bose, and N. Kannan, "Improving the service quality of ocean container carriers: an Indian case study," *Benchmarking: An International Journal*, vol. 19, pp. 709-729, Oct 2012.
- [39] S. Gailus, and C. Jahn, "Ocean container carrier selection in north west-ern europe-qualitative empirical research to-wards a discrete choice model," in *Pioneering Solutions in Supply Chain Performance Management: Concepts, Technologies and Applications*, pp. 69-88, 2013.
- [40] C.-H. Wen, and W.-W. Lin, "Customer segmentation of freight forwarders and impacts on the competitive positioning of ocean carriers in the Taiwan-southern China trade lane," *Maritime Policy & Management*, vol. 43, pp. 420-435, Nov 2016.
- [41] T.-C. Ho, R.-H. Chiu, C.-C. Chung, and H.-S. Lee, "Key influence factors for ocean freight forwarders selecting container shipping lines using the revised dematel approach," *Journal of Marine Science and Technology*, vol. 25, pp. 299-310, 2017.
- [42] P. D. Fanam, H.-O. Nguyen, and S. Cahoon, "An empirical analysis of the critical selection criteria of liner operators: the perspective of freight forwarders," *International Journal of Shipping and Transport Logistics*, vol. 10, pp. 567-586, Oct 2018.
- [43] G. D'este, and S. Meyrick, "Carrier selection in a RO/RO ferry trade Part 1. Decision factors and attitudes," *Maritime Policy & Management*, vol. 19, pp. 115-126, July 1992.
- [44] V. Kannan, "Benchmarking the service quality of ocean container carriers using AHP," *Benchmarking: An International Journal*, vol. 17, pp. 637-656, Aug 2010.

Multi-Criteria Analysis of Capesize Bulk Carrier Design Optimization Model

© Cansu Aksu¹, © Ramazan Yaman²

¹Zonguldak Bülent Ecevit University, Department of Business Administration, Zonguldak, Türkiye

²Istanbul Atlas University Faculty of Engineering and Natural Sciences, Department of Industrial Engineering, İstanbul, Türkiye

Abstract

In engineering problems, the concepts of design and optimization are two basic topics that are related to each other. The problem owner should prioritize the design or optimization on each other. In this regard, two different ways can be followed in engineering problems: firstly designing and then optimizing or using optimized parameters in the design process. In this study, the basic design parameters of a capesize bulk carrier for a specific purpose were created and exemplified on a model. The prototype development problem is handled as a multi-criteria optimization problem by creating appropriate and pareto optimal solutions. Parameter Space Investigation method was used to solve this optimization problem, and this method was applied in a program called Multi-criteria Optimization Vector Identification. As a result of the study, the design parameters of the capesize bulk carrier sample were created and the objective function criteria were obtained better than the prototype and the value in the literature.

Keywords: Ship design parameters, Capesize bulk carrier, Parameter space investigation, Multi-criteria optimization vector identification


1. Introduction

Maritime transportation has played a significant role in the advancement of societies throughout history, facilitating increased commercial activities and contributing to their wealth and power [1]. In recent years, the importance of marine transport in the logistics sector has steadily increased. The cost is cheaper, many materials can be transferred at a party, and delivery conditions are more appropriate are reasons for growing demand in this sector. Increasing competition with globalization and the rapid development of international trade as a result of this have made maritime transportation an important mode of transportation that directly affects the foreign trade level and economic competitiveness of countries [2].

The Coronavirus disease-2019 (COVID-19) pandemic experienced recently has also revealed the importance of logistics and supply chain for countries. Although faced with applications such as restrictions and quarantines during the COVID-19 pandemic, maritime transport was relatively

less affected by the pandemic process among all modes of transport. The “Review of Maritime Transport 2021” report prepared by the United Nations Conference on Trade and Development points out that although the coronavirus pandemic disrupted maritime transport, this decline was not as dramatic as expected. When maritime transportation was interrupted in the first half of 2020, it started to recover in the second half of the year and maritime trade increased by 4.3% in 2021 [3]. Ships provide more than 80% of world trade, so disruptions in ports and shipping routes mean that food, energy, medicine and other essentials do not reach those in need [4]. For this reason, marine transportation and platform needs are expected to grow.

As of January 1, 2022, the countries with the most ships in terms of dead weight tonnage and commercial value were Greece, China, and Japan. The maritime transport supply continues to be dominated by three countries (China, the Republic of Korea and Japan), which together hold 94 percent of the market in 2022 [5]. When examined in Türkiye

 **Address for Correspondence:** Cansu Aksu, Department of Business Administration, Zonguldak Bülent Ecevit University, Zonguldak, Türkiye
E-mail: cansuaksu@beun.edu.tr
ORCID ID: orcid.org/0000-0001-5717-2821

Received: 30.03.2023
Last Revision Received: 13.07.2023
Accepted: 14.07.2023

To cite this article: C. Aksu, and R. Yaman. “Multi-Criteria Analysis of Capesize Bulk Carrier Design Optimization Model.” *Journal of ETA Maritime Science*, vol. 11(3), pp. 168-185, 2023.

©Copyright 2023 by the Journal of ETA Maritime Science published by UCTEA Chamber of Marine Engineers

using all modes of transport in foreign trade activities, the largest share in both imports and exports in the 10-year period covering the years 2011-2021 belongs to maritime transport, based on the value of the goods transported, as seen in Table 1.

The type and characteristics of the ships that make up the merchant fleet, which is the most important element in maritime transport, are of great importance. As can be seen in Table 2, when the DWT and number of ships of 150 GT and above in the Turkish merchant marine fleet are examined in the last 5 years, it is seen that 42 bulk carriers have been owned for 2022 and bulk carriers constitute 25% of the total deadweight [6].

Bulk carriers are used to transport goods (scrap, grain, logs, wood products, sand, etc.) iron ore, coal, and grain are the main cargoes of international bulk freight, as they are transported in large quantities. There are different types and capacities of ships in bulk cargo transportation.

Generally, ships up to 10,000 DWT are known as small bulk carriers, while ships with larger payloads are known by some special names. In this context, Handysize (10,000-30,000 DWT), Handymax (30,000-50,000 DWT), Panamax (50,000-92,000 DWT), Post Panamax (92,000-120,000 DWT), Capesize (120,000-182,000 DWT) abbreviated the names of ships larger than 200,000 DWT as VLBC (Very Large Bulk Carrier) [7]. The design of ships and marine vehicles in general can be counted among the most complex engineering problems [8].

“Ship Design Optimization” is frequently used by designers and shipyards, and it causes different interpretations in the relevant parts of the sector, and its boundaries must be defined [9]. The use of optimization models in ship design dates back to the 1960s. Ship design problems have various conflicting objective functions. Both conventional methods are used in solving multi-criteria problems, and current multi-criteria approaches could be seen.

Table 1. Percentage shares of transportation types in import and export by years (on a value basis)

		Years										
		2011	2012	2013	2014	2015	2016	2017	2018	2019	2020	2021
Road Transportation	Import	21.97	20.26	18.69	18.23	19.09	19.16	18.01	17.88	20.56	21.14	20.79
	Export	37.6	33.35	35.66	35.29	32.7	31.62	29.59	28	30.36	31.61	30.85
Airway Transportation	Import	10.62	12.23	15.21	12.07	11.11	12.83	16.33	14.4	16.17	19.82	11.08
	Export	6.42	14.4	8.61	9.01	12.1	12.54	10.98	8.25	8.28	7.58	8.4
Maritime Transportation	Import	65.85	66.31	65.28	69.11	69.14	67.22	65.1	67.09	62.47	57.96	66.91
	Export	55.05	51.57	55.1	55.11	54.64	55.39	58.99	63.31	60.82	60.04	60.01
Railway Transportation	Import	1.57	1.21	0.83	0.59	0.65	0.8	0.56	0.62	0.8	1.08	1.23
	Export	0.93	0.67	0.64	0.59	0.56	0.45	0.44	0.44	0.54	0.77	0.74

Source: [3]

Table 2. DWT and number development of the Turkish merchant fleet (vessels of 150 GT and above), 2018-2022

The Type of Ship	2018		2019		2020		2021		2022	
	Number	DWT	Number	DWT	Number	DWT	Number	DWT	Number	DWT
Dry Bulk Carriers	323	1,245,588	298	1,148,389	278	10,71119	251	945,737	196	807,374
Bulk Carriers	64	2,636,897	56	2,225,010	46	17,14108	45	1,692,176	42	1,769,522
Container Ships	70	1,349,228	57	1,047,502	56	1,028,620	53	998,316	59	1,097,971
Tankers	184	2,023,011	178	2,085,755	181	2,188,978	185	2,179,130	190	2,452,630
Passenger Ships	308	89,923	311	90,924	308	86,697	306	81,458	445	128,165
Services Ships	151	101,339	151	110,122	154	178,484	161	194,784	164	361,413
Tugs	152	2,776	165	2,598	173	2,710	181	2,710	175	18,836
Sea Vessels	258	34,715	272	38,483	286	38,731	297	48,143	314	352,775
Fishing Ships	293	8,358	314	8,503	337	8,542	375	8,586	401	38,932
Sport and Entertainment Boats	222	3,297	222	3,223	234	3,300	246	3,300	116	3,983
Total	2.025	7,495,133	2024	6,760,509	2053	6,321,289	2100	6,154,340	2102	7,031,603

Source: [6]

In prototype development problems, optimization is performed by considering multiple criteria [10]. To solve the prototype development problem, operational development of the prototype requires two phases [11].

Statnikov et al. [10] indicated that the first step is to determine the mathematical model of the object and its parameters based on different tests. To this end, it would be advantageous to solve the identification problem based on certain adequacy criteria (proximity). In the second step, an expert formulates and resolves the multi-criteria optimization problem using the mathematical model and the performance criteria determined in the first step. Depending on the optimization results, the prototype is improved and object tests are repeated. It is repeated until an expert decides to stop the operational development process.

The Parameter Space Investigation (PSI) method was used in multi-criteria analysis in this study, which constructed feasible and Pareto optimal solution sets while also improving the prototype's key performance criteria by altering the constraints of design variables, functional relations and criteria. The PSI method is applied with the Multi-criteria Optimization and Vector Identification (MOVI) program.

Multi-criteria analysis of a ship design model using the PSI technique was first performed at St. Petersburg State Naval Technical University by M. Berezanskii and Y. N. Semenov. A prototype ship (UT-704) was intended to improve performance benchmarks [12].

In this study, the PSI method which has been widely used for the solution of optimization problems related to manufacturing engineering, machine design, and mechanisms and it has been known for more than a quarter of a century, was employed [13].

In order to examine the surface texture of the Ti6Al4V titanium alloy following final turning under both dry and wet cooling conditions, Leksycki and Feldshtein [14] used the PSI method. They conducted research tests with the fewest possible test points. The test points were set sequentially in fixed positions. The steps involved positioning the points in a multidimensional space with their projection points equally spaced apart from one another on the X_1 and X_2 axes, respectively.

The study of Maruda et al. [15] described three cooling techniques for AISI-1045 steel turning: dry machining, minimum amount of cooling (MQC), and MQC with EP/AW (MQC + EP/AW) additives. The PSI method was applied to an increasing number of variables (variation of shear and emulsion mist generation parameters). A Kistler dynamometer type 9129AA was used to measure the shear

force, and an MPS7 network parameter meter was used to measure the power consumption.

A novel approach for the development of force transducers based on strain gauges was put forth by Gavrilencov et al. [16]. The approach depended on multi-criteria optimization techniques and PSI method.

Three elements of total cutting force and changes in chip shape when finishing turning 17-417-4 4 PH (precipitation hardening) stainless steel were analyzed by Leksycki et al. [17]. The cutting speed was 220 m/min, the depth of cut ranged from 0.2 to 1.2 mm, and the variable feed pattern ranged from 0.05 to 0.4 mm per rev. Minimum amount of lubrication was used during the studies which were conducted in both dry and wet cooling conditions. The PSI method was used to conduct this research.

Pagano et al. [18] examined the mechanism that causes the propagation of twist and sausage modes in the solar corona following the collision of counter-propagating flows and how the characteristics of the flows affect the characteristics of the waves produced. They used the PSI method to explain how the collision of coronal flows results in the generation of magnetohydrodynamic waves.

According to Maruda et al. [19], the condition of the machined surface of 1.4310 stainless steel after turning was examined in relation to the anti-wear additive Crodafos EHA-LQ-(MH) added to emulsion mist. In the tests conducted for the formation of emulsion fog, the emulsion's mass flow, the air's volumetric flow, the nozzle's distance from the shear zone range, and the PSI method were all used.

The PSI method was applied for the design of the L1 flight control system installed on the dynamically scaled GTM AirSTAR aircraft powered by two turbines, and the preliminary results were presented in Xargay and Hovakimyan's [20] study.

Anil [21] investigated marine design engineering problems with PSI method. MIT Functional ship design optimization was conducted and pareto optimal solutions of design variables and criteria values were obtained.

In this study, the PSI method studies of Statnikov et al. [10-12] PSI studies, the study of Anil [21] and optimization model of Cudina [22,23] and Zanic and Cudina [24] are taken as the main references for the optimal design of the model ship.

2. Ship Design Optimization

2.1. Motivation of the Study

The main purpose of ship design is to find the most economical alternative among the alternatives that provide the given design conditions. For this, many design calculations and controls need to be implemented for several alternative designs.

Brown and Salcedo [25] point out that there are three components necessary for a systematic approach to ship design, and these three components are;

- The creation of an effective and efficient design space, the objective function of containing well-defined measurable properties, and the use of an effective format for the expression of the design space.
- Maximizing effectiveness.
- Minimizing cost and risk are different characteristics and require different measurement methods.

These three different features cannot be combined into one function. It should be included in problem solving for simultaneous decision making and comparison. The effectiveness of ship designs can be analyzed using wargaming or other complex methods [25]. However, this approach is of little use when evaluating designs in a structured design space. The non-dominated solution represents a feasible solution in which the problem and the constraints are defined and there is only one best solution in the objective function. For example, in Figure 1 there is a problem solution in which cost is minimized and efficiency is maximized. Decision-making authorities will determine preferred concept designs as one of the non-dominated solutions to strike the balance between cost and effectiveness. Although ship design optimization is not new, it is a concept that contains several computational difficulties. The ship design space is non-linear, discrete and bounded by various constraints and thresholds. It is estimated that 80% of a ship's procurement cost remains unused during the design phase. Therefore, making critical design decisions is unable to be superficial. A methodology that will meet user needs, respect critical performance values, and integrate multiple factors into the objective function should be followed [25].

Ship designs were carried out using the basic ship design and the Evans-Buxton-Andrews spiral until the 1990s. In this spiral, it is assumed that the design process will

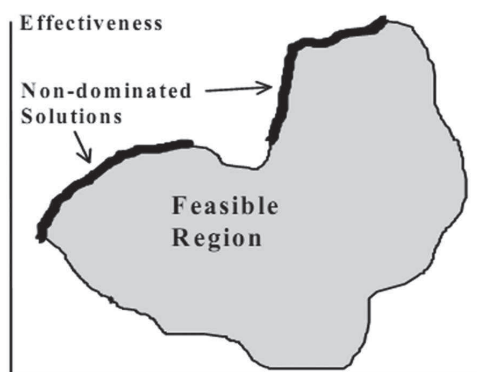


Figure 1. Cost-efficiency design space [25]

be sequential, and the possibility of inclusion of life cycle issues is limited. Mistree et al. [26] proposed a new process for increasing ship design efficiency and effectiveness. This process emphasizes systems philosophy and simultaneous engineering in terms of the life cycle.

Mistree et al. [26] classify design processes in two groups as descriptive and predictive. Predictive methods include three main activities as analysis, synthesis, and evaluation and show a systematic approach. In this context, the Pahl and Bitz method in the literature is a systematic design approach developed in Germany. In this method, which is described as a predictive approach, product design is divided into functional stages. Thanks to the modules that can be designed independently, the design activity is simplified. On the other hand, design studies in the form of independent modules may cause some problems in the integration phase. It is possible to define the method in seven stages. In the first stage, the evaluation criteria are listed and in the second stage, these criteria are weighted. Then, operational measurement values are defined for the criteria, and then numerical values are assigned to each criterion. After finding the value of each criterion by multiplying the weights with the numerical values, the total value is reached. Alternatives are evaluated, with the highest value being the most optimal result. In the final stage, the results are checked to eliminate uncertainties and ensure consistency. On the other hand, descriptive approaches work under the leadership of a designer, and a solution is sought. The approach includes four activities as problem analysis, conceptual design, final design, and detail design. In addition, concurrent engineering design is an approach that considers the product life cycle from the conceptual design stage to inventory removal. It is an approach that focuses on the demands and priorities of the concurrent engineering needs authority, believes that quality occurs as a result of process improvement, and has the philosophy that process improvement is the unending responsibility of the entire enterprise. Although the concurrent design approach has a wide variety of application forms, three activities are generically valid in all of them. These; use of multifunctional teams for design, production and support processes; including computer-aided programs, and the search for solutions with various analytical methods to optimize product design, production and support processes [26].

Mistree et al. [26] state that Evans' spiral model forms the basis of ship design activities. Brinati et al. [27] also state that the most used one among the different design models is the one developed by Evans.

As can be seen in Figure 2, transactions take place in sequential order [28]. It is also a labor-intensive and

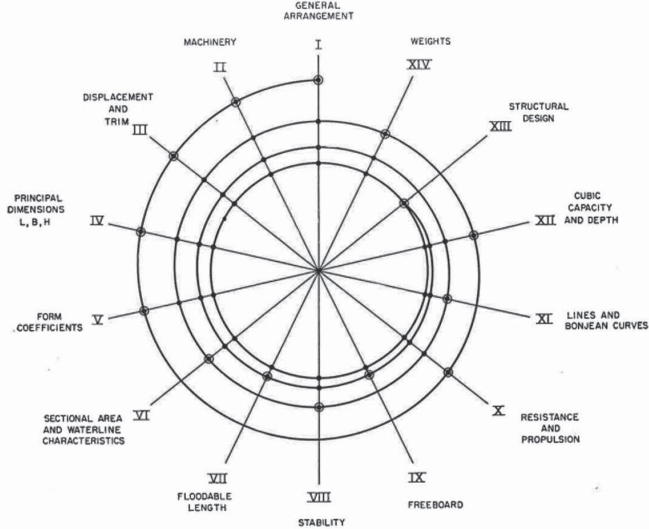


Figure 2. Evans spiral model [27]

expensive system. It is far from model information systems, which was used extensively in ship design in the past and has increased detail [26,27]. Although it is still used today, information systems are used for the solution. Optimization models are also used. According to Mistree et al. [26], optimization models shorten the calculations, the required amount of design variables and constraints can be included in the solution, and the optimal solution defined in the objective function can be found automatically. While single-criteria decision-making models were used in the past, multi-criteria decision-making models have been used. For example, an optimization model was developed by sequential linear programming by Mistree et al. [26]. Thus, simultaneous engineering applications took place in ship design optimization applications, similar to Figure 3.

As stated by Shin and Han [29], in ship design optimization models, designers' own variable spaces are formed and solution sets are created using very different programs. For example, while researchers were working with a computer-aided design program, McGookin et al. [30] used a genetic algorithm for cruise control system optimization. On the other hand, Diez and Peri [31] applied the stochastic study to the ship design, thus reflecting the differences in expected value and standard deviation to the objective function, and based on the worst-case scenario conditions for the constraints. Yaakob et al. [32] remodeled the durability of fishing boats to reduce their cost, achieving 12% fuel savings with a slight modification. Papanikolaou [33] sought a solution for ship design optimization by applying system approach.

Brinati et al. [27] stated that weight calculations such as structure, the machine group, and exterior design excluding cargo could be made with regression. Design models for

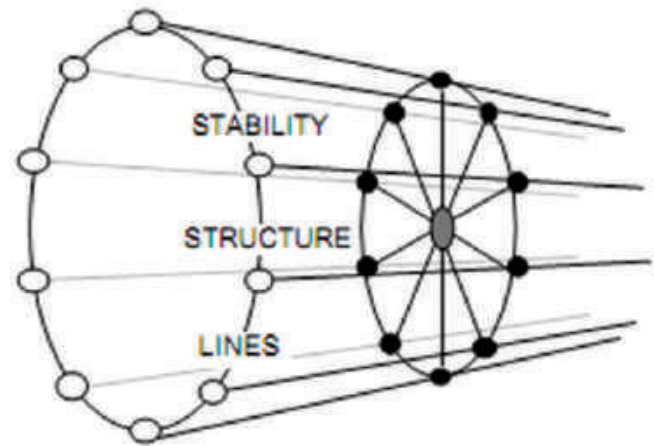


Figure 3. Simultaneous design in a spiral model [26]

other criteria were also presented by the researchers. Solutions of multi-objective combinatorial problems were examined by Ölçer [34] and it was indicated to use solution methods reached by evolutionary calculations. Ray et al. [35] developed a multi-criteria decision-making model and a ship design optimization model. Researchers using container design combined a general optimization tool, a decision-making model, and many ship architectural prediction models in this model. Structural design modeling requires the application of many more factors together than other modeling applications. For example, while range, speed, mobility, and control efficiency are important for missile capacity, speed, surface and underwater forms, dimensions, stabilization, and load status gain importance in ships [36]. Tanıl [36] derived an algorithm run in the MATLAB program to be used for missile exterior design. Thus, it is aimed to obtain the optimum configuration considering the parameters entered by the user during the conceptual design phase. Türkmen and Turan [37] used the multi-criteria decision-making methodology to improve the passenger ship structural design and achieved gains in terms of safety and economy. Arslan and Gürel [38] tried to find an optimal solution by applying fuzzy logic methodology. Along with these, a solution can be found using a genetic algorithm [27].

Özdemir [9] states that the subject of ship design optimization, which is frequently used by designers and shipyards in recent years, is perceived as a subject that causes different interpretations in the relevant parts of the sector and whose boundaries need to be defined. The use of optimization models in ship designs dates back to the 1960s.

Ship design optimization problems have several conflicting objective functions. In the solution of multi-objective problems, classical methods can be used in the light of

assumptions and current multi-criteria approaches. For example, the use of the analytic hierarchy process to combine the efficiency function for evaluating designs.

Lee and Lee [39] emphasize that designers can only design based on their experience and available data. The limited data available at the preliminary design stage further highlight the designer's freedom of knowledge. Lee and Lee [39], who refer to a wide variety of designs, especially in line with the wishes of the ship owners, mention the necessity of making comparisons with similar ships and using the values of their main characteristics at the conceptual design stage.

Tahara et al. [40] state that hull design is a multi-criteria decision-making problem. For example, reducing resistance, eliminating noise, minimal wave height, and increasing certain movements can be the goal of the design process. In addition, designers should consider values related to engine power or maintenance costs. Increasing some values may prevent others from reaching the desired values. Since it is generally impossible to create a perfect design in every respect, the main task of the designer is to provide a balanced integrity among the different functions expected from the ship [41]. Therefore, a multi-objective optimization approach is appropriate.

Genç and Özkök [42] focus on the sea trial stage in the ship production, which is the last phase of tests performed on ships before their delivery. Sea trial is optimized by planning and simulating the tests using computer programs. The objective is to suggest improvements that can shorten the duration of the sea trial, reduce costs, and expedite ship delivery. The results show that the new simulation model reduces the testing time by 2.75 hours (9.76%) compared to the initial model, indicating a more efficient sea trial process. The authors conclude that using simulation programs such as SIMulation Modeling framework based on Intelligent Objects-SIMIO can help shipyards optimize their production processes, reduce costs, and improve on-time delivery performance.

A comprehensive examination of the literature reveals that the establishment of an effective design space is crucial in ship design. This entails creating a framework that allows for efficient exploration and evaluation of design alternatives for different ship types and sizes. Additionally, defining measurable objective functions with specific attributes is essential for accurate assessment and comparison of design solutions. By incorporating quantitative metrics such as efficiency, cost, and risk, designers can make informed decisions and optimize their designs.

2.2. PSI Method

It is necessary to mathematically formulate multi-criteria optimization problems to describe the "Parameter Space

Investigation-PSI" method. In this method, the system relies on design variables. The vector of design variables is as follows [12,21].

$$\alpha = \alpha_1, \dots, \alpha_r \quad (1)$$

The Capesize bulk carrier optimization model's design variables are length between perpendicular (L_{pp}), breadth (B), draft (d_s), block coefficient (C_b), ship speed (v_{tr}), cargo volume (V_{car}), and the machine database number (I_{mei}). Design variable vector;

$$\alpha = (L_{pp}, B, d_s, C_b, v_{tr}, V_{car}, I_{mei}) \quad (2)$$

Every design variable has constraints. These constraints are;

$$\alpha_j^* \leq \alpha_j \leq \alpha_j^{**} \quad j = 1, \dots, r \quad (3)$$

is displayed as α_j^* and α_j^{**} shows the lower and upper limit values of variable α [12,21].

When the model consists of two design variables, $\alpha = \alpha_1, \alpha_2$ design variable constraints $\alpha_1^* \leq \alpha_1 \leq \alpha_1^{**}$ and $\alpha_2^* \leq \alpha_2 \leq \alpha_2^{**}$ is expressed [12,21].

Functional relationships that are functions of the design variables exist for every design optimization problem. These functional constraints are shown as;

$$C_l^* \leq f_l(\alpha) \leq C_l^{**}, \quad l = 1, \dots, t \quad (4)$$

is displayed as $f_l(\alpha)$ functional relations, C_l^* and C_l^{**} consist of lower and upper boundaries of this functional relations [12,21].

The design model has characteristics that should be minimized or optimized in performance criteria. The criteria restrictions determine the performance criteria. The criteria constraints can be written as;

$$\Phi_v(\alpha) \leq \Phi_v^{**}, \quad v = 1, \dots, k \quad (5)$$

Here $\Phi_v(\alpha)$ indicates performance criteria, Φ_v^{**} indicates the worst value of $\Phi_v(\alpha)$ and " \leq " sign is used in equation (5) because minimization is the most common form for demonstration purposes [12,21].

Performance criteria,

$$\Phi(\alpha) = (\Phi_1(\alpha), \dots, \Phi_k(\alpha)) \quad (6)$$

Expressed as vector. Functional constraints are sometimes not correctly identified. In practice, feasible solutions may remain beyond constraints. To include these feasible solutions in the feasible solution set, the constraints need to be rearranged. $\Phi_{k+1}(\alpha) = f_l(\alpha)$ expressed as pseudo-criterion instead of $f_l(\alpha) \leq C_l^{**}$ $l = 1, \dots, t$. To find constraint Φ_{k+1} , the test table containing $\Phi_{k+1}(\alpha)$ the must be compiled (There are test tables containing performance criteria $\Phi_v(\alpha) \leq \Phi_v^{**}$, $v = 1, \dots, k$) [21].

Generally, all performance criteria and pseudo-criteria are considered when it is desired to find the feasible solution set (D). The problem is now

$\Phi_v(\alpha) \leq \Phi_v^{**}$, $v = 1, \dots, k, k+1, \dots, k+t$ solved with constraints. Thus, in order to define the feasible solution set, the problem should be considered with $k+t$ criteria [11].

The Pareto optimal solution set (P) can be discovered by figuring out the optimal solution between the vectors in the feasible solution set (D). The Pareto optimal solution set in minimization problems can be defined as $\Phi(P) = \min_{\alpha \in D} \Phi(\alpha)$. $P \subset D$; is expressed as the Pareto optimal solution set. However, the pseudo criteria are not taken into account while creating this Pareto optimal solution set. They are the criteria values in the Pareto optimal solution calculated using $P(\Pi)$. Φ^p is prototype is value, that is the current design or desired design that needs to be developed [21].

Uniformly distributed LP sequences or random number generators are used in the PSI approach to create vectors (points) in the design variable space. LP-Tau generates uniformly distributed sequences and supports up to 51 design variables and 2^{20} tests. These sequences are used to compute N test points $\alpha^1, \dots, \alpha^N$ in the design variable space [43].

3. Mathematical Model of Capesize Bulk Carrier

Many approaches have been developed to solve multi-criteria optimization problems. In this study, the technique of "Parameter Space Investigation-PSI" developed in the former Soviet Union was used. PSI method studies conducted by Statnikov et al.'s [10-12,43] and Anil [21] are taken as the main reference of this study. As a starting point, this study used the structure of Cudina [22,23] and Zanic and Cudina's [24] optimization model. When solving optimization problems, the MOVI software uses a mathematical model that expresses the properties of the problem under consideration.

This research focuses on the optimization problem of bulk carrier design employing PSI technique to address the challenges posed by multiple and contradictory criteria. A prototype was developed based on existing ship designs found in the literature, and this prototype was further enhanced and refined. The design optimization model was examined using the PSI technique with MOVI software. Subsequently, the obtained results were compared with the findings from Zanic and Cudina's [24] study as reported in the literature.

This study focuses on the optimization of ship design parameters. Design parameters identified in the literature were employed in the study. Note that the limitation of this study lies in the predefined set of ship design parameters. However, these parameters can be expanded or reduced based on specific needs and requirements. Furthermore, future research can involve the development of a prototype model to further explore and enhance the optimization of ship design parameters.

The problem has seven design variables, five functional relations, three criteria, and four pseudo-criteria. Functional constraints are sometimes not correctly identified. In practice, feasible solutions may remain beyond constraints. In order for these feasible solutions to be included in the feasible solution set, the constraints need to be rearranged. Instead of $f_i(\alpha) \leq C_i^{**}$ $i = 1, \dots, t$ the pseudo-criteria $\Phi_{k+1}(\alpha) = f_i(\alpha)$ is used.

Before solving an optimization problem, the properties of the objective function, constraints, and the state of the decision variables are important [44]. This mathematical model is valid only for the "Capesize" case. For other ship types, calculation factors, engine database, power, and cost parameters need to be rearranged in Appendix [24,45]. Also, the minimum freeboard calculation is calculated for the "Capesize (bulk carrier)" type [24]. It needs to be rearranged for other ship types.

Terms used in the mathematical model and their definitions:

Length Between Perpendiculars (Lpp): The horizontal distance between the front and rear perpendiculars is called the length between perpendiculars. It is fixed for a particular ship and does not depend on the ship's loading condition [46].

Breadth (B): The breadth of the ship at its widest point is called the beam [46].

Draft (ds): The vertical distance at any point along the length between the waterline and the deepest part of the ship is the draft [46].

The block coefficient (C_b): C_b is the ratio of the displacement volume to the volume of a rectangular block whose sides are equal to the tip width, the average draft, and the length between perpendiculars [47].

Depth (D): The vertical length between the lowest point and the highest point of the ship [48].

Deadweight Tonnage (DWT): This weight measure shows the total weight a ship can carry [48].

Gross Tonnage (GT): It is a measure of the volume of all the spaces of the ship contained within the hull, bulkheads, and decks [48].

vtr: Trial speed is the speed measured at the ship's sea trial [49].

V_{service}: It is the speed at which the ship performs while navigating its route determined in real weather conditions [49].

Cargo Volume (V_{car}): The cargo of a ship is the goods that it is carrying [50].

MCR: Maximum Continuous Service Rating is the maximum power output engine can produce while running continuously at safe limits and conditions [51].

SMCR: Specified Maximum Continuous Rating [52].

Freeboard: Freeboard is the distance from the waterline to the freeboard deck of a fully loaded ship [53].

Wst: Wst includes the weight of all elements of the ship's steel structure (tonnage) [54].

There are also some dimensionless ratios that are commonly used to describe ship geometry and in systematic analysis studies. These can be expressed as design parameters in modeling. The main dimensions of the dimensionless ratios can be listed as follows [7]:

Length Between Perpendiculars - Beam Ratio: L_{pp}/B

Length Between Perpendiculars - Draught Ratio: L_{pp}/d_s

Length Between Perpendiculars - Depth Ratio: L_{pp}/D

Breadth - Draught Ratio: B/d_s

These ratios should be as low as possible and should not be correlated with each other in a way that defines the ship form in the model.

3.1. Design Variables and Constraints

There are seven design variables in this problem, and four of them are defined as main dimension design variables. The design variables that were developed from the model of Cudina [22] were listed as follows [45]:

Main Dimensions:

p1: L_{pp} Length between perpendiculars (m)

p2: B Breadth (m)

p3: d_s Scantling draught (m)

p4: C_B Block coefficient (-)

Other Design Variables:

p5: V_{car} Volume of cargo space (m^3)

p6: v_{tr} Required trial speed (kn)

p7: IME MAN B&W 6S70MC-C, mark 7, IME (Main engine identifier) = 1 (MCRi = 18660; (kW at 91 rpm) maximum continuous rating)

MAN B&W 5S70MC-C, mark 7, IME (Main engine identifier) = 2 (MCRi = 15550; (kW at 91 rpm) maximum continuous rating)

The design variable vector is shown as $\alpha = (L_{pp}, B, d_s, C_B, v_{tr}, V_{car}, \text{IME})$ and design variable constraints are also shown as $\alpha_j^* \leq \alpha \leq \alpha_j^{**}$ $j = 1, \dots, r$. Constraints of design variables are defined in the range of minimum and maximum values.

$$265 \leq p1 \leq 280$$

$$43 \leq p2 \leq 45$$

$$17.5 \leq p3 \leq 17.95$$

$$0.85 \leq p4 \leq 0.875$$

$$185000 \leq p5 \leq 195000$$

$$14.5 \leq p6 \leq 15.5$$

$$p7 = 1 \text{ or } 2$$

3.2. Functional Relations and Functional Constraints

The functional relations used in the model are expressed as follows. There are five functional relations in this model. These functional relationships and constraints were developed from Cudina's [22] model [45].

f1: L_{pp}/B Length/Breadth ratio

f2: L_{pp}/d_s Length/Scantling draught ratio

f3: B/d_s Breadth/Scantling draught ratio

f4: L_{pp}/D Length/Depth ratio

f5: $(D-d_s)-F_{B60}$ Freeboard control

The freeboard $(D-d_s)$ should be at least "about minimum freeboard" (F_{B60}).

The functional relationship constraints used in the model are shown as follows:

$$5.8 \leq f1 \leq 6.5 \quad L_{pp}/B$$

$$15.3 \leq f2 \leq 16.2 \quad L_{pp}/d_s$$

$$2.3 \leq f3 \leq 2.7 \quad B/d_s$$

$$11.0 \leq f4 \leq 11.9 \quad L_{pp}/D$$

$$0 \leq f5 \quad (D-d_s)-F_{B60}$$

3.3. Pseudo-Criteria and Pseudo-Criteria Constraints

At the beginning of the research, functional relationships that lack strict functional restrictions can be referred to as pseudo-criteria.

Pseudo-criteria used in the model are "engine power control, the volume of cargo space and the required trial speed". Pseudo-criteria used in the model and their features are as follows [22,45]:

f6: MCR_i - SMCR MINIMIZE the "Engine Power Control"

f7: DWT MAXIMIZE the deadweight (t)

f8: V_{car} MAXIMIZE the volume of cargo space (m^3)

f9: v_{tr} MAXIMIZE the required trial speed (kn)

Machine Power Control: The power of the selected machine should be more than the power requirement. In other words, the difference between the power of the selected machine and the power requirement must be greater than zero ($0 < f6$). On the other hand, f6 should also be minimized as the machine may be a lower powered machine supplying the power requirement in the database. Therefore, f6 will be included in the pseudo-criteria section, and the condition of being greater than zero will be evaluated as a "pseudo-criteria constraint", not a "functional constraint". The design variables Cargo Volume (p5) and Ship Speed (p6) are also pseudo-criteria.

3.4. Criteria and Criteria Constraints (Performance Criteria Constraints)

The “design” criteria, also called the “Objective Function”, used in the model were “the weight of steel structure”, “the power requirement”, “the cost of newbuilding”. These criteria are adapted from Cudina’s [22] model. The criteria included in the model have the feature of minimization. There are no criterion constraints in the model [45].

- c1: L_{st} MINIMIZE the weight of steel structure (t)
 c2: SMCR MINIMIZE the power requirement (kW)
 c3: CNB MINIMIZE the cost of new building the (US DOLLAR)

3.5. Prototype

The prototype model was determined based on the characteristics of the ships produced in IHHI, Koyo Dock, Namura, NKK shipyards located in the Far East and the characteristics of the capesize bulk carriers. The specifications of the ships are shown in Table 3.

Based on the characteristics of the ships indicated in Table 3, a prototype model was created. The prototype values used in the model are as follows [45]:

- p1: L_{pp} (m)= 279
 p2: B (m)= 43

- p3: d_s (m)= 17.5
 p4: C_b (-)= 0.875
 p5: V_{car} (m³)= 185000
 p6: v_{tr} (knots)= 15.27
 p7: lme_i (-)= 1

4. Multi-Criteria Optimization of Capesize Bulk Carrier

Optimization is a discipline that helps to make managerial decisions by developing mathematical models for solving a problem [44]. In single-criteria optimization, it is tried to obtain a single design or decision that is best for a purpose, which is usually a global minimum or global maximum based on the minimization or maximization problem [66]. Almost all designs or challenges in the real world necessitate simultaneous optimization of several conflicting objectives. In the case of several objectives, there may not be a single optimal all-purpose solution. In this situation, selecting a solution from a limited number of consensus options is required of the decision-maker. The optimal solution ought to have performance adequate for all needs.

The Pareto optimum has been integrated into the development of multi-objective optimization algorithms. In this way, depending on its objective values, a feasible

Table 3. Characteristics of ships produced in shipyards and their types

		L_{pp} (m)	B (m)	d_s (m)	D (m)	The capacity of cargo (m ³)	DWT (t)	GT (t)	$V_{kn, service}$	Main engine	SMCR (kw/rev)
Shipyards	IHHI	277	45	17.6	23.8	186,668	48,338	83,849	14.8	6RTA72	8160/124
	Koyo Dock	280	45	17.6	23.8	188,205	45,908	85,379	14.6	6S70MC	9267/110
	Namura	277	45	17.7	24.1	191,255	44,881	85,868	14.8	6S70MC	8240/122
	NKK	279	45	17.81	24.1	191,582	47,400	87,522	14.7	6S70MC	8310/123
Capesize Bulk Carriers	Cape Riviera	280	47	17.95	24.4	205,722	185,875	93,006	14.7	Kawasaki MAN B&W 6S70MC Mk VI diesel	16860 kW x 91 rpm
	Cape Heron	279	45	17.95	24.4	197,049	177,656	88,494	15	Mitsui MAN B&W 6S70MC diesel	16860 kW x 91 rpm
	Royal Chorale	279	45	17.95	24.4	197,050	177,544	88,491	15	Mitsui MAN B&W 6S70MC diesel	16860 kW x 91 rpm
	Ocean Comet	279	45	17.93	24.4	198,964	176,943	89,603	14.6	MAN B&W 6S70MC Mk VI diesel	16860 kW x 91 rpm
	Frontier Neige	288	45	18.2	24.7	203,226	182,737	93,288	15.3	Kawasaki MAN B&W 6S70MC-C7 diesel	17780 kW x 87 rpm

Source: [24,55-65]

solution may be the best, the worst, or indistinguishable from the other options. The phrase “optimal solution” refers to a solution that is not just better than the alternatives for at least one objective while not being worse for any of the goals. A solution that is not suppressed by any other solutions in the search space is the optimal solution. According to Osyczka [66], Dias and Vasconcelos [67], Sağ [68], and Deb [69], the collection of such optimum solutions is known as a pareto optimal solution set.

When solving optimization problems, MOVI software uses a mathematical model that expresses the properties of the problem under consideration. The mathematical model explains the relationships between output functions and input parameters (design variables) [21,45]. Model using MOVI software:

- Retrieves input parameters (design variables) created by MOVI.
- Calculates output functions based on input parameters.

In general, the model may contain data files, programs, etc.. No matter how complex the model structure is, the model interface provides the interaction between MOVI and the model, as shown in Figure 4. Dynamic Link Library (DLL file), Matlab M-function (M-file), and executable EXE file are supported for the model interface file. Matlab M-file was used in this study.

Matlab M-function (M-file): Output model functions are calculated with an M-function in a Matlab environment. Input parameters are passed to the M-function as input arguments. Output functions are expressed by the output vector of the M-function [21,45].

Once the M-file interface is generated, MOVI can begin optimization. In this study MOVI 1.4 and MATLAB R2009a software were used.

MOVI uses histograms to show the distribution of feasible and pareto optimal solutions. The intervals of the histograms are divided into 10 subintervals. Analysing the histograms elicits how feasible and pareto sets are distributed in the design variable set. Histograms play a major role in correcting constraints of design variables.

4.1. The First Run Optimization

The optimization model was defined in MOVI via the corresponding menus. LP Tau was chosen as the number

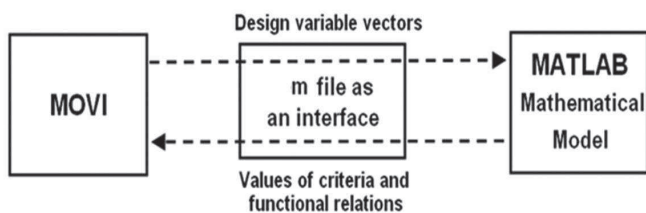


Figure 4. Data exchange between MOVI 1.4 and the user model [21]

generator for this optimization model. LP-Tau generated uniformly distributed arrays and supported 51 design variables and 220 tests. After the prototype values were entered, 8192 (2^{13}) tests were performed using the Run Test interface. This meant that 8192 design variable vectors could be generated by MOVI. As a result of these tests, 3069 of the vectors could enter the test table, while 5123 could not meet the constraints. Prototype values were expressed with the vector “0”. To find better values than the prototype, the prototype value was taken as the constraint and 7 vectors were included in the feasible solution set. Only two of these seven feasible solutions (#7371, #5145) were Pareto optimal solutions. The vectors containing Pareto optimal solution were the 7371 and 5145 vectors. Table 4 shows the feasible and pareto optimal solutions for the first optimization.

By means of histograms, the analysis of the design variables in the feasible solution could be made. Histograms show the distribution of variables over certain intervals. Thus, to achieve a more uniform distribution, the lower and upper limits of variables could be determined again. In the histograms, the values of the pareto optimal solutions are shown as green circles, and the ranges in which the feasible solutions were collected are shown in the red circle. The prototype value is shown as ∇ symbol in the optimization process. The feasible solution intervals of the design variables are shown in Figure 5.

According to the histograms of the design variables shown in Figure 5; the lower limit for the design variable p_1 (length between perpendicular) needed to be adjusted. The lower bound should also be adjusted for the design variable p_3 (draft). Both the upper and lower limits must be set for the design variable p_6 (ship speed).

4.2. The Second Run Optimization

The boundaries of the design variables were rearranged. Lower limit for p_1 was redefined as 273; lower limit for p_3

Table 4. Feasible and pareto optimal solutions for the first run optimization

	1 st Run	2 nd Run	3 rd Run
Test Performed	8192	8192	8192
Test Table Contains	3069	4112	5162
Feasible Set Contains	7	102	282
The Number of Pareto Optimal Solutions	2	9	6
Numbers of Pareto Optimal Solutions Vectors:	#7371, #5145	#2794, #3220, #6096, #741, #3240, #3561, #903, #4307, #1935	#3240, #1944, #57, #4307, #1935, #207

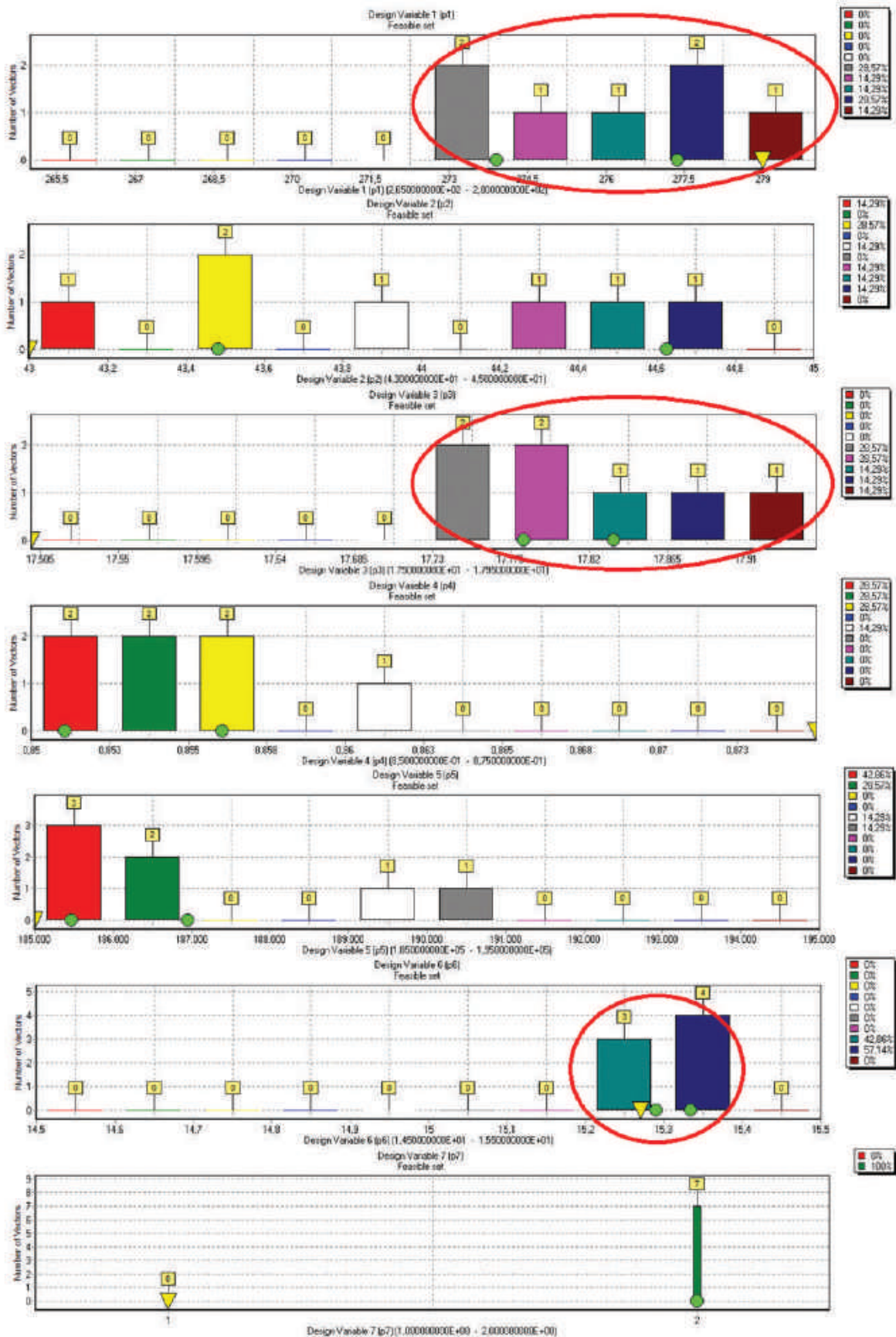


Figure 5. Feasible solution intervals of design variables for the first optimization

was redefined as 17.74; lower limit for p_6 was 15.26; and the upper limit was redefined as 15.4. For the second run of optimization, 8192 tests were performed using rearranged limits. As a result of this test, 4112 vectors could enter the test table. The 4080 vectors did not satisfy the constraints. Again, in order to find better values than the prototype, the prototype value was used as the constraint and 102 vectors were included in the feasible solution set. Only 9 of them were pareto optimal solutions in 102 feasible solutions. Table 4 shows the feasible and pareto optimal solutions for the second run optimization.

The lower and upper limit values of the variables should be determined again through histograms. Figure 6 indicates the boundaries that need to be rearranged. The upper bound for the design variable p_4 (block coefficient) and p_5 (cargo volume) needed to be rearranged.

After the second run optimization, pareto optimal values of design variables are listed in Table 5.

4.3. The Third Run Optimization

The boundaries of the design variables were rearranged. The upper bound for the design variable p_4 was changed to 0.864 and the upper bound for the design variable p_5 to 191,000. As a result of these tests, 5162 of 8192 tests could enter the test table, while 3030 could not. Prototype values were taken as constraints and 282 vectors were included in the feasible solution set. In the end of 8192 tests, 282 feasible solutions were found with better results than the prototype values, and 6 of them were pareto optimal solutions. Table 4 shows the feasible and pareto optimal solutions for the third run optimization.

By means of histograms, the lower and upper limit values of the variables are shown in Figure 7. When the histograms

in Figure 7 are examined, there are no intervals in which the constraints of the continuous variables are defined, where there is no feasible solution. For this reason, the fourth round was not passed and the variable constraints were not rearranged.

As a result of the first run optimization, vectors #7371 and #5145 contain the pareto optimal result. In the end of the second run of optimization, the pareto optimal vectors are #2794, #3220, #6096, #3741, #3240, #3561, #903, #4307, #1935. After the third run optimization, pareto optimal values of design variables are listed in Table 5. "0" number of vector has prototype values and "#57", "#207", "#1935", "#1944", "#3240", "#4307" number of vectors has pareto optimal values of design variables.

The prototype values and the values of Zanic and Cudina [24] found as a result of optimization and the pareto optimal values found as a result of the optimization process are shown in Table 5 for design variables, Table 6 for pseudo criteria, and Table 7 for criteria.

After the completion of the optimization process, pseudo-criteria values were calculated as Table 6.

When the pseudo-criteria in Table 6 are examined, it is seen that the values of the minimum feature f6 (Engine Power Control) criterion are lesser than the prototype value.

Considering the f7 (deadweight) and f8 (cargo volume) criteria which have maximum properties, it is seen that the values in the pareto optimal solution set values are higher than the prototype value.

When the f9 (required trial speed criterion), which is also in the maximum structure, is examined, it is seen that the values in the pareto optimal solution sets values are higher than both the prototype value and the value obtained by Zanic and Cudina [24] (15.03), which is used as a reference.

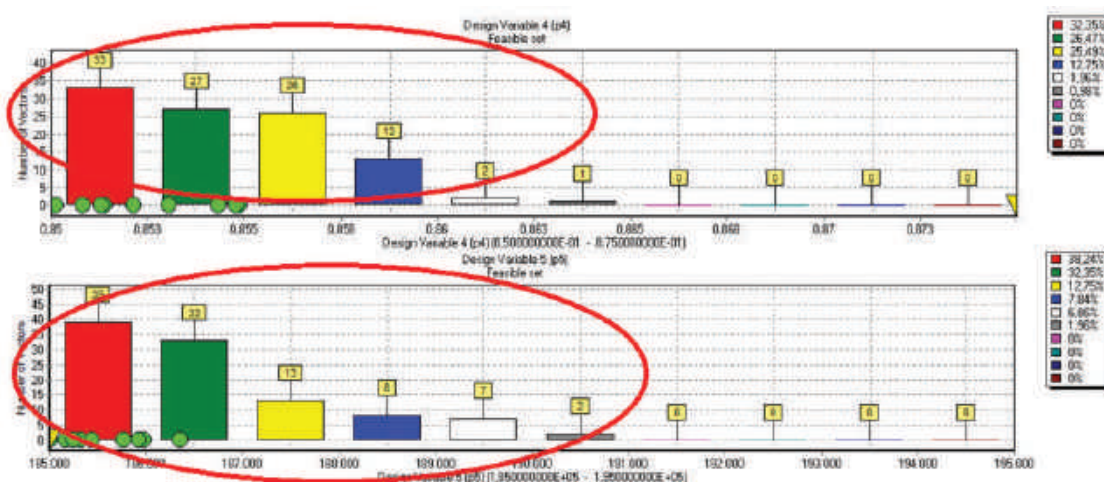


Figure 6. The feasible solution intervals of design variable 4 and 5 for the second run optimization

Table 5. Pareto optimal values of the design variables obtained as a result of the first, second, third optimization runs and reference study

	Design Variables	p1 L _{pp}	p2 B	p3 d _s	p4 C _B	p5 V _{car}	p6 v _{tr}	p7 I _{ME}
	Prototype Values # 0	279	43	17.5	0.875	185,000	15.27	1
1 st Run	Lower Bounds	273.915	43.483	17.783	0.851	185,47	15.291	2
	Upper Bounds	277.376	44.626	17.834	0.856	186,95	15.334	2
	Pareto Optimal # 7371	277.376	43.483	17.783	0.856	185,47	15.334	2
	Pareto Optimal # 5145	273.915	44.626	17.834	0.851	186,95	15.291	2
2 nd Run	Lower Bounds	273.326	43.124	17.763	0.850	185,002	15.274	2
	Upper Bounds	279.614	44.417	17.928	0.855	186,350	15.386	2
	Pareto Optimal # 2794	275.387	44.197	17.851	0.851	185,164	15.328	2
	Pareto Optimal # 3220	274.126	44.057	17.817	0.854	185,256	15.350	2
	Pareto Optimal # 6096	273.326	44.417	17.763	0.851	185,768	15.296	2
	Pareto Optimal # 3741	278.071	43.434	17.919	0.850	185,442	15.386	2
	Pareto Optimal # 3240	273.579	44.151	17.860	0.851	186,350	15.287	2
	Pareto Optimal # 3561	277.148	43.451	17.842	0.855	185,002	15.280	2
	Pareto Optimal # 903	279.173	43.744	17.782	0.852	185,322	15.300	2
	Pareto Optimal # 4307	278.552	43.168	17.925	0.855	185,919	15.274	2
	Pareto Optimal # 1935	279.614	43.124	17.928	0.853	185,981	15.287	2
	3 rd Run	Lower Bounds	273.579	43.124	17.813	0.850	185,026	15.274
Upper Bounds		279.645	44.151	17.928	0.857	185,914	15.288	2
Pareto Optimal # 3240		273.579	44.151	17.860	0.850	185,810	15.287	2
Pareto Optimal # 1944		273.708	43.812	17.882	0.857	185,026	15.274	2
Pareto Optimal # 57		277.266	43.406	17.881	0.854	185,094	15.289	2
Pareto Optimal # 4307		278.551	43.168	15.925	0.853	185,552	15.274	2
Pareto Optimal # 1935		279.614	43.124	17.928	0.852	185,589	15.287	2
Pareto Optimal # 207		279.645	43.540	17.813	0.850	185,914	15.275	2
	Reference [24]	274	44.4	17.85	0.865	189,670	15.03	2

The Pareto optimal values of the criteria obtained as a result of the first, second, and third optimization runs are listed in Table 7.

The prototype value for the minimized c1 = Wst ton (Steel Structure Weight) criterion is 18,911 tons, and the value that Zanic and Cudina [24] obtained as a result of the optimization is 19,001 tons. As a result of third run of optimization with MOVI, six solutions entered the Pareto optimal solution set. Looking at the c1 value of these six solutions, these values vary between 18,611 and 18,897. All six solutions are better than Zanic and Cudina's [24] result for c1 (steel structure weight). Also, the values of vectors 57, 1935, 1944, 3240 and 4307 are better than the value of c1 calculated using prototype values.

The prototype value for the minimized c2 = SMCR kW (Power Requirement) criterion is 15,670 kW, and the value that Zanic and Cudina [24] obtained as a result of the optimization is 15,268 kW. Considering the c2 value of the six pareto optimal solutions, these values vary between

14,744 and 15,431. Five of these six solutions are better than Zanic and Cudina's [24] result for the c2 - power requirement) (values of vectors 57, 207, 1935, 3240 and 4307). The c2 criterion value of all six solutions is better than the c2 value calculated using the prototype values.

For the minimized c3 = CNB US\$ (New Shipbuilding Cost) criterion, the prototype value is 93,696,607 US\$, result of Zanic and Cudina [24] optimization is 93.037.000 US\$. As a result of the third run of optimization with MOVI, six solutions entered the pareto optimal solution set. Looking at the c3 value of these six solutions, these values are between 91.9 million and 92.19 million US\$. All six solutions are better for c3 (new shipbuilding cost) than Zanic and Cudina's [24] value and prototype.

To find these criteria values, the design variables values in Table 5 should be taken as input parameters. The criteria values found in the end of the analysis were better than the prototype values and the values of Zanic and Cudina [24].

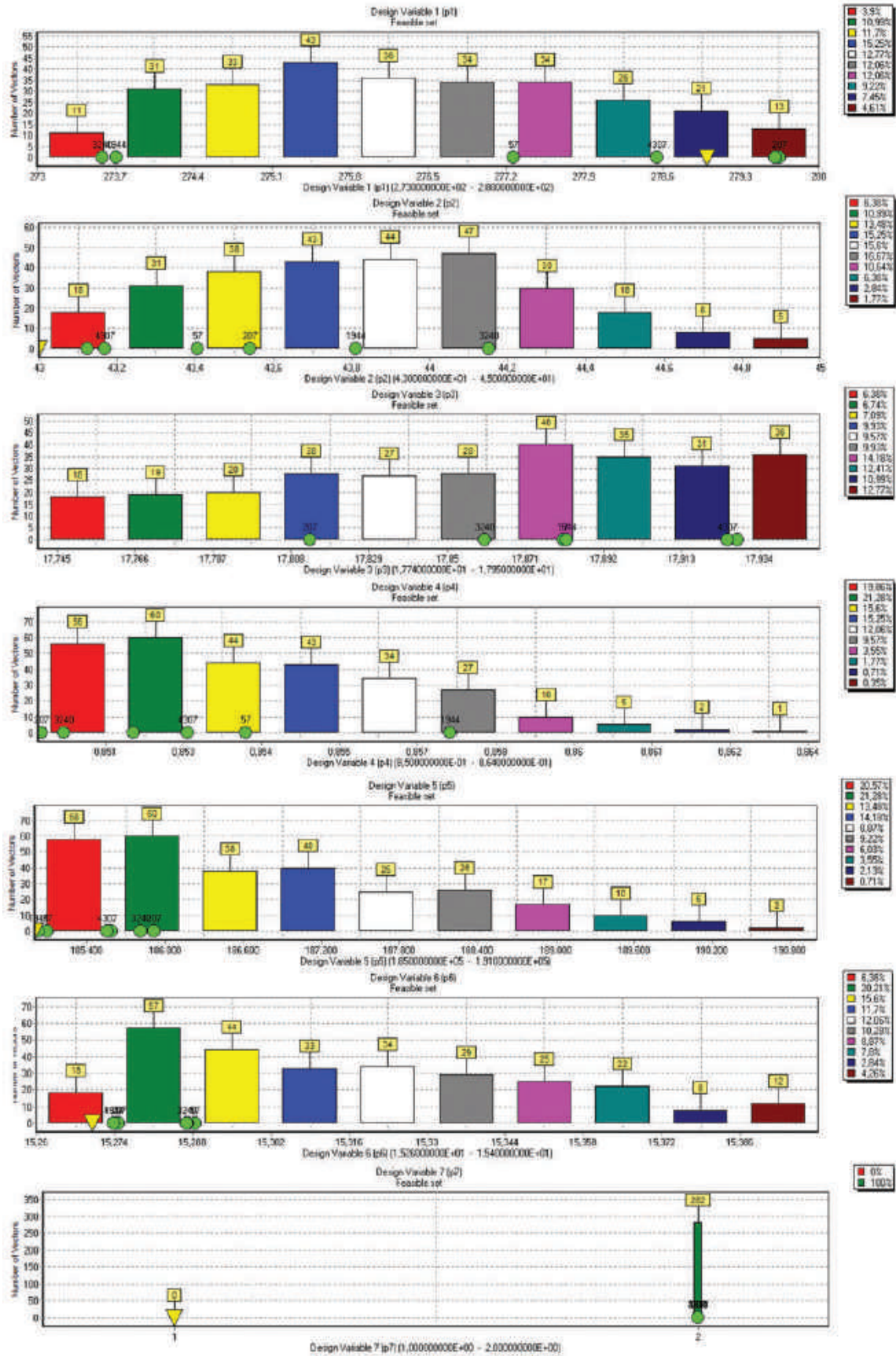


Table 6. Pareto optimal values of the pseudo-criteria obtained as a result of the third optimization run

	Pseudo Criteria	f6: MCR ₁ - SMCR (Min)	f7: DWT (Max) (t)	f8: V _{car} (Max) (m ³)	f9: v _{tr} (Max) (kn)
	Prototype Values # 0	2,989.309	166,933.132	185,000.000	15.27000
3 rd Run	Pareto Optimal # 57	497.926	167,178.378	185,093.750	15.28843
	Pareto Optimal # 207	806.262	167,696.279	185,914.062	15.27476
	Pareto Optimal # 1935	728.881	167,528.841	185,588.867	15.28700
	Pareto Optimal # 1944	119.429	167,370.242	185,026.367	15.27387
	Pareto Optimal # 3240	437.172	166,960.617	185,810.058	15.28689
	Pareto Optimal # 4307	687.037	167,233.339	185,551.513	15.27382

Table 7. Pareto optimal values of the criteria obtained because of the first, second, third optimization runs and reference study

	Criteria	c1 = Wst (Min)	c2 = SMCR (Min)	c3 = CNB US \$ (Min)
1 st Run	Prototype Values # 0	18,911	15,670	93,696,607
	Lower Bounds	18,778	15,322	92,162,223
	Upper Bounds	18,806	15,336	92,218,814
	Pareto Optimal # 5145	18,806	15,322	92,162,223
	Pareto Optimal # 7371	18,778	15,336	92,218,814
2 nd Run	Lower Bounds	18,665	14,911	91,960,962
	Upper Bounds	18,898	15,540	92,218,230
	Pareto Optimal # 903	18,898	15,029	92,168,457
	Pareto Optimal # 1935	18,848	14,911	92,218,230
	Pareto Optimal # 2794	18,742	15,318	91,960,962
	Pareto Optimal # 3220	18,665	15,540	91,968,406
	Pareto Optimal # 3240	18,669	15,137	92,013,004
	Pareto Optimal # 3561	18,730	15,090	92,028,224
	Pareto Optimal # 3741	18,765	15,180	92,000,807
	Pareto Optimal # 4307	18,804	15,005	92,205,640
3 rd Run	Pareto Optimal # 6096	18,679	15,234	91,969,018
	Lower Bounds	18,611	14,744	91,917,124
	Upper Bounds	18,897	15,431	92,191,529
	Pareto Optimal # 57	18,724	15,052	92,005,445
	Pareto Optimal # 207	18,897	14,744	92,191,529
	Pareto Optimal # 1935	18,819	14,821	92,115,028
	Pareto Optimal # 1944	18,611	15,431	91,956,770
	Pareto Optimal # 3240	18,643	15,113	91,917,124
Reference [24]	19,001	15,268	93,037,000	

5. Conclusion

Decision making has always been exceptionally critical, particularly for the leading of different purposes. Deciding on ships and comparative plans with a life span of approximately 30-40 years, in terms of making them more economical, competitive and environmentally friendly, maintains and will preserve its significance as a subject that should be examined very well compared to numerous decisions.

The model used in this study will form the basis for ship designs using multi-criteria optimization methods.

The designs produced using the design spiral method have been transformed by the use of optimization methods. Finding the feasible solution and the Pareto optimal solution set in multi-criteria optimization problems is of great importance, especially when the prototype is being developed.

In this study, the prototype development problem of a Capesize-type bulk carrier was addressed by the PSI method using visualization techniques such as histograms and analysis methods.

The model was developed in MATLAB environment and solved again in MOVI. By finding the feasible solution set and pareto optimal solution set with MOVI, better results were obtained than the results of Zanic and Cudina [24] and the prototype.

At the end of this study, the prototype design of Capesize bulk carrier was developed. After analyzing the Pareto optimal results, the user can choose the model that suits him/her or continue the optimization process. This study presents a case study on the development of ship design problems.

For future studies, the design process can be improved by expanding databases of mathematical models specific to various ship types and sizes. The PSI method presented in this paper introduces a program that generates histograms and test tables, providing decision-makers with unprecedented opportunities for analyzing and synthesizing alternative designs.

Acknowledgment

The authors would like to thank Kıvanç Ali Anıl for the construction and multi-criteria analysis of the model.

Peer-review: Externally and internally peer-reviewed.

Authorship Contributions

Concept design: R. Yaman, Data Collection or Processing: C. Aksu, Analysis or Interpretation: C. Aksu, R. Yaman, Literature Review: C. Aksu, Writing, Reviewing and Editing: C. Aksu, R. Yaman.

Funding: The author(s) received no financial support for the research, authorship, and/or publication of this article

References

- [1] M. Kafalı, and E. Aksu, "A Multi-objective optimization model for determining the performance of a sailboat." *Journal of ETA Maritime Science*, vol. 10, pp. 177-184, Aug 2022.
- [2] L. Zhao, "An evaluation study of logistics service ability of marine logistics enterprises," *Journal of Coastal Research*, vol. 107 pp. 49-52, Aug 2020.
- [3] UTİKAD, "Lojistik sektör raporu 2021," *UTİKAD Rapor*. <https://www.utikad.org.tr/images/HizmetRapor/utikadlojistiksektoruraporu2021-1654.pdf>
- [4] United Nations Conference on Trade and Development, "Review of maritime transport 2021," United Nations Publications, UNCTAD/RMT/2021, 2021. https://unctad.org/system/files/official-document/rmt2021_en_0.pdf
- [5] United Nations Conference on Trade and Development, "Review of maritime transport 2022," *United Nations Publications*, UNCTAD/RMT/2022 and Corr.1, 2022. https://unctad.org/system/files/official-document/rmt2022_en.pdf
- [6] General Directorate of Maritime Affairs, DWT and Number Development of the Turkish Merchant Fleet (Vessels of 150 GT and Above) 2017-2022. <https://denizcilikistatistikleri.uab.gov.tr/filo-istatistikleri>
- [7] R. Baykal, *Gemiler ve Açık Deniz Yapıları*. İstanbul: Birsen Yayınevi, 2011.
- [8] U. Demir, and Y. Ünsan, "Yüksek süratli teknelerde temel optimizasyon yöntemleri ve uygulama alanları," *GİDB Dergi*, pp. 35-52, Dec 2017.
- [9] M. Özdemir, "Amaç esaslı gemi yapım standartları (Goal based ship construction standards - GBS)," presented at Gemi Mühendisliği ve Sanayimiz Sempozyumu, 24-25 Dec 2004.
- [10] R. Statnikov, K. A. Anıl, A. Bordetsky, and A. Statnikov, "Visualization tools for multicriteria analysis of the prototype improvement problem," *Proceedings of the 2007 IEEE Symposium on Computational Intelligence in Multicriteria Decision Making*, pp. 341-347, May 2007.
- [11] R. Statnikov, K. A. Anıl, A. Bordetsky, and A. Statnikov, "Visualization approaches for the prototype improvement problem," *Journal of Multi-Criteria Decision Analysis*, vol. 15, pp. 45-61, Apr 2008.
- [12] R. Statnikov, and A. Statnikov, *The Parameter Space Investigation Method Toolkit*, Boston/London: Artech House, 2011.
- [13] R. W. Maruda, et al. "Metrological analysis of surface quality aspects in minimum quantity cooling lubrication," *Measurement*, vol. 171, vol. 108847, Feb 2021.
- [14] K. Leksycki, and E. Feldshtein, "The surface texture of ti6al4v titanium alloy under wet and dry finish turning conditions," *Lecture Notes in Mechanical Engineering, Industrial Measurements in Machining*, pp. 33-44 Jul 2020.
- [15] R. W. Maruda, S. Legutko, R. Mrugalski, D. Debowski, and S. Wojciechowski, "Analysis of cutting force and power under the conditions of minimized cooling in the process of turning AISI-1045 steel with the use of the parameter space investigation method," *Lecture Notes in Mechanical Engineering, Industrial Measurements in Machining*, 2020.
- [16] S. I. Gavrilin, S. S. Gavriushin, and V. A. Godzikovsky, "Multicriteria approach to design of strain gauge force transducers," *Journal of Physics: Conference Series*, vol. 1379, pp. 012010, Nov 2019.
- [17] K. Leksycki, E. Feldshtein, J. Lisowicz, R. Chudy, and R. Mrugalski, "Cutting forces and chip shaping when finish turning of 17-4 ph stainless steel under dry, wet, and mql machining conditions," *Metals*, vol. 10, pp. 1187, Sep 2020.
- [18] P. Pagano, H. J. Van Damme, P. Antolin, and I. De Moortel, "MHD simulations of the in situ generation of kink and sausage waves in the solar corona by collision of dense plasma clumps," *Astronomy and Astrophysics*, vol. 626, pp. 12, Jun 2019.
- [19] R. W. Maruda, S. Legutko, G. Krolczyk, C. Lukianowicz, and A. Stoić, "Effect of anti-wear additive on cutting tool and surface layer of workpiece state under mql conditions," *Tehnički Vjesnik*, vol. 22, pp. 1219-1223, 2015.
- [20] E. Xargay, and N. Hovakimyan, "L1 adaptive flight control system: systematic design and verification and validation of control metrics," *AIAA Guidance, Navigation, and Control Conference*, 2 - 5 Aug 2010, Toronto, Ontario, Canada.

- [21] K. A. Anıl, "Multi-criteria analysis in naval ship design," *Naval Postgraduate School*, Mar 2005.
- [22] P. Cudina, "Design procedure and mathematical models in the concept design of tankers and bulk carriers," *Brodogradnja (Shipbuilding)*, vol. 59, pp. 323-339, 2008.
- [23] P. Cudina, "Nova metodologija projektiranja trgovackih brodova (A new design methodology merchant ships)," *Sveuciliste U Zagrebu (University of Zagreb)*, 2010.
- [24] V. Zanic, and P. Cudina, "Multiattribute decision making methodology in the concept design of tankers and bulk carriers," *Brodogradnja (Shipbuilding)*, vol. 60, pp. 19-43, 2009.
- [25] A. Brown, and J. Salcedo, "Multiple-objective optimization in naval ship design," *Naval Engineers Journal*, vol. 115, pp. 49-61, 2003.
- [26] F. Mistree, W. F. Smith, B. A. Bras, J. K. Allen, and D. Muster, "Decision-based design: A contemporary paradigm for ship design," in *The Society of Naval Architects and Marine Engineers Annual Meeting*, 1990. <https://citeseerx.ist.psu.edu/viewdoc/download?doi=10.1.1.84.4236&rep=rep1&type=pdf>
- [27] H. L. Brinati, O. B. Augusto, and M. B. De Conti, "Learning aspects of procedures for ship conceptual design based on first principles," in *International Conference on Engineering Education - ICEE 2007*, Jan 2007.
- [28] J. H. Evans, "Basic design concepts," *A.S.N.E. Journal*, Nov 1959. https://edisciplinas.usp.br/pluginfile.php/3072978/mod_resource/content/1/EVANS_1959_Basic_design_concepts.pdf
- [29] Y. Shin and S. Han, "Data enhancement for sharing of ship design models," *Computer-Aided Design*, vol. 30, pp. 931-941, 1998.
- [30] E. W. McGookin, D. J. Murray-Smith, Y. Li, and T. I. Fossen, "Ship steering control system optimisation using genetic algorithms," *Control Engineering Practice*, vol. 8, pp. 429-443, Apr 2000.
- [31] M. Diez, and D. Peri, "Robust optimization for ship conceptual design," *Ocean Engineering*, vol. 37, pp. 966-977, Aug 2010.
- [32] O. Yaakob, E. L. Teoh, Y. W. Liew, and K. K. Koh, "Design of Malaysian fishing vessel for minimum resistance," *Jurnal Teknologi*, pp. 1-12, Jan 2005.
- [33] A. Papanikolaou, "Holistic ship design," *Computer-Aided Design*, vol. 42, pp. 1028-1044, Nov 2010.
- [34] A. İ. Ölçer, "A hybrid approach for multi-objective combinatorial optimisation problems in ship design and shipping," *Computers & Operations Research*, vol. 35, pp. 2760 - 2775, Sep 2008.
- [35] T. Ray, R. P. Gokarn, and O. P. Sha, "A global optimization model for ship design," *Computers in Industry*, vol. 26, pp. 175-192, May 1995.
- [36] Ç. Tanıl, "Optimal external configuration design of missile," Msc. Thesis, Ortadoğu Teknik Üniversitesi, Ankara, 2009. <https://tez.yok.gov.tr>
- [37] B. S. Türkmen, and O. Turan, "A new integrated multi-objective optimisation algorithm and its application to ship design," *SAOS*, vol. 2, 1, pp. 21-37, Jul 2010.
- [38] Ö. Arslan, and O. Gürel, "Farkli tip ve boyutta gemilerin seçiminin bulanik mantik yöntemiyle incelenmesi," *Havacilik ve Uzay Teknolojileri Dergisi*, vol. 3, pp. 55-60, 2008.
- [39] D. Lee, and K.-H. Lee, "An approach to case-based system for conceptual ship design assistant," *Expert Systems with Applications*, vol. 16, pp. 97-104, 1999.
- [40] Y. Tahara, S. Tohyama and T. Katsui, "CFD-based multi-objective optimization method for ship design," *International Journal for Numerical Methods in Fluids*, vol. 52, pp. 499-527, Feb 2006.
- [41] İ. Özyiğit, "Gemi inşaatında planlama ve üretim kademeleri," Msc. Thesis, Yıldız Teknik Üniversitesi, İstanbul, 2006.
- [42] Y. Genç, and M. Özkök, "Simulation-based optimization of the sea trial on ships," *Journal of ETA Maritime Science*, vol. 8, pp. 274-285, 2020.
- [43] R. Statnikov, et al. "Software package MOVI 1.4 for windows: User's manual, USA, Registration Number TXU 1-698-418, May 2010.
- [44] R. Sarker, *Evolutionary Optimization. USA: Kluwer Academic Publishers*, 2002.
- [45] C. Aksu, "Gemi dizaynında optimizasyon ve uygulama örneği", Msc. Thesis, *Balikesir Üniversitesi*, 2013.
- [46] Ship Hydrostatics, "Dimensions and measurements," http://faculty.nps.edu/fapapoul/1/2_basics.htm#.
- [47] K.J. Rawson, and E.C. Tupper, "Some tools," in *Basic Ship Theory*, Editor(s): K. J. Rawson, E. C. Tupper, Ed. 5th ed. Butterworth-Heinemann, pp. 7-51, 2001.
- [48] Milli Eğitim Bakanlığı, *Gemi yapimi alani: Temel endaze çizimi*, Ankara, 2011. http://www.megep.meb.gov.tr/mte_program_modul/moduller_pdf/Temel%20Endaze%20%C3%87izimi.pdf
- [49] Gemi Dizayni, "Gemi hizi (ship speed)", 2012. <http://gemidizayni.blogspot.com/2012/06/gemi-hz-ship-speed.html>
- [50] Cargo, "Cargo volume" <https://www.collinsdictionary.com/dictionary/english/cargo>
- [51] C. Karan, "14 Terminologies used for power of the ship's marine propulsion engine", 2021. <https://www.marineinsight.com/main-engine/12-terminologies-used-for-power-of-the-ships-marine-propulsion-engine/#:~:text=Maximum%20Continuous%20Rating%20or%20MCR,of%20the%20marine%20diesel%20engine>.
- [52] Y. Li, and T. Tang, "Performance analysis and optimization of a series heat exchangers organic rankine cycle utilizing multi-heat sources from a marine diesel engine," *Entropy*, vol. 23, pp. 906, 2021.
- [53] Freeboard. <https://www.britannica.com/technology/freeboard-navigation>
- [54] Ship Design, "Methodologies of preliminary design", 2022. https://edisciplinas.usp.br/pluginfile.php/5730141/mod_resource/content/1/2014%20-%20Papanikolaou%20-%20Weight%20Estimation.pdf
- [55] Japan Ship Exporters' Association, *Sea Japan*, 2003. https://www.jsea.or.jp/wp_2022/wp-content/uploads/2015/06/Sea296.pdf
- [56] Japan Ship Exporters' Association, *Sea Japan*, 2005. https://www.jsea.or.jp/wp_2022/wp-content/uploads/2015/06/Sea310.pdf
- [57] Japan Ship Exporters' Association, *Sea Japan*, 2006. https://www.jsea.or.jp/wp_2022/wp-content/uploads/2015/06/Sea316.pdf
- [58] Japan Ship Exporters' Association, *Sea Japan*. 2006. https://www.jsea.or.jp/wp_2022/wp-content/uploads/2015/06/Sea318.pdf
- [59] Shipspotting, *Shin Sho - IMO 9324124*. <https://www.shipspotting.com/photos/1298513>.

- [60] Japan Ship Exporters' Association, *Sea Japan*, 2008. https://www.jsea.or.jp/wp_2022/wp-content/uploads/2015/06/Sea330.pdf
- [61] Japan Ship Exporters' Association, *Sea Japan*, 2010. https://www.jsea.or.jp/wp_2022/wp-content/uploads/2015/06/Sea340.pdf
- [62] Japan Ship Exporters' Association, *Sea Japan*, 2010. https://www.jsea.or.jp/wp_2022/wp-content/uploads/2015/06/Sea339.pdf
- [63] Japan Ship Exporters' Association, *Sea Japan*, 2011. https://www.jsea.or.jp/wp_2022/wp-content/uploads/2015/06/Sea348.pdf
- [64] Japan Ship Exporters' Association, *Sea Japan*, 2011. https://www.jsea.or.jp/wp_2022/wp-content/uploads/2015/06/Sea349.pdf
- [65] Japan Ship Exporters' Association, *Sea Japan*, 2012. https://www.jsea.or.jp/wp_2022/wp-content/uploads/2015/06/Sea350.pdf
- [66] A. Osyczka, "Evolutionary algorithms for single and multicriteria design optimization", *Physica-Verlag*, 2002.
- [67] A. H. F. Dias, and J. A. de Vasconcelos, "Multiobjective genetic algorithms applied to solved optimization problems," *IEEE Transactions on Magnetics*, vol. 38, pp. 1133-1136, Mar 2002.
- [68] T. Sağ, "Çok kriterli optimizasyon için genetik algoritma yaklaşımları," Msc. Thesis, *Selçuk Üniversitesi*, 2008.
- [69] K. Deb, "Multi-objective genetic algorithms: Problem difficulties and construction of test problems, *IEEE Inst. on Evolutionary Computation*, vol. 7, pp. 205-230, 1999.

APPENDIX

A. Constants and Parameters

The following factors for computations, engine database, power parameters, cost parameters and constants are valid only for the Capesize (bulk carrier) model.

A.1. Factors for Computations [22,23,24,45]

ffc1 = 5 Impact of high-strength steel on reducing the weight of steel structures.

ffc2 = 0.0282 Empirical factor

ffc3 = 450 Addition of the mass of the steel structure

ffc4 = 800 Empirical factor

ffc5 = 0.9 CSR/SMCR ratio

ffc6 = 0.28 Empirical factor

ffc7 = 100 Addition of the weight of ship equipment

Af = 29 Compensation factors Af and Bf for calculation of cGT

Bf = 0.61

$\kappa = 0.64$ specific voluminosity of the ship

$\text{kappa} = V_{\text{car}} / (L_{\text{pp}} * B * D)$

A.2. Engine Database [22,23,24,45]

MAN B&W 6S70MC-C, mark 7 MCR: 18660

CME: 8400000 \$ KCSR: 1.022

MAN B&W 5S70MC-C, mark 7 MCR:15550

CME: 7400000 \$ KCSR: 1.022

A.3. Power Parameters [22,23,24,45]

a1 = 0.00571

a2 = -0.1465

a3 = 1.072

a4 = 0.8145

a5 = 3.843

a6 = 3.589

a7 = 0.0006634

A.4. Cost Parameters [22,23,24,45]

cst = 1000 Average unit steel costs (\$/tonne)

rWgst (Wgst/Wst) = 1.12 The ratio of the gross mass of steel to the weight of the steel structure

Cfix (\$) = 26000000 Other costs, including costs related to other materials and equipment

PcGT = 35 Shipyard productivity (hrs/cGT) cGT: the gross tonnage accounted for, according to the OECD.

VL = 30 Unit hourly wage (\$/hour of employment)

Coc = 7000000

Vcam = 5000 The volume of the camber (m³)

Vsup = 11000 Volume of the accommodation (m³)

Vfc = 0 The volume of the forecastle (m³)

KCBD (CBD) = 0.005285 Constant for approximating the block coefficient to the molded depth.

A.5. Constants

$\gamma_{\text{tot}} = 1.0279$: Density of sea water, including influence of shell plating and ship appendages (t/m³) [22,23,24,45].

Neuroscience Approach to Situational Awareness: A Research on Marine Navigation

© Serkan Kahraman¹, © Durmuş Ali Deveci², © İbrahim Öztura³, © Dilara Mermi Dibek⁴

¹Dokuz Eylül University, The Graduate School of Natural and Applied Sciences, İzmir, Türkiye

²Dokuz Eylül University Faculty of Maritime, Department of Maritime Transportation Business Management, İzmir, Türkiye

³Dokuz Eylül University Faculty of Medicine, Department of Neurology Diseases, İzmir, Türkiye

⁴Dokuz Eylül University, The Institute of Health Sciences, İzmir, Türkiye

Abstract

This study investigates the cognitive levels of tugboat captains, key players during port manoeuvres, which are a crucial part of sea navigation. The objective is to reveal the main neurophysiological findings related to the measurements of the tugboat captains' brain activity during both rest and actual manoeuvring performance and to investigate the relationship between this brain activity and situational awareness. The study employed an experimental research method. Brain waves of the tugboat captains were recorded using the Emotiv X EEG device and the Emotiv Pro v2.0 program during real port manoeuvres which is a part of the sea navigation. Situational awareness levels were tried to be determined by analysing the obtained values in the Brain Products Vision Analyzer 2.1 software. The study examined the cognitive states of four tugboat captains during 16 manoeuvres and resting, focusing on the Fast Fourier Transform (FFT)/Band power graph values. Within the scope of the research non-parametric Friedman Test with five variables [Resting State (RS), 1st Manoeuvre Group, 2nd Manoeuvre Group, 3rd Manoeuvre Group, and 4th Manoeuvre Group] to analyse the FFT values of the participants. Post-hoc comparisons were calculated using Bonferroni correction. The results showed no difference in alpha wave power, while delta, theta, beta, and gamma power decreased. The primary outcome of the research indicates that professional tugboat captains, who were the participants of the study, exhibited consistent situational awareness levels both during manoeuvring and resting moments.

Keywords: Situational awareness, EEG, Tugboat captains, Fast Fourier Transform, FFT, Sea navigation

1. Introduction

Sea navigation involves ships traveling from one point to another around the world. Ship handling or maneuvering is crucial for managing the forces that affect the ship's movement [1]. In this study, tugboats were selected as the representative ship type, and tugboat captains were chosen as the navigators. Tugboats with towing and pulling capabilities are provided for manoeuvring support during the processes of docking and undocking in ports for ships that are considered to be insufficient or at risk of posing a risk to themselves, other vessels, port and coastal facilities, and the environment if they were to maneuver on their own [2]. During the provision of this service, tugboat captains comply with the instructions of the pilot captain on board

the ship. Pilotage and towage services provided within the scope of technical navigation services are interconnected services [3].

Among the various factors contributing to maritime accidents, the human factor is considered the primary cause. Human factors in the maritime industry include mental workload, emotion, attention, pressure, and fatigue [4]. Safety investigations by the European Maritime Safety Agency [5] from 2014 to 2020 revealed that human factors played a role in 75% to 96% of incidents and accidents. Even with the latest technological advancements in marine vessels, it is essential to have qualified ship users (ship's master, maritime pilot, officer on watch or tugboat captains) who can operate them safely. Ship captains



Address for Correspondence: Serkan Kahraman, Dokuz Eylül University, The Graduate School of Natural and Applied Sciences, İzmir, Türkiye
E-mail: cptkahraman@gmail.com
ORCID ID: orcid.org/0000-0001-6941-1367

Received: 25.04.2023
Last Revision Received: 20.07.2023
Accepted: 02.08.2023

To cite this article: S. Kahraman, D. A. Deveci, İ. Öztura, and D. Mermi Dibek. "Neuroscience Approach to Situational Awareness: A Research on Marine Navigation." *Journal of ETA Maritime Science*, vol. 11(3), pp. 186-197, 2023.

©Copyright 2023 by the Journal of ETA Maritime Science published by UCTEA Chamber of Marine Engineers

must consider various ship and weather conditions, make accurate and timely decisions, and have contingency plans for emergencies. Furthermore, as per Rightship's article in 2023 [6], half of the vessel incidents occurred within port limits. Ship maneuvering within port limits for berthing and unberthing is a very critical stage of ship navigation, where many external factors, variables, and much more data flow are involved for situational awareness. Therefore, a very crucial part of navigation is ship maneuvers in ports, and tugboat captains are one of the key players.

Situational awareness (SA) originated in the aviation industry and refers to being aware of what is happening around and understanding the meaning of information in the present and future. Endsley [7] developed a widely used approach to define situational awareness on three levels: perception, comprehension, and projection. Effective situational awareness is measured by making correct decisions and taking appropriate actions. The cognitive state of individuals is directly related to the components of situational awareness, such as mental workload, attention, stress, information processing, and memory [8]. There are significant similarities between workload and situational awareness. Both constructs are distinct from behavior and performance and can be measured using physiology, performance and subjective assessments combined with task analysis and computational modeling [9]. Mental workload is an influencing factor in human performance, and it is a non-independent variable in measuring human factors in the maritime industry [4].

Electroencephalography (EEG) is a widely used medical instrument for measuring the brain activity based on sensor voltage fluctuations. Early studies have demonstrated that the

level of mental workload under different task complexities and difficulty levels can be classified into distinct classes by analyzing the temporal variation of the EEG Power Spectral Density (PSD) or the time-frequency characteristics of EEG time series data [9]. With the development of technology and the availability of physiological data collection equipment, EEG has found applications in various fields and environments. EEG is a non-invasive technique that records signals from the brain using electrodes placed on the scalp [10]. The use of EEG to measure the brain activity offers several advantages, including high temporal resolution and ease of application. EEG devices are equipped with software that enables the measurement of human brain activities. Consequently, there is growing interest in exploring human factors through the analysis of physiological data [11].

Researchers have used EEG in multidisciplinary studies, employing machine learning technology and signal processing. Its use has expanded beyond medicine into various disciplines, as shown in Table 1. In transportation, EEG has been used to measure driver behavior and investigate arousal changes during conflict detection and adjustment processes.

For instance, in the domain of land transportation, Abut et al. [12] employed different data collection tools along with EEG to measure driver behavior. Johnson et al. [13] investigated the impact of arousal changes on conflict detection and conflict adjustment processes during normal arousal fluctuations in behavioral and informatics. In the maritime industry, studying the physiological behavior of crew members has become crucial in identifying the primary causes of human errors and the direct factors contributing to accidents [4,14].

Table 1. Literature review with the EEG device

Authors	The field of Study	Research focus	Method
Tong et al. [15] 2017	Medical	Cognitive	EEG-HRV
Loris et al. [16] 2017	Medical	Cognitive	ECoG and EEG-DABS
Başar et al. [17] 2018	Medical	Cognitive	EEG, ANOVA test
Tsekoura and Foka [18] 2020	Medical	Brain-computer interface	EEG- EEGLAB toolbox
Johnson et al. [13] 2020	Medical	Cognitive	EEG - Behavioural Data Analysis
Çelik et al. [19] 2021	Medical	Cognitive	EEG-SCL-90
Mheich et al. [20] 2021	Medical	Cognitive	EEGLAB
Koctúrová and Juhár [21] 2021	Medical	Cognitive	Open BCI- EEG
Yakobi et al. [22] 2021	Human Factors	Cognitive	EEG- Go/No-Go Task
Wal et al. [23] 2020	Human Factors	Behavioural	EEG task and behavioral performance
Kirschner et al. [24] 2020	Human Factors	Cognitive/Behavioural	EEG-PES, PERI
Kaur et al. [25] 2020	Human Factors	Cognitive	EEG, fMRI, SA Index, PRAA, and PRAFA
Ma et al. [26] 2021	Human Factors	Cognitive	EEG-SVM-LTSM

Table 1. Continued

Jin et al. [27] 2021	Human Factors	Cognitive	Temperaments Inventory
Nann et al. [28] 2021	Human Factors	Brain-computer interface	EEG-EOG-HOV
Berka et al. [29] 2006	Military	Cognitive	EEG/Naval Command Task simulation
Schnell et al. [30] 2008	Aviation	Cognitive	EEG-Cognitive Avionics Tool Set (CATS)
Borghini et al. [31] 2014	Aviation and Transportation	Cognitive	EEG, EOG, and HR data
Galant and Merksiz [32] 2017	Aviation	Cognitive	EEG; simulator-NASA TLX and SWAT
Trapsilawati et al. [33] 2019	Aviation	Cognitive	AT-SAT Test, EEG
Flumeri et al. [34] 2019	Aviation		EEG-eye tracking-Asa TLX
Klaproth et al. [35] 2020	Aviation	Cognitive	ACTR, EEG
Polat and Özerdem [36] 2016	Computer Engineering	Brain-computer interface	EEG- Power Spectral Density
Sözer and Fidan [37] 2019	Computer Engineering	Brain-computer interface	Brain-computer interface-EEG
Alakuş and Türkoğlu [38] 2018	Computer Engineering	Brain-computer interface	EEG-IAPS
Iqbal et al. [39] 2020	Computer and Chemical Engineering	Cognitive	EEG-Theta power spectral density
Ackermann et al. [40] 2016	Mechanical Engineering	Cognitive	EEG-DAEP
Kaya et al. [41] 2017	Machine Learning	Brain-computer interface	EEG-BCI Model
Yin and Zhang [11] 2014	Automation	Cognitive	Mental Workload Calculation -EEG
Roy et al. [42] 2021	Multidisciplinary	Cognitive	EEG-CPCA-MATLAB
Abut et al. [12] 2009	Transportation	Cognitive	EEG, CAN, Bus, IVMC Tool-eye tracking-laser sensor-pedal sensor
Xiaolil et al. [43] 2009	Transportation	Cognitive	EEG-PVT
Kim et al. [44] 2014	Transportation	Cognitive	EEG-WMS
He et al. [45] 2016	Transportation	Behavioural	EEG, head nodding angle, eye-tracking signal-Driving Model
Lee and Yang [46] 2019	Automotive Technology	Cognitive	EEG power spectrum analysis
Hu et al. [47] 2019	Transportation	Cognitive	EEG multichannel analysis
Siddharth and Trivedi [48] 2020	Transportation	Cognitive	EEG, PPG, GSR
Fu et al. [49] 2020	Transportation	Cognitive	EEG Scaling Analysis
Şahan [50] 2016	Business	Cognitive	EEG-Eye tracking-SPSS
Şeker [51] 2017	Cognitive Science	Cognitive	EEG-WEKA
Kısacık [52] 2018	Multidisciplinary	Cognitive	EEG-DEHB
Çetin [53] 2020	Artificial intelligence	Cognitive	EEG- Wavelet Package Transformation
Saymaz [54] 2020	Medical	Cognitive	EEG discrete wavelet transforms
Liu et al. [55] 2016	Sea Navigation	Cognitive	EEG-SVM
Fan et al. [4] 2017	Sea Navigation	Cognitive	EEG-NIFS
Fan et al. [56] 2017	Sea Navigation	Cognitive	EEG-SVM
Wu et al. [57] 2018	Sea navigation	Cognitive	EEG-NASA -TLX
Orlandi and Brooks [58] 2018	Ship Handling	Cognitive	EEG, ECG, and Simulation
Liu et al. [59] 2020	Sea Navigation	Cognitive	EEG-SVM
Taç [60] 2012	Sea Navigation	Cognitive	EEG-ANAM4
Yılmaz [61] 2012	Sea Navigation	Cognitive	EEG: Simulator sleep scoring criteria
Taç [62] 2018	Sea Navigation	Cognitive	EEG-CBT-GTDA-NASA TLX

Borghini et al. [31] conducted a literature review on neurophysiological measurements of pilots and automobile drivers, associating certain aspects of brain activity with concepts such as mental workload, mental fatigue, and

situational awareness. They found that the accuracy of detecting the mental states of drivers and pilots using neurophysiological signals such as EEG, electrooculography (EOG), and heart rate (HR) approaches 90%. Schnell et

al. [30] employed a neurocognitive assessment system called the Cognitive Avionics Toolkit (CATS) in aviation to assess pilot workload before flight using physiological and neurocognitive markers, rather than conducting an actual flight. Other studies have also investigated the potential use of EEG in evaluating the psychophysical condition of pilots and air traffic controllers (ATCo) [32]. Trapsilawati et al. [33] examined the stress levels and brain activity of ATCo operators during conflict resolution, whereas Flumeri et al. [34] studied the human-machine interface and alertness levels of ATCo operators in the context of a highly automated system. The latter proposed a system called the "Vigilance and Attention Controller" that combined EEG and eye tracking techniques.

In the maritime domain, Wu et al. [57] explored the relationship between heart rate and EEG values during maritime operation tasks conducted by maritime students in a simulation environment. Liu et al. [55] developed an EEG-based psychophysiological assessment system for monitoring, training, and assessing seafarers in marine simulators. They used raw EEG data to identify different brain states, including cognitive workload and stress, and provided recommendations based on EEG-based cognitive workload and stress recognition. Taç [60] conducted research on seafarers' cognition and its impact on operational processes, considering factors such as fatigue-drowsiness, noise, and thermal strain. Using EEG devices, Taç observed that fatigue increased, especially during the last quarter of a shift, and that cognitive performance was negatively affected by heat and noise [60]. Yilmaz [61] examined the sleep and fatigue conditions of watchkeeping officers during working and resting hours on a short sea voyage, analyzing EEG data within scenarios prepared in a simulator system. The study revealed that mistakes could occur during navigational shifts due to intense work, unrelated to lack of information, or extraordinary situations. Furthermore, Taç [62] conducted human factor research in the maritime field, finding statistically significant differences in cognitive abilities between ship captains and watch officers through Computer-Based Training (CBT). Proficiency was inversely related to situational awareness levels, and self-evaluation of situational awareness did not significantly correlate with performance.

While previous studies on simulator systems have focused on scenarios, this study aims to investigate the main neurophysiological findings related to measurements of tugboat captains' brain activity during both resting moments and actual navigation performance.

2. Model

The flow model is shown in Figure 1 below the article.

3. Methods

3.1. Electroencephalography and Fast Fourier Transform

In this section, the materials and methods used in this study are described. The brain wave data of the tugboat captains were recorded using an EEG device called Emotiv X and the compatible software Emotiv Pro v2.0. The EEG device was used during real sea navigation, employing an experimental research method. Fourteen standard electrode placements on the scalp, following the international 10-20 system, were used to obtain brain wave data. These electrodes were used to measure the electrical activity of the brain at specific locations. According to the FFT

Fast Fourier Transform/Band power graph values were examined in four maneuvers and compared with the resting and on-duty situations of four tugboat captains. Figure 1 shows the FFT value graph taken at the moment of maneuver by a tugboat captain participating in the research.

FFT was employed to process the brain wave data. FFT is a signal processing technique that converts the information contained in a signal into a usable data format. It decomposes a signal into its frequency components, expressing it as the sum of the cosine and sine fundamental components with different amplitudes, frequencies, and phases [63] (Figure 2).

Alpha waves (8-13 Hz) are commonly observed in awake individuals when they are relaxed or with their eyes closed. They are often detected in the occipital region of the brain and are associated with a state of relaxation or idleness. Alpha waves can be spontaneously generated when there is no specific mental activity. The mu rhythm, a type of alpha wave, is relevant in Brain-Computer Interface (BCI) applications and can be observed in sensorimotor areas. It decreases or disappears when the individual performs or imagines movement. The changes in the alpha activity have been observed during working memory retention, indicating its involvement in cognitive processes [58,64].

Beta waves (13-30 Hz) are typically found in the parietal and frontal lobes of individuals who are awake and actively concentrating. The enhanced beta wave activity is associated with activities such as focused attention, problem-solving, and deep concentration [24]. It can be observed in the anterior and central areas of the brain during such tasks. Studies have reported increased beta band strength in the occipital regions during spatial discrimination tasks and visual attention [11,64].

Delta waves have a frequency range of 0.5-4 Hz and are predominantly observed during slow-wave sleep in infants and adults. These are high-amplitude brain waves associated with deep sleep stages. However, delta waves are not limited

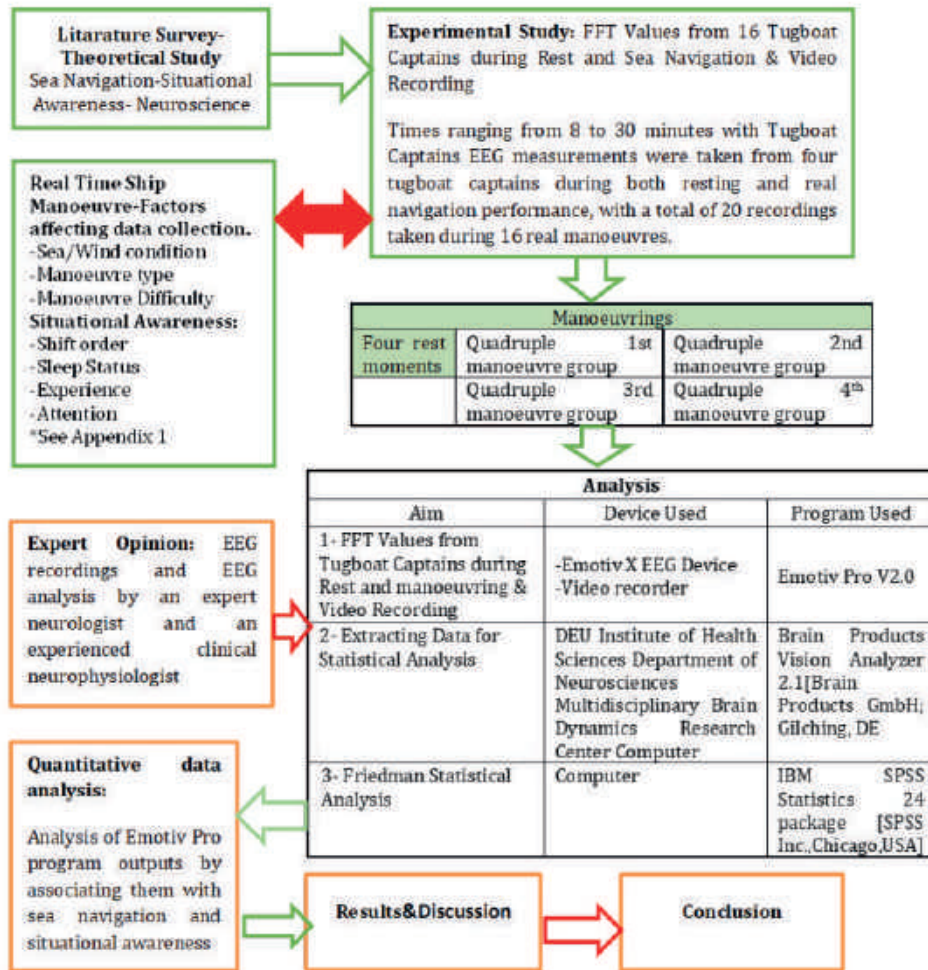


Figure 1. Model

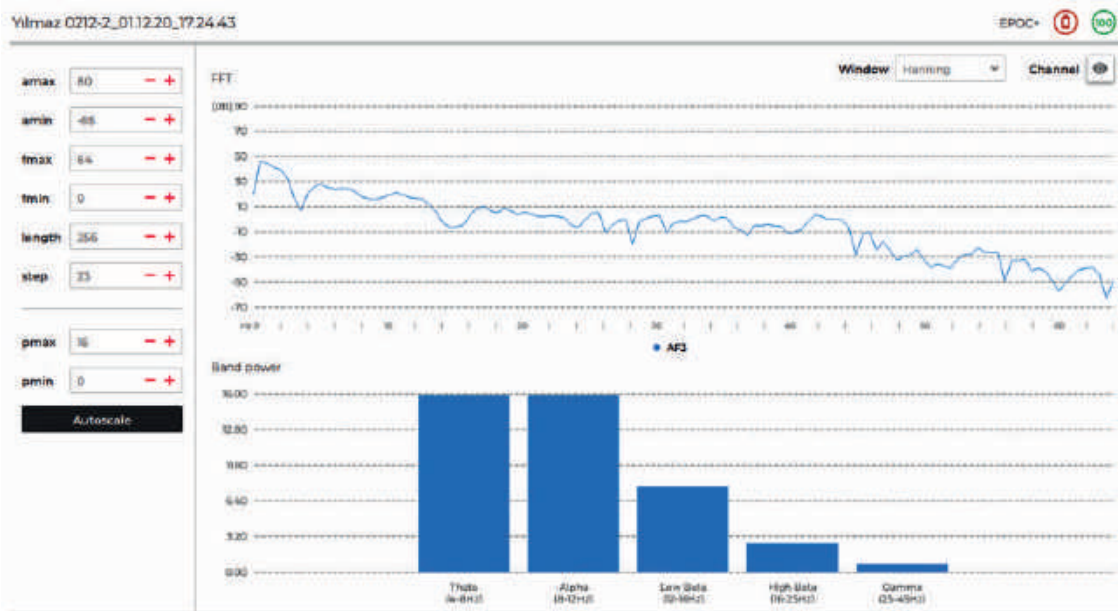


Figure 2. Fourier transform sample chart

to sleep and can also be detected in awake individuals. High frontal delta waves during wakefulness are associated with plasticity and cognitive processing [64].

Theta waves (4-8 Hz) are often associated with drowsiness or idleness in both children and adults. They have been linked to short-term memory and have been identified as a reliable measure of mental workload. Theta wave activity is observed in a drowsy state and is more common in children [11]. In adults, high theta activity without any attention or cognitive activity is considered abnormal and may be associated with certain brain disorders. However, theta activity is critical to attention processing and working memory [64].

Gamma waves have a frequency range of 30-100 Hz or higher and are commonly observed during tasks involving short-term memory and multisensory integration. Fast oscillations typically associated with conscious perception. Gamma activity is involved in attention, working memory, and long-term memory processes. While gamma waves have received less attention than other brain waves, recent studies have reported their relevance in motor tasks and their use in BCIs [9]. High gamma activity at temporal locations is associated with memory processes [64].

3.2. Experiment, Data Collection and Limitations

In this experimental study, data were collected from tugboat captains who worked shifts at the TCDD Izmir Port. These captains assist in the berthing and departure operations of ships at the port. The tugboat captains had an average age of 45 years and an average professional experience of 22 years. Their education levels varied, with two having vocational high school degrees, one with a college degree, and one with a bachelor's degree.

The tugboat captains worked according to a 6-day on (work) and 7-day off (rest) system, operating 24 h a day to accommodate ship traffic at Izmir Port. The experiment focused on real-time sea navigation, capturing brain wave data during the captains' duties. During data collection, moments of blinking and data contamination with artifacts were not considered for evaluation. One limitation of the study is the small number of participants, which is attributed to the difficulty in accessing and obtaining voluntary participation from tugboat captains involved in operationally critical ship maneuvers. However, the similarity in gender and age among the participating captains contributes to the relative homogeneity of the research sample. In addition, the study benefits from optimal conditions for using a mobile EEG device during real-time sea navigation. The small sample size and specific context of the study may limit the generalizability of the findings (Figure 3).



Figure 3. The view of a ship's captain with an EEG device connected while sailing

In the experiment, various data related to navigational conditions and situational awareness were collected from the tugboat captains. EEG measurements were taken from four tugboat captains during both resting and real navigation performance, with four tugboat captains, a total of 20 recordings taken during 16 real maneuvers. The dataset in Appendix 1 includes the following information:

Navigational Data:

- Name of the tugboat
- The type of navigation
- Sea and meteorological conditions
- The type of ship involved in manoeuvre
- The duration of navigation.

Situational Awareness Data:

- Date and time of the experiment
- Age of the captain
- Shift order of the captain
- Sleep status of the captain.

Initially, EEG measurements were taken from the tugboat captains while the tugboat was not navigating. This was done in a quiet environment on the bridge when the tugboat's main engines were not in operation.

Subsequently, the captains of the tugboats, operating in a sequential system based on the Izmir Port traffic, underwent EEG data collection during maneuvers. Each maneuver lasted between 3 and 30 min, and simultaneous video recordings were made.

During the maneuvers, the FFT/Band power graph values were recorded. The tugboats, stationed at a specific location in the port, would depart from their position for each maneuver and navigate to the side of the ship with which they were assisting. The captains then await orders from the maritime pilot responsible for the maneuver either delivering their rope from the bow or stern. According to the captains' statements, all recordings were taken after a minimum of 7 h of sleep.

The following conditions were considered when collecting data from the tugboat captains during real ship maneuvers:

- Ship maneuvers were a part of the sea voyage and were based on the course of the tugboats assisting ships approaching or departing from the port. The berth where the assisted ship would dock or depart from, and the type of vessel involved in the maneuver were also recorded.
- Tugboats and tugboat captains were selected as the sample because of their lower risk to maritime safety and the practical feasibility of the study.
- Although the characteristics of the tugboat were disregarded, the size of the maneuverer ship was considered during the situational awareness stage.
- Weather conditions, including wind strength and direction, sea conditions, current (knots), and visibility (miles), were noted. Local traffic, emergency situations, and accident probabilities were carefully observed during the study.
- Demographic information, such as the age, professional experience, and education status of the tugboat captain, as well as their sleep status (number of hours slept before the experiment) and the day of their current shift, were recorded.
- Because a mobile EEG device was used, the recorded values during the maneuver may have been influenced by other navigational devices present on the ship's bridge.
- The second half of the experimental study was conducted under COVID-19 conditions.

3.3. EEG Analysis

Offline analyzes were performed using Brain Products Vision Analyzer 2.1 [Brain Products GmbH; Gilching, Germany] by Dokuz Eylül University Institute of Health Sciences Department of Neuroscience Multidisciplinary Brain Dynamics Research Centre Specialist (4th author Dilara Mermi Dibek). The sampling rate of continuous EEG recordings was resampled to 256 Hz. Independent Component Analysis [ICA] with classical sphering and infomax algorithm was applied to data to eliminate artifacts. The EEG was filtered with a 0.3 low pass and 50 Hz Notch filter and a 12 dB/octave slope, and then segmented into 2000 ms epochs. Artefacts were manually eliminated following visual inspection. A minimum of 70 epochs were included in the analysis.

FFT was applied to all artefact-free epochs using maximum resolution power, Hanning window function, and non-complex output on the half spectrum with a resolution of 0.5 Hz. The peak power for each frequency (delta: 0.5-3.5 Hz, theta: 4-7.5 Hz, alpha: 8-12.5 Hz, beta: 15-30 Hz, gamma: 30-47.5 Hz) was calculated. The 14 electrodes were grouped as frontal (AF3, AF4, F3, F4, F8, FC5, FC6), temporal (T7, T8), parietal (P7, P8), and occipital (O1, O2).

4. Statistical Analysis

Data were statistically analyzed using IBM SPSS Statistics 24 package (SPSS Inc., Chicago, USA). Because our data did not meet the criteria for parametric analysis, the non-parametric Friedman Test with within-subject design 5 level variable [Resting State (RS), Maneuver-1, Maneuver-2, Maneuver-3, Maneuver-4, and Maneuver-5] was used. Post-hoc comparisons were calculated using the Bonferroni correction.

The Friedman test is a statistical analysis technique used to make meaningful comparisons between dependent groups in cases where the assumption of normality is not provided [65,66]. Citing Daniel (1990) [66] asymptotic efficiency of the Friedman test statistic, it is $0.955k/(k+1)$ if the main mass is normally distributed, $k/(k+1)$ if the main mass is evenly distributed, and $3k/2(k+1)$ if the main mass is double exponentially distributed.

5. Results and Discussion

Situational awareness is an important cognitive ability for a ship captain in sea navigation [67]. It is essential for ship captains to perceive what is happening around them, to understand them in line with their target, and to make decisions by interpreting this information effectively, primarily for environmental safety and for life and environment safety. In conclusion, this experimental study aimed to investigate the relationship between the resting moments of tugboat captains and their neurophysiological brain activity during real sea navigation, focusing on situational awareness. EEG measurements were taken from four tugboat captains during both resting and real navigation performance, with 20 recordings taken during 16 real maneuvers.

The findings of the statistical values obtained from the participants because of the FFT analysis within the scope of the experiment are given below.

Delta wave power: A non-parametric Friedman test produced a significant difference in temporal delta power between Maneuver-4 and the resting state [$X^2=11.00$, $p=0.027$], showing that the temporal delta power decreased during Maneuver-4 [MR=1.75] compared with the resting state [MR=5.00] [$p=0.037$].

Theta wave power: The Friedman test showed a significant difference in temporal theta power [$X^2=9.60$, $p=0.048$] between Maneuver-3 [MR=1.50] and resting state [MR=4.75], indicating that theta power decreased during Maneuver-3 compared with the resting state.

Alpha wave power: The Friedman test showed a significant difference in temporal alpha power [$X^2=11.60$,

$p=0.021$], but post-hoc comparisons showed no significant difference between conditions.

Beta wave power: A non-parametric Friedman test revealed a significant difference in frontal beta power between Maneuver-3 and resting state [$X^2=11.80$, $p=0.019$], and showed reduced frontal beta power during Maneuver-3 [$MR=1.25$] compared to rest [$MR=5.00$] [$p=0.003$].

Gamma wave power: The Friedman test showed significant differences in the frontal gamma [$X^2=10.40$, $p=0.034$] and parietal gamma power [$X^2=9.80$, $p=0.044$]. Both show decreased gamma powers during Maneuver-3 [$MR=1.25$, $MR=1.75$, respectively] compared with the resting state [$MR=4.75$, $MR=5.00$, respectively] [$p=0.017$, $p=0.037$, respectively].

The analysis of the EEG data revealed interesting findings. There was a decrease in theta power and frontal beta power during the third maneuver indicating increased attention and perception. This maneuver seemed to involve higher alertness and attention levels than the other maneuvers previous studies (Kastle et al. [14]; Borghini et al. [31]; Deolindo et al. [67]) have also shown that an increase in theta power and changes in the alpha band are associated with decreased vigilance, whereas an increase in beta power indicates decreased alertness and arousal [68].

Enhanced beta waves were observed in the frontal and central lobes of the brain during activity, anxious thinking, problem-solving, and deep concentration. Gamma activity is involved in attention, working memory, and long-term memory processes [64]. The differences observed in the third maneuver may be attributed to the timing of the maneuvers with two conducted at night and one conducted in the early morning or evening. This suggests that maneuvers may be performed more comfortably during the daytime, and the use of "working memory" may be higher during dark or near-dark times.

During the fourth maneuver which involved berthing larger ships close to the end of the shift, higher mental workload was observed compared with the other maneuvers. However, there was no remarkable change in the alpha frequency throughout all four maneuvers indicating that the maneuvers did not significantly affect the situational awareness of the ship captains.

The study did not find a difference in situational awareness and attention based on professional experience, shift order, or insomnia among the registered tugboat captains. Thus, Endsley's [7] "Situational Awareness Dynamic Decision-Making Model during perception, comprehension, and projection revealed no difference between maneuvering and non-maneuvering moments. This shows that these factors may not significantly impact situational awareness.

6. Conclusion

The key finding of the research suggests that professional tugboat captains who participated in the study demonstrated consistent levels of situational awareness during both maneuvering and resting periods. This study contributes to the limited body of research relating to the cognitive sensory status and situational awareness of ship captains in the international maritime field (Liu et al. [55], Fan et al. [4], Orlandi and Brooks [58], Taç [60-62], Yılmaz [61]). The EEG analysis provides real-time feedback on cognitive processing, assisting ship captains in better understanding their environment and anticipating potential risks. By integrating EEG analysis with decision support systems and other technologies, it may be possible to develop more effective strategies to enhance situational awareness and improve safety in sea navigation. Overall, this study presents novel insights into the cognitive aspects of ship captains (tugboat captains) during real navigation using neuroscience methodologies and contributes to the existing literature on situational awareness in the maritime field.

In future research, the data collection process can be enhanced by increasing the number of participants. Moreover, diversifying the types of ships studied can provide valuable insights. Creating a data pool by examining the special operations of different ship types and their captains, such as ferry boats, fast ferries, passenger ships with higher passenger capacities, container ships with high maneuverability and tanker/chemical tanker ships carrying hazardous loads, can be included.

Additionally, investigating the situational awareness of watch officers involved in Bridge Resource Management (BRM) can offer a more comprehensive understanding of navigational decision-making. As the number of female seafarers in the maritime profession increases, studying female ship captains can provide insights into gender-based differences in situational awareness.

To enhance the effectiveness of the results, it would be beneficial to compare the physiological data acquired from ship masters with those of pilots manoeuvring various ships across different straits, channels, and ports worldwide, similar to what was conducted in this study. Such a comprehensive comparison could provide valuable insights into the cognitive processes of navigators in diverse maritime settings, leading to a broader understanding of situational awareness in sea navigation.

Although previous studies have often used simulator-based approaches, incorporating real-time data into new studies can yield novel findings. Examining navigation data collected during both day and night, in heavy weather and heavy traffic environments, can shed light on the impact of

these factors on situational awareness. Moreover, exploring variations marine life and professional experiences can provide a valuable context for understanding situational awareness.

The neuroscience approach in sea navigation can significantly contribute to navigational science and unveil the underlying brain functions related to situational awareness. As a pioneering real-time study in this field, this research is anticipated to set an example for the maritime sector. It also holds the potential for comparison with similar studies conducted on seafarers from different nationalities, offering cross-cultural insights.

Furthermore, the predictions made by Southampton University's technology department regarding the 2030 maritime trends [69], which encompass unmanned systems, artificial intelligence, sensors, situational awareness, connectivity, cybersecurity, energy management, and sustainability, are highly relevant. The remarkable relationship between situational awareness and artificial intelligence can be further explored using the data obtained from this study. Utilizing the extensive dataset, research techniques can be developed to enhance professional competence and the recruitment process of ship captains, pilots, and watch officers. Ultimately, this can lead to significant advancements in the maritime industry.

Acknowledgements

DEU Institute of Health Sciences, Department of Neurosciences, Multidisciplinary Brain Dynamics Research Centre for data extraction, cleaning, and classification of artifacts (Dilara Mermer Dibeek).

Ethics and App Permissions

- An application was submitted to the DEU Faculty of Medicine Non-Invasive Research Ethics Committee. On 21/09/2020, after the board's correction request, the application was re-applied and finally "Ethics Committee Approval" was received on 28/09/2020 (approval no: 2020/23-23 and date: 28.09.2020).
- In this process, application permits were obtained from the General Directorate of Coastal Safety (16565290-929-E-36761) dated 17.08.2020 and TCDD İzmir Port (51968 number-03.07.2020).

Peer-review: Internally peer-reviewed.

Authorship Contributions

Concept design: S. Kahraman, Data Collection or Processing: S. Kahraman, Analysis or Interpretation: S. Kahraman, D. A. Deveci, İ. Öztura, D. Mermer Dibeek, Literature Review: S. Kahraman, D. A. Deveci, İ. Öztura, D. Mermer Dibeek, Writing, Reviewing and Editing: S. Kahraman, D. A. Deveci, İ. Öztura, D. Mermer Dibeek.

Funding: The Emotiv X EEG device and Emotiv Pro V2.0 program used in this study were supported and implemented as part of the Dokuz Eylül University Scientific Research Project, project numbered 2020. KB.FEN .014 (20204).

References

- [1] A. Erol, "Gemi Kullanma", *İstanbul: Güryay Matbaacılık Tic. Ltd. Şti*, 1987.
- [2] S. Nas, "Teknik seyir hizmetlerinde kaynakların simülasyon modellemesi yöntemiyle optimizasyonu: römorkör park yeri seçimi," *Dokuz Eylül Üniversitesi Denizcilik Fakültesi Dergisi*, vol. 5, pp. 57-81, 2013.
- [3] S. Nas, E. D. Özkan, and E. Uçan, "The determination of the number of tugboats in the area of towage service authorization by using simulation modelling technique," *Journal of ETA Maritime Science*, vol. 4 pp. 91-99, 2016.
- [4] S. Fan, X. Yan, J. Zhang, and J. Wang, "A review on human factors in maritime transportation using seafarers' physiological data," *2017 4th International Conference on Transportation Information and Safety (ICTIS)*, pp. 104-110, Aug 2017.
- [5] Allianz Global Corporate & Specialty, 2020. *Safety and shipping review*. <https://commercial.allianz.com/news-and-insights/reports/shipping-safety.html>
- [6] Right Ship newsletter, 2023. *Half of maritime incidents in 2022 occurred in ports and terminals*. <https://rightship.com/insights/half-maritime-incidents-2022-occurred-ports-and-terminals>, [Accessed: May 25, 2023].
- [7] M.R. Endsley, *Toward a theory of situational awareness in dynamic systems*. Human Factors Lubbock: Human Factors and Ergonomics Society, vol. 37, pp. 32-64, Mar 1995.
- [8] S. Kahraman, *Situational Awareness Analysis of Port Pilotage Services* (Master Thesis). İzmir: Dokuz Eylül University Graduate School of Social Sciences Marine Transportation Engineering Department Maritime Safety, Security and Environment Management Program, 2016. <https://tez.yok.gov.tr/>
- [9] R. Parasuraman, T.B. Sheridan, and C.D. Wickens, "Situation awareness, mental workload and trust in automation: viable, empirically supported cognitive engineering constructs," *Journal of Cognitive Engineering and Decision Making*, Vol. 2, pp. 140-160, 2008.
- [10] R. P. N. Rao, "Brain-computer interfacing an introduction", *Cambridge University Press, Newyork*, pp. 26-27, 2013.
- [11] Z. Yin, and J. Zhang, "Identification of temporal variations in mental workload using locally-linear-embedding-based EEG feature reduction and support-vector-machine-based clustering and classification techniques," *Computer Methods and Programs in Biomedicine*, 115, pp. 119-134, Apr 2014.
- [12] H. Abut, et al. "Real-world data collection with "UYANIK"", *In-Vehicle Corpus and Signal Processing for Driver Behavior New York: Springer Science-Business Media*, pp. 23-43, 2009.
- [13] A. C. Johnson, et al. "Decreased alertness reconfigures cognitive control networks," *The Journal of Neuroscience*, vol. 40, pp. 7142-7154, Sep 2020.
- [14] J. Kastle, B. Anvari, J. Krol, and A. H. Wurdeman, "Correlation between situational awareness and EEG signals," *Neurocomputing*, vol. 432, pp. 70-79, Dec 2021.

- [15] K. Tong, K. Leung, and Y. Leung, "A System for personalized health care with ECG and EEG signals for analysis," *2017 International Smart Cities Conference (ISC2)*, pp. 1-6, 2017.
- [16] Z. B. Loris, M. Danzi, J. Sick, W. D. Dietrich, H. M. Bramlett, and T. Sick, "Automated approach to detecting behavioral states using EEG-DABS." *Heliyon*, vol. 3, e00344, 2017.
- [17] M. D. Başar, A. D. Duru, S. Ş Özgör, C. Özgör, and A. Akan, "Analysis of reduced EEG channels based on emotional stimulus", *26th Signal Processing and Communications Applications Conference*. pp. 1-4, 2018.
- [18] K. Tsekoura, and A. Foka, "Classification of EEG signals produced by musical notes as stimuli," *Expert Systems with Applications*, vol. 159, pp. 113507, Nov 2020.
- [19] S. Çelik, R. B. Doğan, C. S. Parlatan, and B. Güntekin, "Distinct brain oscillatory responses for the perception and identification of one's own body from other's body," *Cognitive Neurodynamics*, vol. 15 pp. 609-620, Jan 2021.
- [20] A. Mheich, et al. "HD-EEG for tracking sub-second brain dynamics during cognitive tasks," *Scientific Data*, vol. 8, pp. 32, Jan 2021.
- [21] M. Kocúrová, and J. Juhár, "A novel approach to EEG speech activity detection with visual stimuli and mobile BCI," *Applied Sciences*, vol. 11, pp. 674, 2021.
- [22] O. Yakobi, J. Boylan, and J. Danckert, "Behavioral and electroencephalographic evidence for reduced attentional control and performance monitoring in boredom," *Psychophysiology*, vol. 58, e13816, Mar 2021.
- [23] M. T. Wal, et al. "Human stereo EEG recordings reveal network dynamics of decision-making in a rule-switching task," *Nature Communications*, vol. 11 pp. 3075, June 2020.
- [24] H. Kirschner, J. Humann, J. Derrfuss, C. Danielmeier, and M. Ullsperger, "Neural and behavioral traces of error awareness," *Cognitive, Affective, & Behavioral Neuroscience*, vol. 21 pp. 573-591, 2021.
- [25] A. Kaur, R. Chaujar, and V. Chinnadurai, "Effects of neural mechanisms of pretask resting EEG Alpha information on situational awareness: a functional connectivity approach," *Human Factors*, vol. 62, pp. 1150-1170, Aug 2020.
- [26] Q. Ma, M. Wang, L. Hu, L. Zhang, and Z. Hua, "A novel recurrent neural network to classify EEG signals for customers decision making behavior prediction in brand extension scenario," *Frontiers in Human Neuroscience*, vol. 15 pp. 610890, Mar 2021.
- [27] X. Jin, Y. Lu, B. D. Hatfield, X. Wang, B. Wang, and C. Zhou, "Ballroom dancers exhibit a dispositional need for arousal and elevated cerebral cortical activity during preferred melodic recall," *PeerJ*, vol. 9, e10658, Jan 2021.
- [28] M. Nann, N. Peekhaus, C. Angerhöfer, and S. R. Soekadar, "Feasibility and safety of bilateral hybrid EEG/EOG brain/neural machine interaction," *Frontiers in Human Neuroscience*, vol. 14, pp. 580105, 2021.
- [29] C. Berka, D. J. Levendowski, G. Davis, M. Whitmoyer, K. S. Hale, and S. Fuchs, "Objective Measures of Situational Awareness Using Neurophysiology Technology," *Augmented Cognition Conference Past, Present and Future, Orlando, FL USA*, pp. 145-154, 2006.
- [30] T. Schnell, M. Keller, and P. Poolman, "Neurophysiological workload assessment in flight," *27th Digital Avionics Systems Conference*. pp. 4, 2008.
- [31] G. Borghini, L. Astolfi, G. Vecchiato, D. Mattia, and F. Babiloni, "Measuring neurophysiological signals in aircraft pilots and car drivers for the assessment of mental workload, fatigue and drowsiness," *Neuroscience and Biobehavioral Reviews*, vol. 44, pp. 58-75, Oct 2012.
- [32] M. Galant, and J. Merksiz, "Analysis of the possibilities of using EEG in assessing pilots' psychophysical condition," *Scientific Journal of the Silesian University of Technology Series Transport* vol. 95, pp. 39-46, Apr 2017.
- [33] F. Trapsilawati, M.K. Herliansyah, A.S.A.N.S. Nugraheni, M.P. Fatikasari, and G. Tissamodie, "EEG-based analysis of air traffic conflict investigating controller's situation awareness stress level and brain activity during conflict resolution," *The Journal of Navigation*, pp. 1-19. Oct 2019.
- [34] D. G. Flumeri, et al. "Brain-computer interface-based adaptive automation to prevent out-of-the-loop phenomenon in air traffic controllers dealing with highly automated systems," *Frontiers in Human Neuroscience*, vol. 13, Sep 2019.
- [35] O. W. Klaproth, C. Vernaleken, L. R. Krol, M. Halbruegge, T. O. Zander, and N. Russwinkel, "Tracing pilots' situation assessment by neuroadaptive cognitive modeling," *Frontiers in Neuroscience*, vol. 14, Aug 2020.
- [36] H. Polat, and M. S. Özerdem, "Reflection of emotions based on different stories onto EEG signal," *Türkiye Bilişim Vakfı Bilgisayar Bilimleri ve Mühendisliği Dergisi*, vol. 9, pp. 2618, 2016.
- [37] A. T. Sözer, and C. B. Fidan, "Emotiv epoc ile durağan hal görsel uyarılmış potansiyel temelli beyin bilgisayar arayüzü uygulaması," *BEU Journal of Science*, vol. 8, pp. 158-166, 2019.
- [38] T. B. Alakuş, and İ. Türkoğlu, "EEG based emotion analysis systems," *Türkiye Bilişim Vakfı Bilgisayar Bilimleri ve Mühendisliği Dergisi*, Vol. 11, pp. 26, 2018.
- [39] M. U Iqbal, B. Srinivasan, and R. Srinivasan, "Dynamic assessment of control room operator's cognitive workload using Electroencephalography (EEG)," *Computers and Chemical Engineering*, vol. 141, pp. 106726, Oct 2020.
- [40] P. Ackermann, C. Kohlschein, J. A Bitschx, K. Wehrlex, and S. Jeschke, "EEG-based automatic emotion recognition:feature extraction, selection and classification methods," *IEEE 18th International Conference on e-Health Networking, Applications and Services*, pp. 1-6, 2016
- [41] M. Kaya, M. Cömert, and Y. Mishchenkoa, "Brain-computer interface detection of right- and left-hand movement imageries from EEG Data Using the SVM machine learning method," *TÜBAV Bilim*, vol. 10, pp. 1-20, 2017.
- [42] T. S. Roy, S. Mazumder, and K. Das, "Wisdom of crowds benefits perceptual decision making across difficulty levels", *Scientific Reports*, vol. 11, 2021.
- [43] X. Xiaolil, H. Jiangbi, L. Xiaoming, L. Pingsheng, and W. Shuyun, "The EEG changes during night-time driver fatigue". *IEEE Intelligent Vehicles Symposium*, pp. 935-939, 2009.
- [44] H. Kim, Y. Hwang, D. Yoon, W. Choi, and C. H. Park, "Driver workload characteristics analysis using EEG data from an urban road," *IEEE Transactions on Intelligent Transportation Systems*, vol. 15, pp. 1844-1849, 2014.
- [45] Q. He, W. Li, X. Fan, and Z. Fei, "Evaluation of driver fatigue with multi-indicators based on artificial neural network," *The*

- Institution of Engineering and Technology*, vol. 10, pp. 555-561, Oct 2016.
- [46] J. Lee, and J. H. Yang, "Analysis of driver's EEG given take-over alarm in SAE level 3 automated driving in a simulated environment," *International Journal of Automotive Technology*, vol. 21, pp. 719-728, 2019.
- [47] J. Hu, F. Liu, and P. Wang, "EEG-based multiple entropy analysis for assessing driver fatigue," *The 5th International Conference on Transportation Information and Safety*, pp. 1290-1294, 2019.
- [48] S. Siddharth, and M. M. Trivedi, "On assessing driver awareness of situational criticalities: multi-modal bio-sensing and vision-based analysis, evaluations, and insights," *Brain Sciences*, vol. 10, 2020.
- [49] R. Fu, M. Han, B. Yu, P. Shi, and J. Wen, "Phase fluctuation analysis in functional brain networks of scaling EEG for driver fatigue detection," *Traffic & Transportation*, vol. 32, pp. 487-495, 2020.
- [50] Y. Şahan, Determination of Web Site Desinging Features Which are Effective on Consumers Tourist Purchasing Decision in Tourism Marketing by The Methods of Electroencephalograph and Eye Tracking from Technique of Neuroimaging (Master Thesis). Çorum: Hitit University Graduate School of Social Sciences Business Administration Program, 2016.
- [51] M. Şeker, Emotiv-Epoc Based Electroencehalographic (Eeg) Responses to Pleasant - Unpleasant Odors Classification Using Machine Learning Algorithms (Master Thesis). Diyarbakır: Department of Electrical and Electronics Engineering Institute of Natural and Applied Sciences University of Dicle, 2017.
- [52] E. Kısacık, The Investigation of Attention Processes on Participants with and Without Attention Deficit Hyperactivity Disorder Symptoms: An EEG Study (PhD Thesis). Ankara: Ankara University Graduate School of Health Sciences, 2018.
- [53] E. Çetin, Mobile EEG Based Hunger and Satiety Classification (Master Thesis). Antalya: Akdeniz University Electrical and Electronics Engineering, 2020.
- [54] A. Saymaz, Evaluation of Happiness Training Effect of EEG Signals with Machine Learning Methods (Master Thesis). İstanbul: İstanbul University-Cerrahpasa Institute of Graduate Studies Department of Biomedical Engineering, 2020.
- [55] Y. Liu, X. Hou, O. Sourina, D. Konovessis, and G. Krishnan, "Human factor study for maritime simulator-based assessment of cadets," *ASME 2016 35th International Conference on Ocean, Offshore and Arctic Engineering*, vol. 49941, pp. V003T02A073, Oct 2016.
- [56] S. Fan, et al. "Effects of seafarers' emotion on human performance using bridge simulation," *Ocean Engineering*, vol. 170 pp. 111-119, Dec 2018.
- [57] Y. Wu, T. Miwa, and M. Uchida, "Using physiological signals to measure operator's mental workload in shipping – an engine room simulator study," *Journal of Marine Engineering & Technology*, vol. 16, pp. 61-69, Jan 2017.
- [58] L. Orlandi, and B. Brooks, "Measuring mental workload and physiological reactions in marine pilots: building bridges towards redlines of performance," *Applied Ergonomics*, vol. 69, pp. 74-92, Jan 2018.
- [59] Y. Liu, et al. "Psychophysiological evaluation of seafarers to improve training in maritime virtual simulator", *Advanced Engineering Informatics*, vol. 44, Apr 2020.
- [60] U. Taç, Modelling the Cognition of Seafarers under Stresor Factors and Its Effect on Operational Processes in Maritime Transportation (Master Thesis). İstanbul: İstanbul Technical University the Graduate School of Natural and Applied Sciences Maritime Transportation and Management Engineering Graduate Program, 2012.
- [61] H. Yılmaz, Determination of Fatigue and Sleep States of Watchkeeping Officers with Help EEG and Bridge Simulator (Master Thesis). Trabzon: Karadeniz Technical University the Graduate School of Natural and Applied Sciences Maritime Transportation and Management Engineering Graduate Program, 2012.
- [62] U. Taç, Modelling Cognitive Abilities of Seafarers with Regards to Situational Awareness (Master Thesis). İstanbul: İstanbul Technical University the Graduate School of Natural and Applied Sciences Maritime Transportation and Management Engineering Graduate Program, 2018.
- [63] Z. Cömert, *Yazılım Mühendisliği Ders notları*. Samsun Üniversitesi, <http://www.zafercomert.com/IcerikDetay.aspx?zcms=157>.
- [64] A.S. Malik, and H.U. Amin, *Designing EEG Experiments for Studying the Brain*, Academic Press, London, pp. 2-4, 2017.
- [65] M. Gola, M. Magnuski, I. Szumska, and A. Wróbel, "EEG beta band activity is related to attention and attentional deficits in the visual performance of elderly subjects," *International Journal of Psychophysiology*, vol. 89, pp. 334–341, May 2013.
- [66] Y. Karagöz, "Nonparametrik tekniklerin güç ve etkinlikleri", *Elektronik Sosyal Bilimler Dergisi*, vol. 9 pp. 18-40, 2010.
- [67] C. Deolindo, et al. "Microstates in complex and dynamical environments: Unraveling situational awareness in critical helicopter landing maneuvers", *Human Brain Mapp*, vol. 42, pp. 1-14, Mar 2021.
- [68] C. Gao, J. Liu, Y. Zhang, C. Li, and S. Wang, "Using EEG to evaluate situational awareness of ship navigators", *Journal of Marine Science and Engineering*, vol. 6, pp. 55, 2018.
- [69] F. Lockwood, et al. "Global Marine Technology Trends 2030", Southampton University, Aug 2017.

Appendix 1. Data Set

No	Date	Time	Captain	Tugboat	Navigation Datas				Situational Awareness Datas						
					Navigation Type	Maneuver	Wind Force	Wave	Wind direction	Wind direction	Air Temperature	Departure Time	Age	Date of duty/Exp. day	Total Sleep Hour
							Beaufort Scale	0-360 degree	Celcius	minutes-seconds	Year				
1	17.09.2020	11:57	1	KIZKULES	#16 Departure	Container	3	2	32	35	27	08:02	41	6/1	8
2	17.09.2020	12:00	1	KIZKULES	#10 Departure	General Cargo	3	2	32	35	27	05:00	41	6/2	8
3	17.09.2020	12:27	1	KIZKULES	#5 Departure	General Cargo	3	2	32	35	27	10:13	41	6/3	8
4	17.09.2020	12:54	1	KIZKULES	#12 Departure	General Cargo	3	2	32	35	27	02:51	41	6/4	8
5	17.09.2020	15:06	1	KIZKULES	#12 Yanaşma	General Cargo	3	2	32	35	27	19:01	41	6/5	8
6	11.10.2020	15:53	1	KIZKULES	Resting	..	5	6	250	250	24	05:06	41	1/1	9
7	11.10.2020	13:49	2	KIZKULES	Resting	..	5	6	250	250	24	04:25	45	1/1	9
8	11.10.2020	14:10	2	KIZKULES	#13 Arrival	Container	5	6	250	250	24	20:00	45	1/1	9
9	11.10.2020	14:35	2	KIZKULES	#26 Arrival	Multi Purpose	5	6	250	250	24	30:53	45	1/1	9
10	11.10.2020	16:38	2	KIZKULES	#7 Departure	General Cargo	5	6	250	250	24	12:52	45	1/1	9
11	3.11.2020	17:19	3	GARP	#26 Departure	General Cargo	2	1	33	35	21	02:58	45	6/1	8
12	3.11.2020	17:40	3	GARP	Resting	..	2	1	33	35	21	04:00	45	6/1	8
13	4.11.2020	16:47	1	KIZKULES	#13 Departure	Container	2	4	40	30	19	22:17	41	5/4	5
14	4.11.2020	17:41	1	KIZKULES	#25 Arrival	Multi Purpose	2	4	40	30	19	35:39	41	5/4	5
15	5.11.2020	14:50	4	ZÜBEYDE ANA	#13 Arrival	Konteyner	4	5	38	35	20	14:40	40	7/3	8
16	5.11.2020	16:11	3	GARP	#12 Arrival	General Cargo	4	5	30	30	20	21:02	45	6/5	7
17	5.11.2020	17:54	3	GARP	#25 Arrival	Tanker	4	5	30	30	20	24:03	45	6/5	7
18	5.11.2020	18:57	3	GARP	#26 Arrival	Multi Purpose	4	5	30	30	20	12:17	45	6/5	7
19	5.11.2020	19:30	3	GARP	#8 Departure	Volgabalt	4	5	30	30	20	13:24	45	6/5	7
20	7.11.2020	14:50	2	KIZKULES	#14 Departure	Container	5	6	35	35	19	12:58	45	5/2	8
21	7.11.2020	16:14	2	KIZKULES	#7 Departure	General Cargo	5	6	35	35	19	07:08	45	5/2	8
22	7.11.2020	16:57	2	KIZKULES	#16 Departure	Container	5	6	35	35	19	05:51	45	5/2	8
23	7.11.2020	17:29	2	KIZKULES	#23 Departure	General Cargo	5	6	35	35	19	11:05	45	5/2	8
24	20.11.2020	14:28	3	GARP	Resting	..	3	2	35	35	16	01:18	45	6/2	5
25	20.11.2020	14:41	3	GARP	#12 Departure	General Cargo	3	2	35	35	16	13:12	45	6/2	5
26	20.11.2020	16:12	3	GARP	#12 Arrival	General Cargo	3	2	35	35	16	18:16	45	6/2	5
27	26.11.2020	08:18	2	KIZKULES	#16 Arrival	Container	3	4	30	30	9	06:06	45	6/3	7
28	26.11.2020	09:09	2	KIZKULES	#3 Arrival	Multi Purpose	3	4	30	30	9	19:40	45	6/3	7
29	1.12.2020	13:22	3	GARP	#26 Arrival	Tanker	3	4	35	35	16	17:23	45	8/2	6
30	1.12.2020	17:24	3	GARP	#12 Arrival	General Cargo	3	4	35	35	14	23:11	45	8/2	6
31	1.12.2020	18:19	3	GARP	#7 Departure	General Cargo	2	1	30	30	10	12:25	45	8/2	6
32	1.12.2020	19:35	3	GARP	#7 Arrival	General Cargo	2	1	30	30	10	21:24	45	8/2	6
33	2.12.2020	11:30	3	GARP	#10 Departure	General Cargo	2	1	40	40	8	08:38	45	8/3	7
34	2.12.2020	12:15	3	GARP	#25 Arrival	General Cargo	2	1	40	40	8	14:51	45	8/3	7
35	2.12.2020	12:59	3	GARP	#8 Departure	General Cargo	2	1	40	40	8	14:40	45	8/3	7
36	2.12.2020	13:58	3	GARP	#10 Arrival	General Cargo	2	1	40	40	8	21:21	45	8/3	7
37	7.12.2020	16:54	4	ZÜBEYDE ANA	Resting	..	3	3	25	25	17	01:18	40	5/3	4
38	7.12.2020	17:19	4	ZÜBEYDE ANA	#4-5 Arrival	Bulk Carrier	3	3	25	25	17	18:05	40	5/3	4
39	7.12.2020	18:25	3	GARP	#10 Arrival	General Cargo	3	3	25	25	17	15:29	45	7/7	7
40	10.12.2020	05:51	4	ZÜBEYDE ANA	#17 Arrival	Container	4	2	225	220	11	28:08	40	5/5	3
41	10.12.2020	06:54	4	ZÜBEYDE ANA	#16 Arrival	Container	4	2	225	220	11	26:54	40	5/5	3
42	10.12.2020	08:01	5	Kurtarma 1	#13 Arrival	Container	4	2	225	220	12	27:14	42	5/4	0

Estimation of Human Errors During Cargo Unloading Operations on Bulk Carriers Using SLIM and Interval Type 2 Fuzzy Sets

✉ Ahmet Lutfi Tunçel^{1,2}, ✉ Pelin Erdem², ✉ Osman Turan²

¹Istanbul Technical University, Department of Maritime Transportation and Management Engineering, İstanbul, Türkiye

²University of Strathclyde, Department of Naval Architecture, Ocean and Marine Engineering, Glasgow, United Kingdom

Abstract

Cargo unloading operations on bulk carriers are critical shipboard operations. Many tasks are expected to fulfill by the ship's personnel to safely complete this type of operation. However, many human errors may occur during this process, and this situation threatens the safety of life and property. In this respect, this study predicts potential human errors and probabilities that may occur during cargo unloading operations on bulk carrier ships. In this study, an integrated human error prediction approach is proposed using interval type 2 fuzzy sets and the success likelihood index method. Thus, within the scope of this study, a model was obtained that allows human errors to be evaluated both qualitatively and quantitatively. Because of the analyzes made, it has been found that the most common human errors that occur while unloading cargo operations on bulk carriers occur in the processes of following the ballast operation and performing the tasks to prevent excessive trim/list formation on board ship, respectively. In addition, it was concluded that the factors that most shape the performance of the ship's personnel are education, communication, and experience.

Keywords: Unloading operation, SLIM, IT2FS, Human error prediction, Bulk carrier

1. Introduction

Global maritime transport is rapidly growing and has become an even more significant mode for the import and export of bulk cargoes. This expanding volume of global trade causes an enormous rise in port cargo handling capacity and, accordingly, operational vulnerabilities. According to bulk cargo trade data, the global average for loading capsize dry bulk vessels was 34.9 tons per minute, while this quantity reached 6.3 tons per minute for dandyize vessels in 2021 [1]. This means that a high volume of bulk cargo is handled onboard the ship at once, which poses a big challenge to planning and managing cargo handling operations. In particular, cargo handling performance increases with ship size because large vessels can be handled by large cranes, conveyor belts, and other advanced technological equipment.

Humans are considered a key element and a contributing factor to most casualties in the maritime transportation industry. In this regard, the International Maritime Organization emphasizes that the safety performance and competence of seafarers are of critical importance in increasing safety and reducing the risk of possible accidents in operations conducted at sea [2]. Indeed, maritime accidents or incidents occur mostly because of human errors [3,4]. Thus, maritime operations and navigation safety can be enhanced by strengthening the focus on the human element

Cargo unloading operations are critical operations that are expected to perform different tasks simultaneously by the ship crew. In this process, factors such as stress and fatigue may compel the crew in charge to neglect pivotal activities that must be properly performed [5]. In this case, different



Address for Correspondence: Ahmet Lutfi Tunçel, İstanbul Technical University, Department of Maritime Transportation and Management Engineering, İstanbul, Türkiye

E-mail: tuncel.ahmet@itu.edu.tr

ORCID ID: orcid.org/0000-0003-2306-6996

Received: 07.06.2023

Last Revision Received: 15.08.2023

Accepted: 21.08.2023

To cite this article: A. L. Tunçel, P. Erdem, and O. Turan. "Estimation of Human Errors During Cargo Unloading Operations on Bulk Carriers Using SLIM and Interval Type 2 Fuzzy Sets." *Journal of ETA Maritime Science*, vol. 11(3), pp. 198-208, 2023.

©Copyright 2023 by the Journal of ETA Maritime Science published by UCTEA Chamber of Marine Engineers

types of accidents can occur during the cargo unloading operations due to many reasons such as not following the ballast operation [6], deterioration of the stability of the ships [6], and the for reasons related to improper use of deck cranes, especially [7].

However, to prevent potential incidents or accidents that may be encountered during cargo unloading operations and to make operational processes safer, it is expected that the determined tasks will be fulfilled completely by the ship crew. Furthermore, it is thought that the completion of the tasks that must be performed by the ship crew during the cargo unloading operations is of critical importance not only for the safety of life and property but also for the protection of the marine environment.

Probabilistic risk assessments pointing out the human contribution to operational risks should be the focal point of the research because human error has emerged as a significant factor in unsafe cargo handling operations and maritime accidents in recent decades. Risk determination being distinguished from the safety performance of the responsible crew will cause insufficient detection in maritime incidents, accidents, or any undesired events [5].

In the view of literature research, despite some applicable methods presented related to human reliability assessments in high-risk industries such as offshore [8-12], nuclear [13,14], railway [15,16], chemical [17], and maritime [5,18-21] the research directly focusing on human error contributions in bulk cargo loading/unloading operations is quite limited. At this point, a quantitative approach systematically evaluating the potential human error in critical bulk carrier shipboard operations must reduce operational vulnerabilities and enhance safety.

Although determining the impact of human performance on risks arising in operational processes is a critical issue, most human reliability analysis (HRA) techniques are limited in evaluating human performance in all aspects [22]. To illustrate, first-generation HRA techniques, such as the technique for human error rate prediction [23], the success likelihood index method (SLIM) [24], and the human error assessment and reduction technique [25], facilitate human error quantification. Although they are good at emphasizing the success/failure of activities, they have less consideration for human behaviors. On the other hand, a technique for human error analysis [26], cognitive reliability and error analysis method [27], accident dynamics simulator-information, decision, action in crew context, and standardized plant analysis risk-human reliability analysis [28] are considered second-generation approaches that can be used to evaluate the occurrence of human errors, cognitive processes, and human performance. However, it is necessary to analyze organizational factors

very well in determining the failures in studies using these approaches. Third-generation HRA methods, such as the Bayesian network [29], focus on the factors that contribute to the emergence of human errors and other dependent elements associated with these factors, and they are still in progress. Apart from all these, the lack of data is the most significant source of uncertainty in most HRA methods [30]. In particular, data scarcity is the biggest obstacle to HRA applications planned for evaluating human performance during ship operations. In this regard, an effective and consistent HRA implementation must be able to access the data needed for operational processes and evaluate them by an appropriate expert team.

This article aims to quantify the potential human-induced failures in the tasks expected to be performed by ship personnel during the cargo unloading operations of bulk carriers and to provide an idea of what measures may be necessary to prevent future losses. The scarce data for human failure in cargo unloading operations of bulk carrier vessels is the motivation for applying the proposed model consisting of the integration of Type-2 fuzzy logic (T2FL) and SLIM. The SLIM technique is heavily based on domain experts' evaluations that are based on the knowledge and experiences to predict human error. At this point, SLIM has been extended with fuzzy logic to improve consistency and reduce the subjectivity of experts' evaluations. Interval type-2 fuzzy sets (IT2FS) are highly functional for coping with subjectivity and vagueness in the process of using experts' evaluations. While the integrated approach addresses human error probability assessment, the results highlight the importance of human factors in critical cargo unloading operations on bulk carrier vessels.

This paper consists of 5 sections. This section briefly details the human factors, bulk carrier cargo operations, and motivation behind the research. Section 2 introduces the methodologies used in this study and the proposed integrated HRA approach. Chapter 3 estimates human errors and HEPs that may arise during cargo-unloading operations in bulk carrier ships. Section 4 evaluates the outputs of the research. Finally, section 5 concludes the research and advises on future studies.

2. Methodology

2.1. Interval Type 2 Fuzzy Sets (IT2FS)

The conventional fuzzy set, introduced by Zadeh [31] to cope with uncertainties encountered in decision-making processes, was developed as a type-2 fuzzy set (T2FS) in the following years [32]. Although the basic philosophy of both clusters is quite similar, there are also some divergence points. The most obvious aspect of this is that while the membership functions of the traditional fuzzy set consist

of exact values, the membership functions of the T2FSs are fuzzy numbers [5]. In addition, T2FSs has more parameters than the traditional fuzzy set [33,34].

Interval type 2 fuzzy sets (IT2FSs) can be expressed as a more specialized version of the T2FS set [5]. Compared to T2FSs with more general cluster characteristics, IT2FS has a lower computation process for expert feedback to be digitized and converted to crisp values [19]. In addition, thanks to the linguistic evaluation scale it provides, it contributes to experts in making better and more effective decisions. Thus, they are more effective in eliminating possible uncertain conditions. In this respect, IT2FSs have been used in various academic studies based on the expert evaluation recently [5,19,35]. Expressions of mathematical operations performed using IT2FS and T2FS are detailed as follows [19,36-38]:

Expression 1: Let us assume that a T2FS \tilde{A} in the universe X is expressed through a type-2 membership function $\mu_{\tilde{A}}(x,u)$. Here, J_x symbolizes an interval in $[0, 1]$ and can be detailed in the following equation (1) [36-38]:

$$\tilde{A} = \{(x,u), \mu_{\tilde{A}}(x,u) | \forall x \in X, \forall u \in J_x \subseteq [0,1], 0 \leq \mu_{\tilde{A}}(x,u) \leq 1\} \quad (1)$$

In addition, assuming that fuzzy numbers are continuous, T2FS \tilde{A} can be symbolized with the following equation (2) [36]:

$$\tilde{A} = \int_{x \in X} \int_{u \in J_x} \mu_{\tilde{A}}(x,u) / (x,u) = \int_{x \in X} \left(\frac{\int_{u \in J_x} \mu_{\tilde{A}}(x,u)}{u} \right) / X \quad (2)$$

Here, $J_x \subseteq [0,1]$. Also, \int represents session over all admissible x and u figures.

Expression 2: Let us assume that \tilde{A} is a T2FS in the universe of X , as demonstrated via the type-2 membership function $\mu_{\tilde{A}}(x,u)$. Assuming that all $\mu_{\tilde{A}}(x,u) = 1$, in this case \tilde{A} is defined as an IT2FS [19]. In addition, it can be expressed as shown in equation (3) [33,36]:

$$\tilde{A} = \int_{x \in X} \int_{u \in J_x} 1 / (x,u) = \frac{\int_{x \in X} \left(\frac{\int_{u \in J_x} 1}{u} \right)}{x} \quad (3)$$

Here, $J_x \subseteq [0,1]$.

Expression 3: Within the scope of this study, an approach based on taking and evaluating expert opinions using IT2FS is presented. In this direction, the representation of IT2FS covering the upper and lower membership functions is shown in Figure 1. In this respect, the IT2FS used in this study exhibits trapezoidal characteristics.

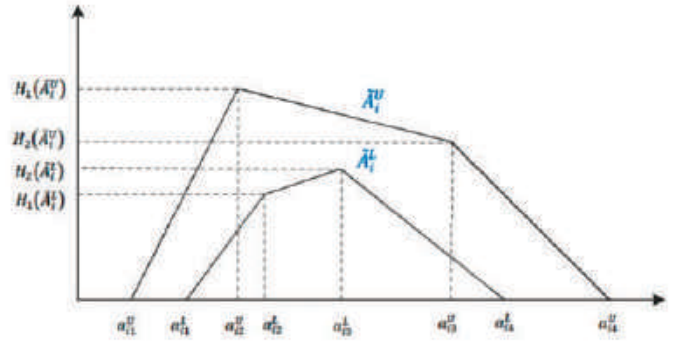


Figure 1. IT2FS membership functions [36]

IT2FS with trapezoidal character

$$\tilde{A}_i = (\tilde{A}_i^u, \tilde{A}_i^l) = \left((a_{i1}^u, a_{i2}^u, a_{i3}^u, a_{i4}^u; H_1(\tilde{A}_i^u), H_2(\tilde{A}_i^u)), (a_{i1}^l, a_{i2}^l, a_{i3}^l, a_{i4}^l; H_1(\tilde{A}_i^l), H_2(\tilde{A}_i^l)) \right)$$

where \tilde{A}_i^u and \tilde{A}_i^l are type-1 fuzzy sets in this expression [19]. In addition, $a_{i1}^u, a_{i2}^u, a_{i3}^u, a_{i4}^u, a_{i1}^l, a_{i2}^l, a_{i3}^l, a_{i4}^l$ are reference points of the IT2FS \tilde{A}_i [5,36,39]. However, $H_j(\tilde{A}_i^u)$ symbolizes the membership value of the parameter $a_{i(j+1)}^u$ in the upper side of the membership function \tilde{A}_i^u , $H_j(\tilde{A}_i^l)$ stands for the membership value of the parameter $a_{i(j+1)}^l$ in the lower side of the membership function \tilde{A}_i^l . Here, j can vary to include 1 and 2 [39].

Expression 4: The center of area (CoA) technique is used for defuzzification and ranking of IT2FS. In the implementation of this operation, the following equation (4) is used [40]:

$$\text{Defuzzified}(\tilde{A}_i) = \frac{(a_{i4}^u - a_{i1}^u) + (H_1(\tilde{A}_i^u) \cdot a_{i2}^u - a_{i1}^u) + (H_2(\tilde{A}_i^u) \cdot a_{i3}^u - a_{i1}^u) + a_{i1}^u + (a_{i4}^l - a_{i1}^l) + (H_1(\tilde{A}_i^l) \cdot a_{i2}^l - a_{i1}^l) + (H_2(\tilde{A}_i^l) \cdot a_{i3}^l - a_{i1}^l) + a_{i1}^l}{2} \quad (4)$$

There are also more advanced mathematical operations that can be performed using IT2FSs. These will be detailed below [37,38]:

i. Equation (5) is used when performing aggregation between two IT2FS.

$$\begin{aligned} \tilde{A}_1 &= (\tilde{A}_1^u, \tilde{A}_1^l) = \left((a_{11}^u, a_{12}^u, a_{13}^u, a_{14}^u; H_1(\tilde{A}_1^u), H_2(\tilde{A}_1^u)), (a_{11}^l, a_{12}^l, a_{13}^l, a_{14}^l; H_1(\tilde{A}_1^l), H_2(\tilde{A}_1^l)) \right) \\ \tilde{A}_2 &= (\tilde{A}_2^u, \tilde{A}_2^l) = \left((a_{21}^u, a_{22}^u, a_{23}^u, a_{24}^u; H_1(\tilde{A}_2^u), H_2(\tilde{A}_2^u)), (a_{21}^l, a_{22}^l, a_{23}^l, a_{24}^l; H_1(\tilde{A}_2^l), H_2(\tilde{A}_2^l)) \right) \\ \tilde{A}_1 \oplus \tilde{A}_2 &= (\tilde{A}_1^u, \tilde{A}_1^l) \oplus (\tilde{A}_2^u, \tilde{A}_2^l) \\ &= \left((a_{11}^u + a_{21}^u, a_{12}^u + a_{22}^u, a_{13}^u + a_{23}^u, a_{14}^u + a_{24}^u; \min(H_1(\tilde{A}_1^u), H_1(\tilde{A}_2^u)), \min(H_2(\tilde{A}_1^u), H_2(\tilde{A}_2^u))), \right. \\ &\quad \left. (a_{11}^l + a_{21}^l, a_{12}^l + a_{22}^l, a_{13}^l + a_{23}^l, a_{14}^l + a_{24}^l; \min(H_1(\tilde{A}_1^l), H_1(\tilde{A}_2^l)), \min(H_2(\tilde{A}_1^l), H_2(\tilde{A}_2^l))) \right) \end{aligned} \quad (5)$$

ii. When extract two IT2FS, equation (6) given below is used.

$$\begin{aligned} \tilde{A}_1 \ominus \tilde{A}_2 &= (\tilde{A}_1^u, \tilde{A}_1^l) \ominus (\tilde{A}_2^u, \tilde{A}_2^l) \\ &= \left((a_{11}^u - a_{21}^u, a_{12}^u - a_{22}^u, a_{13}^u - a_{23}^u, a_{14}^u - a_{24}^u; \min(H_1(\tilde{A}_1^u), H_1(\tilde{A}_2^u)), \min(H_2(\tilde{A}_1^u), H_2(\tilde{A}_2^u))), \right. \\ &\quad \left. (a_{11}^l - a_{21}^l, a_{12}^l - a_{22}^l, a_{13}^l - a_{23}^l, a_{14}^l - a_{24}^l; \min(H_1(\tilde{A}_1^l), H_1(\tilde{A}_2^l)), \min(H_2(\tilde{A}_1^l), H_2(\tilde{A}_2^l))) \right) \end{aligned} \quad (6)$$

iii. If multiplication is to be performed between two IT2FS, the following equation (7) is implemented.

$$\begin{aligned} \tilde{A}_1 \otimes \tilde{A}_2 &= (\tilde{A}_1^u, \tilde{A}_1^l) \otimes (\tilde{A}_2^u, \tilde{A}_2^l) \\ &= \left((a_{11}^u \times a_{21}^u, a_{12}^u \times a_{22}^u, a_{13}^u \times a_{23}^u, a_{14}^u \times a_{24}^u; \min(H_1(\tilde{A}_1^u), H_1(\tilde{A}_2^u)), \min(H_2(\tilde{A}_1^u), H_2(\tilde{A}_2^u))), \right. \\ &\quad \left. (a_{11}^l \times a_{21}^l, a_{12}^l \times a_{22}^l, a_{13}^l \times a_{23}^l, a_{14}^l \times a_{24}^l; \min(H_1(\tilde{A}_1^l), H_1(\tilde{A}_2^l)), \min(H_2(\tilde{A}_1^l), H_2(\tilde{A}_2^l))) \right) \end{aligned} \quad (7)$$

iv. If an arithmetic operation is to be performed, equations (8) and (9) given below are used, respectively .

$$k\tilde{A}_1 = \left(\left(k \times a_{11}^u, k \times a_{12}^u, k \times a_{13}^u, k \times a_{14}^u; H_1(\tilde{A}_1^u), H_2(\tilde{A}_1^u) \right), \left(k \times a_{11}^l, k \times a_{12}^l, k \times a_{13}^l, k \times a_{14}^l; H_1(\tilde{A}_1^l), H_2(\tilde{A}_1^l) \right) \right) \quad (8)$$

$$\frac{\tilde{A}_1}{k} = \left(\left(\frac{1}{k} \times a_{11}^u, \frac{1}{k} \times a_{12}^u, \frac{1}{k} \times a_{13}^u, \frac{1}{k} \times a_{14}^u; H_1(\tilde{A}_1^u), H_2(\tilde{A}_1^u) \right), \left(\frac{1}{k} \times a_{11}^l, \frac{1}{k} \times a_{12}^l, \frac{1}{k} \times a_{13}^l, \frac{1}{k} \times a_{14}^l; H_1(\tilde{A}_1^l), H_2(\tilde{A}_1^l) \right) \right) \quad (9)$$

2.2. SLIM

SLIM is a type of human reliability assessment technique that allows the prediction of the probability of human error (HEP) in the process of performing specified tasks in a particular job [41]. In the stages of obtaining HEP values with this technique, factors called performance shaping factors (PSFs) and thought to have a positive or negative effect on the fulfillment of specific tasks are also considered. In addition, the effects/weights of each PSF determined by the SLIM technique on the occurrence of human errors in specific tasks can also be measured. In the literature, the SLIM technique, which is used to perform HRA in many fields such as the petrochemical industry [42], railway driving process [43], maintenance of offshore facilities [44], and lifting operations [45], has a very common usage area. Furthermore, the SLIM technique was used in HRA studies conducted in various fields for the maritime transportation sector [46-48].

Although the SLIM technique allows for very practical HRA, it requires expert judgments in the process of obtaining HEP values [5,41]. PSFs are digitized by expert judgments, and then the Success Likelihood Index (SLI) values are reached for each determined task [5]. Afterward, calibration is performed for the obtained SLI and HEP values are obtained [49]. Thus, the HEP values in the process of performing each task are determined.

2.3. Integration of the Methodology

This section describes the estimation process of human errors that occur during a cargo unloading operation of bulk carrier ships by integrating SLIM and interval type 2 fuzzy sets. The conceptual framework designed for the study is shown in Figure 2.

The application stages of the proposed hybrid approach are detailed below.

Stage 1. Determining related tasks

First, the tasks expected to be fulfilled within the scope of the specific operation type examined are determined. If there is any follow-up order among the defined tasks, hierarchical task analysis is performed among the tasks [5].

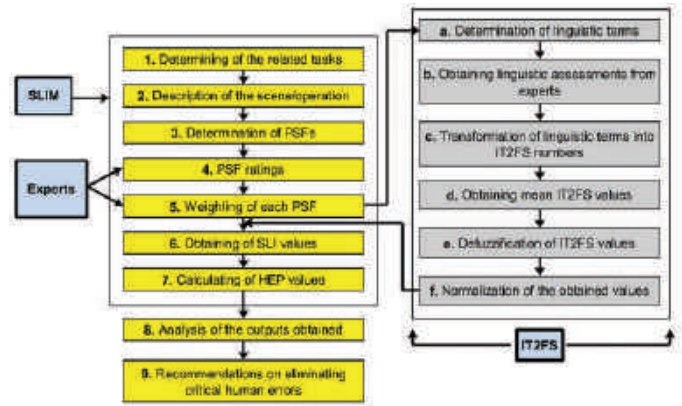


Figure 2. Conceptual framework for the proposed hybrid HEP prediction approach

Stage 2. The description of the scene/operation

At this stage, it is considered under which conditions the specific tasks determined are carried out. In this context, a scenario that coincides with real operations is produced by referring to written sources and expert opinions.

Stage 3. Determination of the PSFs

In this section, attention is drawn to the factors that are thought to have a positive or negative effect on the duties expected to be fulfilled. Sometimes this can be human-related factors such as stress, fatigue, and commercial pressure, and sometimes environmental factors such as rain, limited visibility, and sea and wave conditions. All of these factors may vary depending on the conditions under which the specific type of operation to be analyzed is performed. In this respect, PSFs that have a serious impact on the specific type of operation examined are determined in the presence of experts.

Stage 4. PSF ratings

In this section, the effects of the PSFs determined on the fulfillment of each task are evaluated by experts. For this, a linear scale consisting of numbers ranging from 1 to 9 is used. The effects of PSFs on tasks are selected inversely proportional to the magnitude of the values used in the linear scale.

Stage 5. Weighting of each PSF

PSFs have relatively different weights in the fulfillment of the determined tasks [49]. While percentage values are used in the conventional SLIM technique to determine these relative weights, IT2FS is used in the determination of these weights in the proposed approach. In other words, PSF weights are calculated using the linguistic scale within the scope of IT2FS. Thus, possible subjective and ambiguous evaluations by experts are avoided, thus contributing to obtaining more sensitive and realistic results [5].

Stage 6. Obtaining SLI values

The process that needs to be performed immediately after the rating and weighting of the determined PSFs is the obtaining of the SLI values. The SLI value, which plays a critical role in determining the probabilities of the emergence of human errors, is calculated using equation (10) given below [5,50,51].

$$SLI = \sum_{j=1}^Q r_j w_j, \quad 0 \leq SLI \leq 1 \quad (10)$$

Here, Q represents the number of PSFs, r_j represents the rating scale of PSFs, and w_j represents the relative importance weight of each PSF.

Stage 7. Calculation of HEP values

After obtaining the SLI values, the HEP values were calculated for each task. This operation is performed using the logarithmic function specified in equation (11).

$$\text{Log (HEP)} = mSLI + N \quad (11)$$

The m and N values specified in equation (11) are constant figures and are used for the calibration of the obtained SLI values [5,52].

3. Estimating Human Error Probabilities in Cargo Unloading Operations in Bulk Carrier Vessels

3.1. Cargo Unloading Operations in Bulk Carrier Ships

For the safe performance of unloading operations on bulk carriers, a number of tasks must be fulfilled both before and after arrival at the discharging port. The tasks that must be performed by the ship's personnel, especially during cargo watch at port, are critical not only for the safety of the unloaded cargo but also for ensuring the safety of the ship and its personnel. For example, implementation of the prepared discharging plan, monitoring the ballast operation, checking deck cargo cranes, grabs, and checking the stability of the ship can be shown among these tasks.

Some ship staff have been charged with responsibilities within the scope of the company Safety Management System (SMS) to keep safe cargo watch at the discharging ports. The ship master, chief officer, officer of watches (OOWs), electro-technical officer (ETO), and other deck crew can be shown as examples. In order for the ship discharging operations to be completed safely, each member of this team is expected to work effectively and in coordination. In company SMS, OOWs are generally expected to keep cargo watches at port alternately under the supervision and control of the ship's captain and chief officer during ship unloading operations. In addition, the ETO and other ship crews are requested to assist in this process. Cargo watches at the discharging port continue until the unloading of the cargo is completed.

3.2. Problem Statement

Because of technological developments, the cargo handling capacities of bulk cargo terminals have increased [1]. This significantly reduces the length of the stay of bulk carriers in ports. In this respect, the intensity of the duties that the ship's bulk carrier staff must fulfill in routine cargo shift increases. This situation increases the risk of encountering accidents during unloading operations for seafarers, who have a perilous and challenging working environment. Moreover, seafarers try to cope with many factors that can prevent or delay the fulfillment of their assigned duties, such as stress, environmental factors, and fatigue, during a cargo watch carried out as part of the discharging operation. Considering that most accidents/incidents are caused by human errors [19,53], estimating the HEP in the tasks expected to be completed by the ship's staff during a cargo watch at the discharging operation is of critical importance in terms of preventing possible accidents. For this, the method of finding HEP values for each determined task is followed.

3.3. Prediction of the Human Error Probability

Because of the examination of the reports of classification societies [54], circulars of the maritime authorities [55], company SMSs, and consulting expert opinions, the tasks that the ship's personnel must fulfill during a bulk carrier unloading operation have been determined. The determined tasks were then divided and categorized in the presence of experts. The identified and categorized tasks are detailed in Table 1.

To conduct a realistic and effective risk analysis, it is critical to utilize the right experts with sufficient knowledge and experience on the specific subject under investigation. In this regard, 10 marine experts who have served on bulk carriers for many years and are familiar with unloading operations were used in this study. The profiles of the experts who contributed to this study are detailed in Table 2.

Later PSFs that could have a positive or negative impact on the tasks expected to be fulfilled during cargo unloading operations on bulk carrier ships were determined with the help of the experts detailed in Table 2. The PSFs derived in this context are given in Table 3.

In the next stage, the effect of the determined PSFs on each task was evaluated by the experts using a dinner scale varying between 1 and 9. In this context, PSF ratings were performed by 10 experts for each task. Table 4 gives the geometric means of the PSF ratings performed by 10 experts.

In this step of the study, IT2FS was used to obtain the relative weights of the PSFs. In this context, IT2FS numbers

Table 1. Tasks and subtasks to be fulfilled during the bulk carrier unloading operation

Task/Sub-tasks	The description of tasks and subtasks
1	Tasks related to the unloading operation follow-up
1.1	Become familiar with the unloading sequence plan
1.2	Monitor the start of the discharge operation and record the time
1.3	Maintain constant communication with the foreman to avoid potential delays in the unloading operation.
1.4	Make sure the discharged cargo is correct and in good condition
2	Ship stability/ballast operation-related tasks
2.1	Do not allow the excessive trim/list formation on the ship
2.2	Check ship drafts at regular intervals using an electronic gage
2.3	Check ship drafts at regular intervals from draft marks on hull
2.4	Ensure that the ballast operation continues in the scheduled order
2.5	Monitor soundings from ballast tanks against possible overflow
3	Other ship/crew/cargo safety-related tasks
3.1	Check that the bulldozers and grabs are working without damaging the cargo holds, frames, and tank top.
3.2	Record and report damage to both ship and cargo during the unloading operation to the Chief Mate/Master
3.3	Check mooring ropes/lines with the deck crew at regular intervals
3.4	Ensure the hatch lights are working properly at night
3.5	Check that the non-return valves fitted to the hatch comings are functional.
3.6	Check bilge high-level alarms at routine intervals
3.7	Periodically check the weather reports and report any expected adverse weather conditions to the Chief Mate/Master.
3.8	Record all events during the unloading process in the port/deck logbook
3.9	Ensure that stoppers are rigged/secured after opening hatch covers
3.10	Ensure that no one is in the cargo hold before closing the hatch covers.
3.11	Ensure that there are no obstructions in the hatch chamber when closing hatch covers.
3.12	Make sure personal protective equipment is always used on deck
3.13	Control that the gangway or accommodation ladder is properly positioned.
3.14	Monitor the hoisting and luffing wires of deck cargo cranes against possible twisting at routine intervals
3.15	Ensure the limit switches of deck cargo cranes are set correctly to use the proper angle

corresponding to the linguistic evaluations taken by experts are needed. Table 5 lists the IT2FS linguistic terms used by experts and their equivalent IT2FS numbers. In addition, Table 6 represents the linguistic evaluations made by the experts for each PSF.

Linguistic evaluations performed by marine experts to obtain PSF weights were converted to corresponding IT2FS numbers. Then, the mean IT2FS values for each PSF were obtained and defuzzified using equation (4) [40]. In the following process, normalization was performed. The average IT2FS numbers and normalized weights corresponding to each PSF are given in Table 7.

In the following process, SLI values for each task were obtained using equation (10) [5,50,51], and HEP values were computed using equation (11) [5,52]. In this context, the SLI, log (HEP), and HEP values obtained for each task are given in Table 8.

4. Findings and Discussion

In this study, HEP values were obtained for each subtask expected to be performed by the ship's personnel during the cargo-unloading operation on bulk carrier ships. The subtask with the highest HEP value during unloading operations carried out on such ships was found to be 2.4 (Make sure the ballast operation continues in the scheduled order) with a HEP value of 9.74E-01. This result shows that the subtask is (2.4), where the probability of the ship crew making a mistake during the unloading of bulk carriers is the highest. It is thought that the increase in the cargo discharging capacities of the ports and the failure to comply with the planned unloading sequence have a significant impact on this. During ship-unloading operations, ballast is taken simultaneously with the discharged cargo holds [54]. For this, the capacity of the ship's ballast pumps and the cargo discharge capacity of the port are considered. If a compromise cannot be reached between these two critical parameters, undesirable situations, such as delays or premature termination, may occur in the scheduled ballast operations. In addition, the indifference of the ship personnel responsible for the ballast operation to the operation, not having the tank water levels measured on time, and not using the ballast pumps efficiently can also be an obstacle to the fulfillment of subtask 2.4. To eliminate this risk, it is necessary to reach a full agreement between the ship and the port on the cargo discharge plans before the cargo unloading operation begins [55]. Ship personnel responsible for ballast operation should always be careful, check tank levels at regular intervals, and use ballast pumps at the appropriate level and capacity.

The subtask with the second highest HEP value was obtained as 2.1 (Do not allow excessive trim/list formation on board

Table 2. Profile details of the experts

Marine Expert	Professional Position	Competency	Educational Level	Experiences with Bulk carriers (Years)	Age
1	Operational Manager	Oceangoing Master	Bachelor's Degree	25	52
2	Designated Person Ashore	Oceangoing Master	Master's Degree	24	50
3	Designated Person Ashore	Oceangoing Master	Bachelor's Degree	25	51
4	Designated Person Ashore	Oceangoing Master	Master's Degree	25	53
5	Superintendent	Oceangoing Master	Master's Degree	25	54
6	Superintendent	Oceangoing Master	Master's Degree	26	50
7	Designated Person Ashore	Oceangoing Master	Master's Degree	24	50
8	Operational Manager	Oceangoing Master	Master's Degree	24	51
9	Designated Person Ashore	Oceangoing Master	Bachelor's Degree	23	54
10	Designated Person Ashore	Oceangoing Master	Bachelor's Degree	24	51

Table 3. PSFs that impact the specified tasks

PSF No	The description of the PSFs
PSF 1	Fatigue
PSF 2	Training
PSF 3	Experiences
PSF 4	Stress level
PSF 5	Safety culture
PSF 6	Complexity
PSF 7	Communication

ship) with an HEP value of 9.20E-01. It is thought that the lack of experience and training of the responsible personnel is of great importance in the emergence of failures during the fulfillment of this task. In addition, it should not be overlooked that it is very tedious to constantly check the ship list and trim in a working environment where cargo discharge continues rapidly and many tasks are carried out by the personnel simultaneously. In this respect, the distribution of duties must be made clearly and precisely in order not to exceed the ship's stability limits and to safely complete the load unloading operation. In addition, this should be stated in writing in the company's safety SMS. In addition, before joining the ship, it should be tested that the officer responsible for cargo and stability and other ship personnel assisting in this regard have sufficient knowledge and experience. In addition, detailed training should be provided to the ship's personnel in this regard.

The third subtask with the highest HEP value was found to be 3.10 (Ensure that no one is in the cargo holds before closing the hatch covers) with an HEP value of 8.93E-01. Closing hatch covers can have devastating consequences if port workers or ship crew is present inside the hold, on the stairs, or on platforms. As a result of closing the hatch covers, a dark environment will be created inside the cargo holds. This situation may cause injury or even death of

Table 4. Geometric means of PSF ratings based on marine experts' judgments

Sub-Tasks	PSFs						
	Fatigue	Training	Experiences	Stress	Safety Culture	Complexity	Communication
1							
1.1	5	4	4	5	5	5	5
1.2	4	5	4	6	5	5	5
1.3	5	5	5	6	4	6	3
1.4	4	5	5	5	3	5	3
2							
2.1	3	3	3	3	3	3	3
2.2	4	4	5	6	3	4	4
2.3	3	3	3	3	2	3	3
2.4	4	3	3	3	2	3	2
2.5	4	5	4	6	4	5	5
3							
3.1	4	4	4	6	4	5	6
3.2	5	5	5	5	5	5	3
3.3	4	4	3	5	2	5	5
3.4	5	4	5	6	3	5	6
3.5	5	4	5	6	4	5	5
3.6	5	5	5	6	3	5	5
3.7	5	4	4	5	3	6	3
3.8	5	5	4	6	3	5	5
3.9	4	5	5	5	4	5	5
3.10	3	4	3	3	2	3	2
3.11	4	5	4	6	4	4	4
3.12	5	3	3	6	2	7	6
3.13	4	3	4	4	2	3	3
3.14	4	4	4	6	3	4	5
3.15	3	2	3	3	2	4	3

Table 5. Linguistic terms and the corresponding IT2FS numbers [5]

Linguistic Terms	Abbreviations	Equivalent IT2FS numbers
Very Low	VL	((0.0;0.0;0.0;0.1;1.0;1.0), (0.0;0.0;0.0;0.05;0.9;0.9))
Low	L	((0.0;0.1;0.1;0.3;1.0;1.0), (0.05;0.1;0.1;0.2;0.9;0.9))
Medium Low	ML	((0.1;0.3;0.3;0.5;1.0;1.0), (0.2;0.3;0.3;0.4;0.9;0.9))
Medium	M	((0.3;0.5;0.5;0.7;1.0;1.0), (0.4;0.5;0.5;0.6;0.9;0.9))
Medium High	MH	((0.5;0.7;0.7;0.9;1.0;1.0), (0.6;0.7;0.7;0.8;0.9;0.9))
High	H	((0.7;0.9;0.9;1.0;1.0;1.0), (0.8;0.9;0.9;0.95;0.9;0.9))
Very High	VH	((0.9;1.0;1.0;1.0;1.0;1.0), (0.95;1.0;1.0;1.0;0.9;0.9))

Table 6. Linguistic judgments of marine experts for each PSF determined

PSFs	E.1	E.2	E.3	E.4	E.5	E.6	E.7	E.8	E.9	E.10
Fatigue	H	MH	VH	M	VH	H	H	VH	MH	H
Training	VH	H	VH	VH	VH	VH	H	H	VH	VH
Experience	VH	MH	VH	VH	VH	H	MH	VH	H	VH
Stress Level	MH	MH	ML	L	H	H	M	M	MH	M
Safety Culture	H	MH	H	VH	H	H	H	MH	VH	MH
Complexity	ML	ML	MH	H	M	ML	M	M	H	VH
Communication	H	VH	H	VH	VH	H	MH	VH	VH	VH

Table 7. Calculated mean IT2F values and normalized weights for each PSF

PSFs	Mean , IT2FSs	Normalised Weight
Fatigue	((0.68;0.85;0.85;0.95;1;1) , (0.77;0.85;0.85;0.9;0.9;0.9))	0.148
Training	((0.84;0.97;0.97;1;1;1) , (0.91;0.97;0.97;0.99;0.9;0.9))	0.165
Experience	((0.78;0.92;0.92;0.98;1;1) , (0.85;0.92;0.92;0.95;0.9;0.9))	0.158
Stress Level	((0.39;0.58;0.58;0.76;1;1) , (0.49;0.58;0.58;0.67;0.9;0.9))	0.108
Safety Culture	((0.68;0.86;0.86;0.97;1;1) , (0.77;0.86;0.86;0.92;0.9;0.9))	0.151
Complexity	((0.4;0.59;0.59;0.75;1;1) , (0.5;0.59;0.59;0.67;0.9;0.9))	0.109
Communication	((0.8;0.94;0.94;0.99;1;1) , (0.87;0.94;0.94;0.97;0.9;0.9))	0.161
Total		1

the personnel on the platforms or on the stairs inside the cargo holds by falling. In addition, it may cause the death of personnel exposed to an airless environment after a certain period. In this respect, the hatch covers of the ship must be checked in detail before closing. These controls should be done not only by looking from the hatch coamings but also by entering the cargo holds safely, and it should be reported by walkie talkie that there is no one in the hatch.

Another subtask with the highest HEP value was calculated as 3.15 (make sure the limit switches of deck cargo cranes are set correctly to be used proper angle) with HEP values of 6.39E-01. On bulk carriers, unloading operations can sometimes be performed by the ship's own deck cargo cranes. Therefore, limit switches play a decisive role in the safe use of deck cargo cranes by adjusting the tilt angle. In this regard, adjustments outside the safe limits may cause

damage or even breakage of the deck cranes. It is thought that the selection of unsuitable personnel, the lack of training and experience are quite effective in making this mistake quite often. In this respect, according to the company SMS, it is necessary to be very meticulous in the selection of personnel held responsible for this subtask. It should be ensured that the selected personnel have experience with crane bulk carrier vessels. In addition, necessary checks for deck cranes and limit switches should be performed before each cargo unloading operation, and improper limit switch angle adjustments that could lead to possible unsafe use should be avoided [56].

Because of the analysis performed for PSFs, it is understood that the most effective PSF on the tasks/subtasks expected to be fulfilled by the ship's personnel is training with 0.165 weighting value. This was followed by communication with a weight value of 0.161. In addition, another effective PSF was

Table 8. Obtained SLI and HEP values for each task

Sub-Task	Calculated SLI	Log -HEP	HEP
1.			
1.1	4.51	-4.23	5.90E-05
1.2	4.70	-4.71	1.96E-05
1.3	4.72	-4.78	1.68E-05
1.4	4.25	-3.54	2.90E-04
2.			
2.1	2.90	-0.04	9.20E-01
2.2	4.24	-3.53	2.98E-04
2.3	2.97	-0.23	5.92E-01
2.4	2.89	-0.01	9.74E-01
2.5	4.70	-4.72	1.90E-05
3.			
3.1	4.80	-4.98	1.05E-05
3.2	4.71	-4.76	1.74E-05
3.3	3.98	-2.85	1.40E-03
3.4	4.74	-4.83	1.49E-05
3.5	4.75	-4.86	1.38E-05
3.6	4.79	-4.96	1.09E-05
3.7	4.24	-3.52	3.04E-04
3.8	4.60	-4.46	3.47E-05
3.9	4.73	-4.79	1.63E-05
3.10	2.90	-0.05	8.93E-01
3.11	4.30	-3.69	2.04E-04
3.12	4.37	-3.87	1.34E-04
3.13	3.30	-1.08	8.34E-02
3.14	4.34	-3.79	1.62E-04
3.15	2.96	-0.19	6.39E-01

obtained with a weight value of 0.158. In this respect, special attention should be paid to these 3 critical PSFs to eliminate possible human errors during unloading operations and to perform safer operations on bulk carrier ships. Therefore, sufficient training should be given to the ship's personnel and attention should be paid to the selection of experienced personnel. Furthermore, during the unloading operation, effective communication should be established between onboard personnel and the shippport.

From another viewpoint, with the human error estimation approach obtained using both SLIM and IT2FS methods, human errors were evaluated both qualitatively and quantitatively. Thus, this study provides an opportunity to express the potential human errors encountered in this process and the possibilities of their occurrence in a more striking way considering numerical data. In addition, this study is the first to predict potential human errors that may occur in cargo unloading operations on bulk carriers and

the probability of these errors occurring. In this respect, this study contributes to the academic literature. In addition, this approach obtained within the scope of this study will contribute to the measurement of human errors and their probability of occurrence in different areas of the maritime industry. Furthermore, because the outputs of the study highlight the human errors that are frequently made during cargo unloading operations on bulk carriers, it will raise awareness among all ship staff to prevent such mistakes. Thus, it will contribute to the execution of safer operations by preventing future accidents during the cargo-unloading operation of bulk carrier ships. This will not only contribute to the prevention of possible loss of life but also to the prevention of economic losses that may be encountered. In addition, by evaluating the most common human errors in unloading operations, new protective and preventive rules can be introduced by policy makers to prevent such errors from recurring. Thus, a more sustainable maritime transport environment will be created.

5. Conclusion

Preventing human errors that may be encountered during cargo unloading operations on bulk carrier ships is of critical importance for increasing operational safety. In this respect, estimating human errors in operational processes is an important approach for preventing possible accidents and loss of life [5]. In this study, the HEP occurring in the tasks/subtasks expected to be performed by the ship's personnel during the cargo unloading of bulk carrier ships has been estimated. Thus, the first three subtasks with the highest HEP values during cargo unloading operations of bulk carriers were found to be 2.4 (Make sure the ballast operation continues in the scheduled order), 2.1 (Do not allow excessive trim/list formation on board ship), and 3.10 (Ensure that no one is in the cargo holds before closing the hatch covers) In addition, the PSFs most effective on the tasks/subtasks to be performed during this operational process have been determined. It has been concluded that these are training, communication, and experience. In addition, a quantitative HEP estimation approach based on SLIM and IT2FS, which can be used for other specific areas in the future, was obtained.

From another point of view, in the estimation of human errors that may occur during cargo unloading operations on bulk carrier ships, the evaluations were made regardless of the type of bulk cargo being unloaded. In this respect, the study has a generic feature and is a source for future cargo-specific studies. It is thought that future studies on the prediction of human errors that may occur during the discharging of bulk cargoes with flammable properties, such as bulk coal or sulfur, will contribute to the literature.

Peer-review: Externally peer-reviewed.

Authorship Contributions

Concept design: A. L. Tunçel, Data Collection or Processing: A. L. Tunçel, Analysis or Interpretation: A. L. Tunçel, P. Erdem, Literature Review: A. L. Tunçel, P. Erdem, O. Turan, Writing, Reviewing and Editing: A. L. Tunçel, P. Erdem, O. Turan.

Funding: The author(s) received no financial support for the research, authorship, and/or publication of this article.

References

- [1] United Nations Conference on Trade and Development (UNCTAD) (2022). Review of Maritime Transport 2022. Geneva: United Nations.
- [2] IMO (2004). Human Element Vision, Principles and Goals for the Organization. Resolution A.947(23). London: IMO.
- [3] K. Pazouki, N. Forbes, R. A. Norman, and M. D. Woodward, "Investigation on the impact of human-automation interaction in maritime operations." *Ocean Engineering*, vol. 153, pp. 297-304, Apr 2018.
- [4] D. A. Wiegmann, and S. A. Shappell, "A human error approach to aviation accident analysis: The human factors analysis and classification system." Routledge. 2017.
- [5] P. Erdem, and E. Akyuz, "An interval type-2 fuzzy SLIM approach to predict human error in maritime transportation." *Ocean Engineering*, vol. 232, pp. 109161, 2021
- [6] International Association Of Classification Societies (IACS). Bulk carriers, Guidance and Information on Bulk Cargo Loading and Discharging to Reduce the Likelihood of Over-stressing the Hull Structure. London: IACS. 2018.
- [7] The North of England P&I Association Limited. Bulk Cargoes: A guide to good practice. The Quayside, Newcastle upon Tyne, UK: The North of England P&I Association Limited. 2015.
- [8] H. Rozuhan, M. Muhammad, and U. M. Niazi, "Probabilistic risk assessment of offshore installation hydrocarbon releases leading to fire and explosion, incorporating system and human reliability analysis." *Applied Ocean Research*, vol. 101, pp. 102282, Aug 2020.
- [9] R. Islam, and H. Yu, "Chapter three - human factors in marine and offshore systems" *Methods in Chemical Process Safety*, vol. 2, pp. 145-167 2018
- [10] D. G. DiMattia, F. I. Khan, and P. R. Amyotte, "Determination of human error probabilities for offshore platform musters." *Journal of Loss Prevention in the Process Industries*, vol. 18, pp. 488-501, July-November 2005.
- [11] D. G. DiMattia, "Human error probability index for offshore platform musters. (Doctoral dissertation)." Halifax, NS, Canada: Dalhousie University. 2004.
- [12] R. G. Bea, "Risk assessment and management of offshore structures." *Progress in Structural Engineering and Materials*, vol. 3, pp. 180-187, Aug 2001
- [13] M. A. B. Alvarenga, P. F. Frutuoso e Melo, and R. A. Fonseca, "A critical review of methods and models for evaluating organizational factors in human reliability analysis." *Progress in Nuclear Energy*, vol. 75, pp. 25-41, 2014.
- [14] I. Jang, A. R. Kim, M. A. S. Al Harbi, S. J. Lee, H. G. Kang, and P.H. Seong, "An empirical study on the basic human error probabilities for NPP advanced main control room operation using soft control." *Nuclear Engineering and Design*, vol. 257, pp. 79-87, April 2013.
- [15] W. Wang, X. Liu, and Y. Qin, "A modified HEART method with FANP for human error assessment in high-speed railway dispatching tasks." *International Journal of Industrial Ergonomics*, vol. 67, pp. 242-258, Sep 2018
- [16] M. Grozdanovic, "Usage of human reliability quantification methods." *International Journal of Occupational Safety and Ergonomics*, vol. 11, pp. 153-159, 2005
- [17] D. E. Embrey, T. Kontogiannis, and M. Green, Guidelines for Preventing Human Error in Process Safety. Center for Chemical Process Safety. New York: American Institute of Chemical Engineers. 1994.
- [18] S. T. Ung, "Evaluation of human error contribution to oil tanker collision using fault tree analysis and modified fuzzy Bayesian Network based CREAM." *Ocean Engineering*, vol. 179, pp. 159-172, May 2019.
- [19] E. Akyuz, and E. Celik, "A quantitative risk analysis by using interval type-2 fuzzy FMEA approach: the case of oil spill." *Maritime Policy & Management*, vol. 45, pp. 979-994, 2018.
- [20] Y. T. Xi, Z. L. Yang, Q. G. Fang, W. J. Chen, and J. Wang, "A new hybrid approach to human error probability quantification-applications in maritime operations." *Ocean Engineering*, vol. 138, pp. 45-54, July 2017.
- [21] B. Wu, X. Yan, Y. Wang, and C. G. Soares, "An evidential reasoning-based CREAM to human reliability analysis in maritime accident process." *Risk Analysis*, vol. 37, pp. 1936-1957, Jan 2017.
- [22] M. Konstandinidou, Z. Nivolianitou, C. Kiranoudis, and N. Markatos, "A fuzzy modeling application of CREAM methodology for human reliability analysis." *Reliability Engineering & System Safety*, vol. 91, pp. 706-716, June 2006.
- [23] A. D. Swain, and H. E. Guttman. Handbook of Human Reliability Analysis with Emphasis on Nuclear Power Plant Applications. Washington, DC: Nuclear Regulatory Commission. 1983.
- [24] D. E. Embrey, P.C. Humphreys, E.A. Rosa, B. Kirwan, and K. Rea. SLIMMAUD: an approach to assessing human error probabilities using structured expert judgement. NUREG/CR-3518. Washington DC : US Nuclear Regulatory Commission. 1984.
- [25] J. C. Williams, "A data-based method for assessing and reducing human error to improve operational performance. In: *Proceedings of IEEE 4th Conference on Human Factor and Power Plants*. Monterey, California, pp. 436-450, 1988
- [26] S. E. Cooper, A. M. Ramey-Smith, and J. Wreathall, "A technique for human event analysis (ATHEANA) - technical basis and methodological description." Upton (NY): Brookhaven National Laboratory; 1996. (US Nuclear Regulatory Commission; report no. NUREG/CR-6350).
- [27] E. Hollnagel. Cognitive Reliability and Error Analysis Method (CREAM). (1st edition). Elsevier. 1998.
- [28] D. I. Gertman, H. S. Blackman, J. L. Marble, C. Smith, and R. L. Boring. The SPAR-H human reliability analysis method. In: Fourth American Nuclear Society International Topical Meeting on Nuclear plant Instrumentation, Controls and human-machine interface technologies (NPIC & HMIT 2004). pp. 1-8, Columbus-Ohio.

- [29] Almond, R. "An extended example for testing graphical belief." *Statistical Science Research Report 6*, 1-18, 1992.
- [30] X. He, Y. Wang, Z. Shen, and X. Huang, "A simplified CREAM prospective quantification process and its application." *Reliability Engineering & System Safety*, vol. 93, pp. 298-306, 2008.
- [31] L. A. Zadeh, "Fuzzy sets." *Information and Control*, vol. 8, 338-353, June 1965.
- [32] L. A. Zadeh, "The concept of a linguistic variable and its application to approximate reasoning-1," *Information Sciences*, vol. 8, pp. 199-249, 1975.
- [33] O. Castillo, and P. Melin, "Type-2 fuzzy logic: theory and applications." Springer-Verlag Berlin Heidelberg, 2008.
- [34] J. M. Mendel, "Advances in type-2 fuzzy sets and systems." *Information Sciences*, vol. 177, pp. 84-110, 2007.
- [35] E. Celik, and E. Akyuz, "Application of interval type-2 fuzzy sets DEMATEL methods in maritime transportation: the case of ship collision." *International Journal of Maritime Engineering*, vol. 158, pp. 359-371, 2016.
- [36] J. M. Mendel, R. I. John, and F. Liu, "Interval type-2 fuzzy logic systems made simple." *IEEE Transactions on Fuzzy Systems*, vol. 14, pp. 808-821, Dec 2006
- [37] S. M. Chen, and L. W. Lee, "Fuzzy multiple attributes group decision-making based on the interval type-2 TOPSIS method." *Expert Systems with Applications*, vol. 37, pp. 2790-2798, 2010
- [38] E. Celik, O. N. Bilisik, M. Erdogan, A. T. Gumus, and H. Baraclı, "An integrated novel interval type-2 fuzzy MCDM method to improve customer satisfaction in public transportation for Istanbul." *Transportation Research Part E: Logistics and Transportation Review*, vol. 58, pp. 28-51, Nov 2013.
- [39] E. Celik, and E. Akyuz, "An interval type-2 fuzzy AHP and TOPSIS methods for decision-making problems in maritime transportation engineering: the case of ship loader." *Ocean Engineering*, vol. 155, pp. 371-381, May 2018.
- [40] C. Kahraman, B. Öztayşı, İ. U. Sarı, and E. Turanoğlu, "Fuzzy analytic hierarchy process with interval type-2 fuzzy sets." *Knowledge-Based Systems*, vol. 59, pp. 48-57, March 2014
- [41] K. S. Park, and J. in Lee, "A new method for estimating human error probabilities: AHP-SLIM." *Reliability Engineering & System Safety*, vol. 93, pp. 578-587, April 2008.
- [42] A. Zare, N. Hoboubi, S. Farahbakhsh, and M. Jahangiri, "Applying analytic hierarchy process and failure likelihood index method (AHP-FLIM) to assess human reliability in critical and sensitive jobs of a petrochemical industry." *Heliyon*, vol. 8, pp. e09509, 2022.
- [43] J. L. Zhou, Z. T. Yu, and R. B. Xiao, "A large-scale group Success Likelihood Index Method to estimate human error probabilities in the railway driving process." *Reliability Engineering & System Safety*, vol. 228, pp. 108809, Dec 2022
- [44] R. Abbassi, F. Khan, V. Garaniya, S. Chai, C. Chin, and K. A. Hossain, "An integrated method for human error probability assessment during the maintenance of offshore facilities." *Process Safety and Environmental Protection*, vol. 94, pp. 172-179, March 2015.
- [45] J. Tu, and Y. Lou. "A SLIM based methodology for human reliability analysis of lifting operations." In *Proceedings of 2013 International Conference on Mechatronic Sciences, Electric Engineering and Computer (MEC)*. IEEE, pp. 322-325, Dec 2013.
- [46] G. Kayisoglu, B. Gunes, and E. B. Besikci, "SLIM based methodology for human error probability calculation of bunker spills in maritime operations." *Reliability Engineering & System Safety*, vol. 217, pp. 108052, 2022.
- [47] R. Islam, H. Yu, R. Abbassi, V. Garaniya, and F. Khan, "Development of a monograph for human error likelihood assessment in marine operations." *Safety Science*, vol. 91, pp. 33-39, Jan 2017.
- [48] F. E. Kizilay, O. Arslan, E. Akyuz, and T. Kececi, "Prediction of human error probability for officers during watchkeeping process under SLIM approach." *Australian Journal of Maritime & Ocean Affairs*, 1-18, Jan 2023.
- [49] E. Akyuz, "Quantitative human error assessment during abandon ship procedures in maritime transportation." *Ocean Engineering*, vol. 120, pp. 21-29, July 2016.
- [50] J. Liu, et al. "Prediction of human-machine interface (HMI) operational errors for maritime autonomous surface ships (MASS)." *Journal of Marine Science and Technology*, vol. 27, pp. 293-306, 2022.
- [51] R. Islam, R. Abbassi, V. Garaniya, and F. I. Khan, "Determination of human error probabilities for the maintenance operations of marine engines." *Journal of Ship Production and Design*, vol. 32, pp. 226-234, Nov 2016.
- [52] E. Stojiljkovic, S. Glisovic, and M. Grozdanovic, "The role of human error analysis in occupational and environmental risk assessment: a Serbian experience." *Human and Ecological Risk Assessment: An International Journal*, vol. 21, pp. 1081-1093, 2015.
- [53] Ö. Uğurlu, E. Köse, U. Yıldırım, and E. Yükkseyıldız, "Marine accident analysis for collision and grounding in oil tanker using FTA method." *Maritime Policy & Management*, vol. 42, pp. 163-185, 2015.
- [54] International Association of Classification Societies (IACS) (2018). Bulk carriers. London: IACS.
- [55] Maritime and Coastguard Agency (MCA). Safe loading and unloading of bulk carriers 2003. Southampton: MCA.
- [56] NAMCO. Crane limit switches. Available at: <https://www.specialtyproducttechnologies.com/namco/applications/crane-limit-switch>. Access Date: 26.04.2023.

Application of Relaxation Times Distribution of Dielectric Permittivity for Marine Engine Oils Analysis

✉ Nikolay Sinyavsky, ✉ Oksana Synashenko, ✉ Natalia Kostrikova

Kaliningrad State Technical University, Kaliningrad, Russia

Abstract

This work is a preliminary dielectric relaxation time distribution analysis of several fresh and used marine engine oils that have not previously been examined for degradation with relaxation time distribution. The correlation of the distribution of relaxation times with other characteristics of oils, particularly the content of additives and wear products, was analyzed. The obtained results can be useful in the development of instrumentation for express diagnostics of the engine. The proposed mechanism for describing the dielectric spectrum using the relaxation time distribution can provide a meaningful interpretation of the processes at the molecular level. Information about the frequency measurements of permittivity can be used in various applied research.

Keywords: Marine engine oils, Engine oil additives, Dielectric relaxation, Relaxation time distribution

1. Introduction

Engine oil plays a key role in marine diesel engines. It consists of a complex mixture of hydrocarbons and a combination of base oil and a set of additives [1]. Lubricating oils in engines are used to reduce friction and keep moving parts clean because they contain both detergent and dispersant additives. Engine oil aging is a complex process that degrades the base oil and depletes its additives. The main aging factors are oxidative high-temperature degradation and contamination from soot, wear metals, fuel, water and coolant.

There are many physical and chemical methods for determining engine oil condition, including ferrography, X-ray fluorescence spectroscopy, visible spectrophotometry. In [2], an attempt was made to combine the magneto-optic method and photon correlation spectroscopy to detect ferromagnetic particles of diesel engine wear products and determine their disperse characteristics. This approach enables recording the low content of magnetic nanosized particles and their dispersion in waste marine engine oil. In this work, experiments were conducted to observe the longitudinal magneto-optic Faraday effect in a model magnetic fluid and in waste engine oil. It is shown that a low

concentration of magnetic particles in waste oil does not allow one to observe the effect of rotation of the polarization plane in a magnetic field. To measure large wear particles washed off the oil filter element, we used the regularities of the process of particle deposition in solution and recorded the absorption of light that varies with time.

In [3], a study of fresh and waste marine engine oil was conducted by high-resolution ^1H nuclear magnetic resonance (NMR) and NMR relaxometry with Laplace transform inversion. A change has been registered in the molar content of functional groups CH , CH_2 and CH_3 for waste oils. It is shown that the spin-spin relaxation times of the protons of waste oil 10W40 are shifted towards lower values, and for waste oil M-4015 they increase. This indicates a change in the mobility of the functional groups of macromolecules caused by a change in the waste oil viscosity.

The possibility of using optical absorption spectroscopy and fluorescence methods to detect wear products in the waste engine oils of marine engines has been studied in [4]. The aim of this work is to develop a method for detecting and determining the concentration of ferromagnetic particles of wear products in waste engine oil by analyzing changes



Address for Correspondence: Nikolay Sinyavsky, Kaliningrad State Technical University, Kaliningrad, Russia

E-mail: n_sinyavsky@mail.ru

ORCID ID: orcid.org/0000-0003-1285-206X

Received: 24.05.2023

Last Revision Received: 15.07.2023

Accepted: 06.09.2023

To cite this article: N. Sinyavsky, O. Synashenko, and N. Kostrikova. "Application of Relaxation Times Distribution of Dielectric Permittivity for Marine Engine Oils Analysis." *Journal of ETA Maritime Science*, vol. 11(3), pp. 209-216, 2023.

©Copyright 2023 by the Journal of ETA Maritime Science published by UCTEA Chamber of Marine Engineers

in the optical density spectra depending on the wavelength when the sample is placed in an external magnetic field. The proposed mechanism for increasing the transparency of waste oils in a magnetic field is described. The possibility of determining the concentration of magnetic particles and hence the degree of engine component wear during operation is shown.

Recently, much attention has been paid to the dielectric properties of industrial lubricants [5]. Methods for analyzing permittivity are relatively fast, simple, and inexpensive. Dielectric spectroscopy [6] is an analytical method for studying the interaction between a dielectric material and electromagnetic energy in the radio frequency range. In [7], dielectric spectroscopy was used to analyze the oxidation process of engine lubricating oil compared with Fourier IR spectroscopy.

The publication [8] compares mineral and hydrocarbon oils in terms of conductivity and relaxation mechanisms in the complex plane of the Cole-Cole diagram and in terms of dielectric losses. Here, dielectric relaxation spectroscopy in the frequency domain is used for various values of the alternating electric field strength.

A previous study [9] studied the permittivity, dielectric losses, and insulating characteristics of paper impregnated with oil with iron oxide nanoparticles. Studies have shown that nanoparticles are bound to impregnated paper fibers with O-H bonds and that the relative permittivity and dielectric loss of nanofluid impregnated paper increase. In this case, the electrical breakdown strength of the paper impregnated with nanofluid can increase.

The publication [10] presents a selection procedure and a computer code for the numerical estimation of the dielectric properties using the relaxation time distribution function. This approach is based on the linear least-squares method. The basis set of the spectra is calculated here using the Debye relaxation model. The method was tested on simulated spectra with certain dielectric relaxation parameters and on some experimental dielectric spectra.

The paper [11] presents the results of measurements of permittivity in the microwave to infrared frequencies for various liquid electrolytes and non-electrolyte systems. Three types of relaxation processes are demonstrated with an almost continuous relaxation time distribution, including a very short one (about 1 ps).

The dielectric properties of asphaltenes deposited from four different oils have been studied [12] in the frequency range 0.01-1000 Hz use frequency domain spectroscopy. It has been shown that an increase in asphaltene aggregation leads to a significant decrease in the anomalous effect of permittivity at low frequencies.

In the article [13], using dielectric spectroscopy, the correlation has been analyzed between the degree of oxidation of engine oil and its dielectric characteristics. In [14], the frequency characteristics of three different types of mineral oil were measured and compared with the simulation results using the polarization model proposed by the authors.

Studies on the analysis of engine oils carried out in [15] confirm the selectivity and sensitivity of dielectric spectroscopy based on measurements of the frequency dependence of the real component of the complex capacitance.

In [16], the effectiveness of dielectric spectroscopy as a tool for studying complex materials was demonstrated. The unique capabilities of the method make it possible to study complex systems on a wide time scale, identify relaxation processes, and reveal structural and dynamic features of materials.

A new approach for estimating dielectric spectra is presented in [17]. It is based on the solution of the Fredholm integral equation of the first kind using the Tikhonov regularization method. This method allows you to resolve several dynamic processes in the sample under study. The main problem when using the Tikhonov regularization technique is the correct choice of the regularization parameter. This parameter is of decisive importance for the correctness of the form of the relaxation time distribution function.

In [18], the Tikhonov regularization method was applied in a wide frequency band to calculate the distribution of dielectric relaxation times to dielectric data of geological material. This method does not require a priori information for analysis, and the results obtained from the distribution of dielectric relaxation times can be used to study the separate mechanisms of the Debye polarization of different dipoles in complex systems.

An important problem in the operation of engine oils is the degradation of their components, functional additives, because the performance characteristics of the oil depend on the concentration of the active substances of the additives.

Currently, the set of dielectric methods for the analysis of engine oils is rather limited and is mainly represented by measurements of their condition based on a comparison, as a rule, of one component of the complex dielectric constant of fresh and used oils. The main disadvantage is that the frequency spectrum of the acting measuring signal is usually quite narrow. However, the dielectric characteristics of engine oils are unevenly distributed over the frequency range. The non-uniformity of the dielectric characteristics is especially pronounced in used engine oils, which are complex dispersed systems. In the single-frequency mode,

this circumstance makes it difficult to effectively control, unambiguous interpretation of the results depending on the structure and composition of the samples under study in the dielectric control of engine oils.

While dielectric relaxation times distributions are used to study various complex systems [16-18], there is no information in the literature on the application of $G(T_r)$ distributions to study the degradation of engine oils during engine operation, identification of oils, engine diagnostics using used oil, or working life forecasting. Although many such studies have used dielectric spectroscopy, they are limited to measurements of the relative permittivity at a fixed frequency, the frequency dependence $\varepsilon = \varepsilon(\omega)$, or measuring one dielectric relaxation time.

An urgent task is to obtain such information about the used oil, which will allow diagnosing the condition of the engine and the malfunctions of its components by changing the composition of hydrocarbons, the content of additives, and wear products. The solution to the problem is possible by applying the method of distribution of dielectric relaxation times for the analysis of used engine oil because oil is a complex dispersed system. This method, as far as we know from the literature, has not yet been used to diagnose used engine oils.

Studies on the potential use of dielectric relaxation time distributions to identify oils and determine changes in used engine oils are lacking in the literature. The novelty of the current paper lies in the use of the advantages of the dielectric relaxation time distribution method for the separate detection of dipoles of engine oil degradation products and additives.

The purpose of this work was to study the state of waste marine engine oils according to their dependence on the frequency of the dielectric constant and the tangent of the dielectric loss angle, to obtain the distribution of the dielectric relaxation times of oils as polar dielectrics, and to determine the presence of functional additives that determine the quality of lubricating oils of various types.

2. Methodology for Conducting Experimental Studies

In this study, a modern precision digital parameter meter LCR TH2827C [19] was used for conducting measurements. The operating frequency range of the device is 20 Hz - 1 MHz, with a resolution of 10 MHz and a frequency accuracy of 0.01%. The basic measurement accuracy of the LCR parameters is 0.05%. The dependence of the capacitance on frequency was measured in the sweep mode (201 points). The frequency dependence of the capacitance of the air capacitor $C_0(\omega)$ and that of the capacitor $C(\omega)$ immersed in the test engine oil were measured. The frequency

dependence of the dielectric constant of the oil was found as $\varepsilon = C(\omega)/C_0(\omega)$. Samples of the studied oils were not subjected to special preparation before measurements. To check the reproducibility and repeatability of the experiment, measurements were performed several times, and the results were compared with each other. A standard air trimmer condenser immersed in the test oil was used as the measurement cell. A total of 8 engine oils were studied at a temperature of $T = 295$ K. The measured dependence of the parameters were transferred to a personal computer via a flash drive for further processing.

Fresh and waste engine oils can be considered polar dielectrics. In an external alternating electric field, if the time required to establish the equilibrium orientation of the dipoles becomes longer than the field oscillation period, the polarization of the sample decreases. For simple liquids, the polarization decay is characterized by a single relaxation time. In this case, the Debye equation for the real part of the relative permittivity is written as [20]:

$$\varepsilon' = \frac{\varepsilon + \varepsilon_\infty \omega^2 T_r^2}{1 + \omega^2 T_r^2} \quad (1)$$

where ω - cyclic frequency, ε_∞ - dielectric permittivity at $\omega \rightarrow \infty$, ε - dielectric permittivity at $\omega \rightarrow 0$, T_r - macroscopic relaxation time. The dielectric loss tangent for the Debye model can be written

$$tg \delta = \frac{(\varepsilon - \varepsilon_\infty) \omega T_r}{\varepsilon + \varepsilon_\infty \omega^2 T_r^2} \quad (2)$$

Engine oil is a complex polar liquid and is characterized by not one, but several relaxation times related to different systems of dipoles. Let us call the relaxation time distribution function $G(T_r)$, and the following can be written:

$$\varepsilon' = \int_0^\infty G(T_r) \frac{\varepsilon + \varepsilon_\infty \omega^2 T_r^2}{1 + \omega^2 T_r^2} dT_r \quad (3)$$

Function (3) is the experimentally measured dependence of the relative permittivity of engine oil on frequency. Knowledge of the relaxation time distribution function $G(T_r)$ will allow analyzing the composition of additives, engine wear products, contaminants and chemical degradation in engine oil.

To determine the $G(T_r)$ function, it is necessary to apply the inversion of the integral transformation (IIT) to Equation (3). To do this, we use the algorithm [21] and the RILT program [22] implemented in the MatLab environment. The desired array of relaxation time distribution is an inverse integral transformation of a set of signals decreasing with increasing frequency, which is a measured array, and is calculated using least squares regularization using the CONTIN algorithm [21].

The stability of the algorithm, obtaining a correct solution to the problem, critically depends on the signal-to-noise ratio

of the dependance $\varepsilon = \varepsilon(\omega)$ measured in the experiment. The signal-to-noise ratio must be at least two. The resolution of the lines of the spectrum of relaxation times depends on the correct choice of the regularization parameter. The error in determining the values of ε and ε_∞ in formula (3) is introduced by the limited frequency range of the LCR meter (0.02-1000 kHz).

3. Results of the Experimental Studies and Their Analysis

The dielectric permittivity provides information about the presence of contaminants and the condition of the oil-additive package. When measuring the dielectric permittivity of waste lubricating oil, changes in its dielectric permittivity may indicate the presence of contaminants such as water, fuel, or wear particles, oil oxidation, or additive depletion. Any increase in dielectric permittivity indicates some contamination or a change in the chemical composition of the oil. In [23], on model samples, the dependence of the permittivity on the amount of aluminum and iron wear products in the sample have been obtained in the form of linear equations:

$$\begin{aligned} \varepsilon &= 0.0031X_{Al} + 2.4049, \\ \varepsilon &= 0.0004X_{Fe} + 2.4036 \end{aligned} \quad (4)$$

where X_{Al} – aluminium concentration in ppm; X_{Fe} – ferrum concentration in ppm. As the temperature increases, the oil

density decreases, and consequently, the dielectric constant of the oil decreases

Mineral-based hydrocarbon-lubricating oils are typically complex mixtures of straight and branched paraffins, naphthenic molecules, and aromatic compounds. They have a dielectric permittivity that typically ranges from 2.1 to 2.4, depending on the viscosity, oil density, paraffinic, naphthenic, and aromatic content, and additive package. An increase in the content of additives increases the dielectric permittivity of the oil because the additives themselves have a higher dielectric permittivity. The dielectric characteristics of engine oils correlate with their viscosity characteristics [20].

The main dielectric characteristics at a temperature $T=295$ K at the beginning and end of the frequency range for the studied oils are given in Table 1.

The dielectric permittivity relaxation of fresh and used oils is caused by the established orientation of the polar molecules of the additives. From the frequency dependence of ε for base oils SN-150 and SN-500, they have no dipole polarization (Figure 1). The authors of [15] came to a similar conclusion: the capacitance of a sensor filled with SN-500 base oil does not depend on frequency, i.e., there is no oil polarization. Among fresh oils, at $f=1$ MHz, TPEO 12/40 oil has the highest dielectric permittivity ($\varepsilon=2.2596$),

Table 1. Dielectric characteristics of base, fresh, and waste engine oils

№	Oil type	Relative dielectric permittivity, ε		Dielectric loss tangent, $\text{tg}\delta$	Dielectric loss coefficient, k_n
		$f=200$ Hz	$f=1$ MHz	$f=1$ MHz	$f=1$ MHz
1	Shell Rimula 15W40				
	fresh	2.2696	2.2115	0.00077	0.001703
	used for 250 h.	2.3059	2.2328	0.00280	0.006252
	used for 500 h.	2.2811	2.2437	0.00031	0.000696
2	Mobil 5W30				
	fresh	2.1747	2.1455	0.00035	0.000751
	used for 170 h.	2.4095	2.3392	0.00369	0.008632
3	Mobil 5W40				
	fresh	2.2056	2.1275	0.00008	0.000170
	used for 160 h.	2.3418	2.2983	0.00407	0.009354
4	Total Disola M4015				
	fresh	2.2811	2.2350	0.00240	0.005364
	used for 300 h.	2.3395	2.2709	0.00279	0.006336
5	Lukoil Navigo TPEO 12/40				
	fresh	2.2832	2.2596	0.00480	0.010846
	used for 300 h.	2.5733	2.4838	0.01010	0.025086
6	Base oil SN-150	2.2207	2.2477	0.00049	0.001101
7	Base oil SN-500	2.2855	2.2940	0.00428	0.009818

and Mobil 5W40 has the lowest permittivity ($\epsilon=2.1275$). The average values of the relative permittivity for oils 5W40 and 15W40, given in [23], are consistent with the data in Table 1. An increase in the dielectric constant of the used oil is also recorded in [24,25]. At a frequency up to $f=1$ MHz, for all the studied oils, other types of polarization (ionic, electronic) do not appear.

Dependence of dielectric permittivity on frequency for base oil SN-150, fresh and used for 250 h, and engine oil Shell Rimula 15W40 are shown in Figure 1.

As can be seen from the diagram, the base oil that does not contain an additive package does not have dipoles that could relax. Dipoles that cause polarization and subsequent relaxation are additive molecules that are used during engine operation. This is also illustrated by the dependence of the loss tangent for the same oils, as shown in Figure 2.

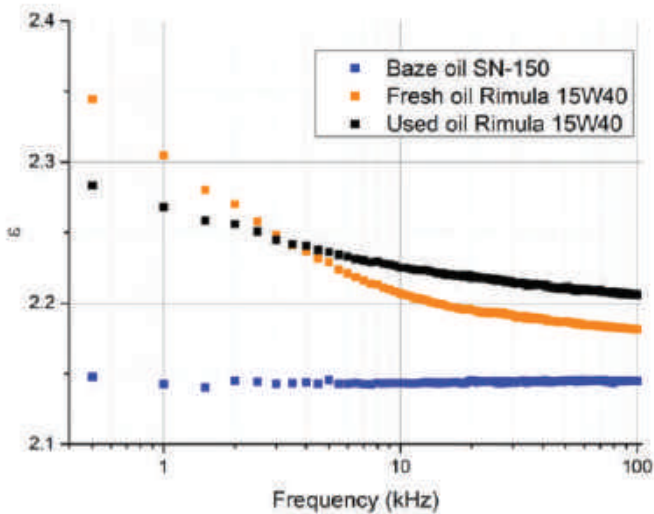


Figure 1. Dependence of the dielectric permittivity on frequency

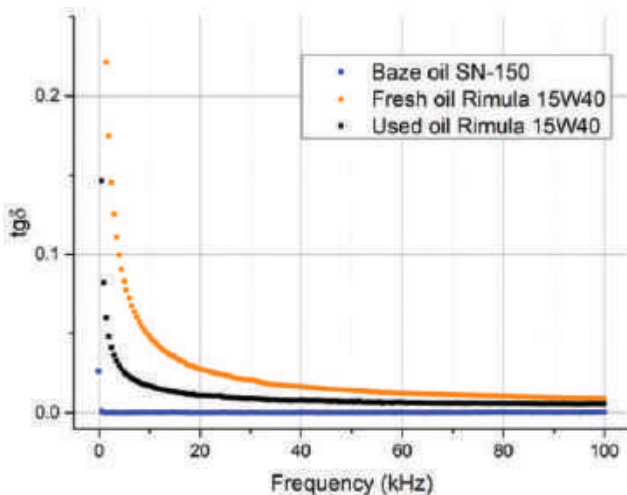


Figure 2. Dependence of the dielectric loss tangent of oils on frequency

Engine oils are dielectrics, which are base oils and a multicomponent dispersed additive system to improve the oil performance. Base oil molecules are composed of bonded atoms with a uniform charge distribution and are non-polar. This leads to the fact that the dielectric permittivity and the loss tangent of the base oils SN-150 and SN-500 do not depend on the frequency.

From the experimental and literature data, when engine oil is used, its dielectric permittivity increases. This is caused by oil oxidation and the appearance of metal wear particles and other contaminants with high electrical conductivity.

To obtain the necessary properties, metal-containing additives are added to the oils, the amount of which affects the dielectric permittivity value and the rate of its relaxation.

The results of integral transformation inversion (3) in the form of distribution functions of relaxation times $G(T_r)$ are shown for fresh and used oils in Figures 3-5. For both oils, the peak in the 0.01 ms interval is likely due to dipoles of the main antiwear, extreme pressure, and antioxidant zinc dialkyldithiophosphate (ZDDP) additive. This antiwear additive is in almost all engine oils. The number of metal-containing additives, including zinc alkyldithiophosphate, can be measured by the sulfate ash content, one of the main parameters of fresh oil. The value of ϵ and sulfate ash of

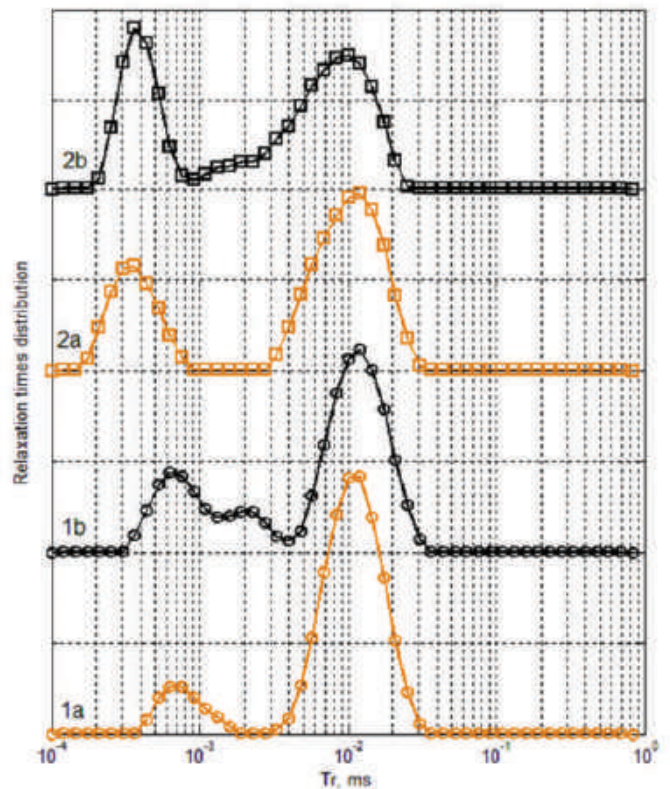


Figure 3. The relaxation time distribution of the dielectric permittivity of fresh and waste oils Total (1a and 1b curves) and TPEO (2a and 2b curves)

some oils are given for comparison in [24]. The second peak for Total M4015 oil is in the interval of $7 \cdot 10^{-4}$ ms, and for TPEO 12/40 oil is in the interval of $3.5 \cdot 10^{-4}$ ms. These peaks are most likely due to other additives. The positions of these peaks in the time spectra do not change in waste oils. In both Total M4015 and TPEO 12/40 waste oils, a third peak appears in the interval of $2 \cdot 10^{-3}$ ms, apparently caused by the thermal decomposition of hydrocarbons. A significant increase in the content of phosphorus, zinc, and boron in the waste oil Total M4015 [26] is apparently caused by contamination of the waste oil with fuel containing antiwear additives.

The relaxation time distributions (Figure 4) for Mobil 5W30 and Mobil 4W40 oils are close to the distributions discussed above. The chemistry of these oils is the same, but Mobil 5W30 is more refined than Mobil 5W40. The viscosity of the first oil is less than that of the second. Waste oil Mobil 5W30 contains a lot of potassium contaminant [26], and the peak with a short relaxation time is shifted to the interval of short times, apparently due to a decrease in viscosity. Potassium in waste oils can be due to fuel additives and antifreeze containing potassium-based additives. The bimodal distribution of oil relaxation times practically does not change its appearance for waste Mobil 5W40 oil (Figure 4).

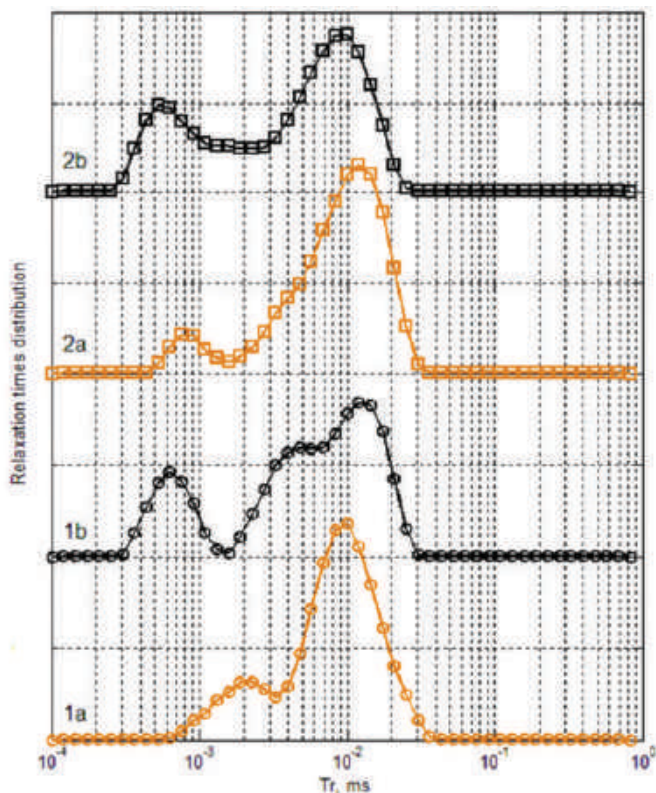


Figure 4. Relaxation times of Mobil 5W30 (1a and 1b curves) and Mobil 5W40 (2a and 2b curves) oils

A distinctive feature of the relaxation time spectra (Figure 5) for Mobil 15W40 and Rimula 15W40 oils is the presence of three relaxation times, and the main peak is almost an order of magnitude larger (0.08 ms) than for the other oils studied. The rest of the spectra are similar. Rimula 15W40 oil, according to [26], has the highest boron content (290 ppm). Boron is found in many engine oils in dispersant additives. In addition, there is boron in the antiwear additive boron nitrite. Fresh Rimula 15W40 oil has a rather significant content of molybdenum [26], which is present in molybdenum dithiocarbamate (MoDTC), an antiwear additive and an effective friction modifier. The main relaxation time for oils, the graphs of which are shown in Figure 5, may be due to the above additives.

Small values of relaxation times are due to dipoles of small molecular groups, for example, highly mobile tails of macromolecules, whereas large values of relaxation times are associated with the motion of large molecules as a whole. Differences in relaxation times can also be caused by the formation of associations involving dipole molecules.

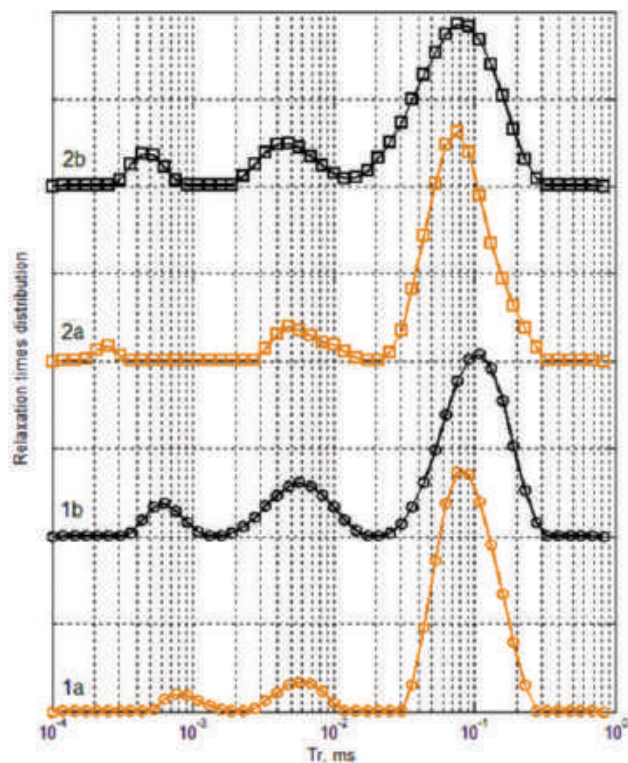


Figure 5. Relaxation times of Mobil 15W40 (1a and 1b curves) and Rimula 15W40 (2a and 2b curves) oils

4. Conclusion

Thus, from the studies performed, it can be seen that the value of the dielectric constant increases in used engine oils. This is due to oil oxidation and metal particles of wear and contamination. Increasing the additive content also

increases the dielectric constant. The dielectric constant of base oils does not depend on frequency, these oils do not have dipole polarization because base oil molecules are non-polar. Fresh engine oils polarize and relax because of the dipoles of the additives. Additives are depleted during operation, which can be seen from the decrease in the dielectric loss tangent for the Rimula 15W40 oil.

The distributions of relaxation times for Total M1015 and TPEO 12/40 oils have 2 peaks each. The main peak in the region of 0.01 ms is probably due to the main antiwear additive ZDDP. The second peak in these oils is caused by the presence of other additives with electric dipole moments. For used oils Total M1015 and TPEO 12/40, the position of the peaks in the distributions does not change, but a third peak appears at 0.002 ms, caused by the thermal decomposition products of hydrocarbons. The distributions of relaxation times for Mobil 15W40 and Rimula 15W40 oils have 3 peaks each, and the relaxation time of the main peak (0.08 ms) is an order of magnitude longer than that of the other oils. This peak for Rimula 15W40 may be due to the antiwear additive MoDTC or the boron nitrite dispersant.

In this work, a new approach was used to analyze the frequency dependence of the dielectric permittivity of engine oils to obtain the dielectric relaxation time distribution. The desired array of the relaxation times distribution has been calculated using regularization by the least squares method. The method uses the Debye relaxation model, but it can be applied to other models as well. The procedure has been previously tested on simulated spectra with known dielectric relaxation parameters and on real dielectric spectra of engine oils, and it turned out to be reliable and fairly stable. The spectra of dielectric relaxation times are a prerequisite for the interpretation of processes in engine oils at the molecular level. Important information not available using other methods can be obtained and used to explain the properties of solutions or mixtures of solutions.

The originality of this work is in the first application of the distributions of dielectric relaxation times to study the degradation of engine oils during engine operation, and the correlation of the distribution of relaxation times with other characteristics of oils, in particular, with the content of additives and with wear products.

In the future, we plan to study used engine oils by dielectric spectroscopy to determine the wear of engine components and identify their malfunctions. The advantage of the described method is the use of a simple electrical parameter meter, which makes it possible to implement express diagnostics of engine oil and engine without the delivery of equipment to a service and repair point, which is especially important for maritime transport.

Peer-review: Internally and externally peer-reviewed.

Authorship Contributions

Concept design: N. Sinyavsky, Data Collection or Processing: O. Synashenko, Analysis or Interpretation: N. Sinyavsky, Literature Review: N. Kostrikova, Writing, Reviewing and Editing: N. Kostrikova.

Funding: The research was conducted with the financial support of the Federal Agency for Fisheries of the Russian Federation (project number: 122030900056-4).

References

- [1] R. Baltenas, A. S. Safonov, A. I. Ushakov, and V. Shergalis, "Engine oils". M., St. Petersburg: Al'falab, pp. 272, 2000 (in Russia).
- [2] N. Ya. Sinyavsky, A. M. Ivanov, and N. A. Kostrikova, "Analysis of wear particles in used marine engine oils", *Marine Intellectual Technologies*, vol. 4, pp. 44-48, 2021.
- [3] N. Sinyavsky, and I. Mershev, "NMR relaxometry used ship oils", *Journal of Eta Maritime Science*, vol. 10, pp. 195-201, 2022.
- [4] I.P. Korneva, N.Ya. Sinyavsky, and N.A. Kostrikova, "Study of marine engine oils with wear products by optical methods", *Marine Intellectual Technologies*, vol. 4, pp. 72-78, 2022.
- [5] L. Guan, X.L. Feng, and G. Xiong, "Engine lubricating oil classification by SAE grade and source based X.L. on dielectric spectroscopy data", *Analytica Chimica Acta*, vol. 628, pp. 117-120, 2008.
- [6] F. Kremer, A. Schönhals (Eds.), "Broadband dielectric spectroscopy", Springer-Verlag Berlin Heidelberg GmbH, 2012.
- [7] L. Guan, X.L. Feng, G. Xiong, and J.A. Xie, "Application of dielectric spectroscopy for engine lubricating oil degradation monitoring", *Sensors and Actuators A: Physical*, vol. 168, pp. 22-29, 2011.
- [8] P. Havran, et al. "Dielectric properties of electrical insulating liquids for high voltage electric devices in a time-varying electric field", *Energies*, vol.15, pp. 391. 2022.
- [9] B. Du, Q. Liu, Y. Shi, and Y. Zhao, "The effect of Fe3O4 nanoparticle size on electrical properties of nanofluid impregnated paper and trapping analysis", *Molecules*, vol. 25, pp. 3566, 2020.
- [10] A. Y. Zasetky, and R. Buchner, "Quasi-linear least squares and computer code for numerical evaluation of relaxation time distribution from broadband dielectric spectra", *Journal of Physics: Condensed Matter*, vol. 23, pp. 025903, 2011.
- [11] J. Barthel, and R. Buchner, "High frequency permittivity and its use in the investigation of solution properties", *Pure and Applied Chemistry*, vol. 63, pp. 1473-1483, 1991.
- [12] H. Vralstad, Ø. Spets, C. Lesaint, L. Lundgaard, and J. Sjoblom, "Dielectric properties of crude oil components", *Energy Fuels*, vol. 23, pp. 5596-5602, 2009.
- [13] Y. Gong, L. Guan, L. Wang, and H. Liu, "Dielectric submicroscopic phase characterisation of engine oil dispersed in jet fuel based on on-line dielectric spectroscopy", *Lubrication Science*, vol. 29, pp. 335-354, Feb 2017.
- [14] Y. Zhou, M. Hao, G. Chen, G. Wilson, and P. Jarman, "Study of the dielectric response in mineral oil using frequency-domain measurement", *Journal of Applied Physics*, vol. 115, pp. 124105, 2014.

- [15] D. Levi, Z. Stoyanov, and D. Vladikova, "Application of permittivity spectroscopy for screening of engine oils lubricating properties", *Bulgarian Chemical Communications*, vol. 49, pp. 254-259, 2017.
- [16] Yu. Feldman, Yu. A. Gusev, and M. A. Vasilyeva, "Dielectric relaxation phenomena in complex systems: Tutorial", Kazan: Kazan University, 2012.
- [17] J. Macutkevicius, J. Banys, and A. Matulis, "Determination of the distribution of the relaxation times from dielectric spectra", *Nonlinear Analysis: Modelling and Control*, vol. 9, pp. 75-88, 2004.
- [18] P. R. J. Connolly, et al. "Dielectric polarization studies in partially saturated shale cores", *JGR Solid Earth*, vol. 124, pp. 10721-10734, 2019.
- [19] TH2826/A High Frequency LCR-Meter. Operation manual. [Online]. Available: http://222.185.248.92:8080/upload/UploadAction2/20200114135540_522.pdf [Accessed: April 01, 2023].
- [20] Yu. A. Gusev, "Fundamentals of dielectric spectroscopy", Kazan: KGU, 2008. (in Russian)
- [21] S. W. Provencher, "A constrained regularization method for inverting data represented by linear algebraic or integral equations", *Computer Physics Communications*, vol. 27, pp. 213-227, 1982.
- [22] I.-G. Marino, *Regularized Inverse Laplace Transform*, 2004, [Online]. Available: <http://www.mathworks.com/matlabcentral/fileexchange/6523-rilt/content/rilt.m> [Accessed: June 26, 2022].
- [23] A. B. Grigorov, and I.S. Naglyuk, "Rational use of engine oils: monograph", Ch., Tochka, 178 p., 2013. (in Russian).
- [24] A.B. Grigorov, P.V. Karnozhitsky, and I.S. Naglyuk, "Changes in the dielectric constant of diesel engine oils in operation" *Automobile transport*. No. 20, 2007, <https://cyberleninka.ru/article/n/izmenenie-dielektricheskoy-pronitsaemosti-dizelnyh-enginenyh-masel-v-ekspluatatsii> (Accessed: April 28, 2023).
- [25] I.V. Izmetiev, and S.A. Konyaev, "Change of dielectric properties some engine oils at their destruction", *Bulletin of the Perm University. Series: Physics*, vol. 1, pp. 85-90, 2012.
- [26] N. Sinyavsky, and N. Kostrikova, "Analysis of the marine engine oils elemental constituents for engine diagnostics", *Jurnal Tribologi*, 2023.



Autonomous Network System with Specialized and Integrated Multi-Sensor Technology for Dynamic Monitoring of Marine Pollution (SMARTPOL)

© Nurten Vardar¹, © Bülent Bayram¹, © Amit Mishra², © Mihai Palade³, © Bekir Şener¹, © Ines Boujmil⁴,
© Jeremy Scerri⁵, © Andre Attard⁵, © İskender Demir⁶

¹Yıldız Technical University Faculty of Naval Architecture and Maritime, Department of Naval Architecture and Marine Engineering İstanbul, Türkiye

²University of Cape Town, Cape Town, South Africa

³Interactive Software, Bucharest, Romania

⁴AquaBioTech Group, Mosta, Malta

⁵Malta College of Arts, Science and Technology, Paola, Malta


⁶Sirena Marine, Bursa, Türkiye

Abstract

This project aims to provide a novel and compact pollution detection, monitoring, and analysis system architecture to monitor marine fields and detect different types of marine pollution that includes hardware and software components. The system will mainly consist of a Shore Control Centre (SCC) and unmanned surface vessels, both equipped with multi-sensor technology and artificial intelligence-based solutions. The SCC will play a key role as a central network hub of the system.

Keywords: Marine pollution, Sensor technology, Remote control

*This project received funding from the Türkiye National Funding Authority (TÜBİTAK) in Türkiye, the Malta Council for Science and Technology (MCST) in Malta, UEFISCDI subordinated to the Ministry of Education and Research in Romania, and the Department of Science & Innovation in South Africa, via the MarTERA – ERA NET co-fund scheme under grant agreement No 728053-MarTERA of H2020 of the European Commission.

 **Address for Correspondence:** Nurten Vardar, Yıldız Technical University Faculty of Naval Architecture and Maritime, Department of Naval Architecture and Marine Engineering İstanbul, Türkiye
E-mail: vardar@yildiz.edu.tr
ORCID ID: orcid.org/0000-0002-9042-7029

Received: 18.08.2023
Last Revision Received: 18.08.2023
Accepted: 04.09.2023

To cite this article: N. Vardar, et al. "Autonomous Network System with Specialized and Integrated Multi-Sensor Technology for Dynamic Monitoring of Marine Pollution (SMARTPOL)." *Journal of ETA Maritime Science*, vol. 11(3), pp. 217-220, 2023.

©Copyright 2023 by the Journal of ETA Maritime Science published by UCTEA Chamber of Marine Engineers

1. Introduction

According to MARPOL 73/78, the principles have been established to prevent pollution of the marine environment. However, illegal discharges by ships above permitted limits in prohibited areas persist. Marine pollutants originating especially from anthropological activities threaten the marine and coastal ecosystems.

Therefore, the 2002 EU Integrated Coastal Area Management Recommendation and the 2008 Marine Strategy Framework Directive were developed to protect all European coasts and marine waters. To address these problems and support EU regulations, the idea of SMARTPOL has emerged with the aim of producing technological solutions for marine pollution detection while establishing data services that can be integrated with existing EU services in synergy with the European Green Deal. From this viewpoint SMARTPOL aims to present a novel and compact pollution detection, monitoring, and analysis system architecture to monitor marine fields and detect different types of marine pollution, consisting of hardware and software components.

2. Project Objectives

Integration of different types of sensors [e.g., remote sensing, unmanned aerial vehicles (UAV), and unmanned surface vessels (USV) integrated Internet of Things (IoT)], development of a marine pollution detection algorithm using sensor data, and state-of-the-art intelligent system technologies, including artificial intelligence (AI)-based image processing, autonomous navigation, and smart communication systems, will be presented as R&I objectives of the project.

The project is in good agreement with the 2019 European Green Deal, which aims to exploit sustainable digital technologies such as AI, 5G, cloud and edge computing, and the IoT. From this viewpoint our project aims to provide a novel and compact pollution detection, monitoring, and analysis system architecture to monitor marine fields and detect different types of marine pollution that includes hardware and software components. The system will mainly consist of a Shore Control Centre (SCC) and USVs, both equipped with multi-sensor technology and AI-based solutions. The SCC will play a key role as a central network hub of the system.

SMARTPOL will validate USVs by monitoring pollutants in specific areas of Türkiye, Malta, and South Africa through sensors identified for pollutants monitoring. USVs will perform local environmental monitoring and data analysis. USVs will also be equipped with pollution detection sensors for data collection. The data will be collected from the sensors, and the results will be transmitted to the SCC. Smartpol network system will provide communication

and reliable data transfer between SCC and USVs will be provided by the SMARTPOL network system. As stated in the European Commission Staff Working Document on Digital Solutions for Zero Pollution, the use of sensors, IoT solutions, and satellite systems integrated with AI technologies can help us make more evidence-based decisions and improve our ability to comprehend and address climatic and environmental issues.

In addition, a pollutant often released into the ocean by scrupulous entities is industrial wastes released by carrying them in small boats. The solution to this issue is an integration of images from European Space Agency's radar satellite Sentinel-1 and Automated Identification System (AIS) tracking of boats. Radar-based satellite images are proven methods to detect industrial waste spills in the ocean. By combining these with real-time monitoring of AIS data, an alarm system will be developed as part of the overall system. The command-and-control software platform that will facilitate the visualization of the pollution alerts, USV positions, and its path tracking will also integrate the data fusion processing (AI based) results and other expected and estimated pollution evolutions so that a proper intervention mechanism could be shared with other authorities/legal institutions. The command-and-control software platform will allow the complete review of pollution detection data series, pollution confirmation data from the USV and additional data sources (UAV, if available), and expected evolution and impact. The command-and-control software will be installed on the SCC, and in addition to the visualization of data results, it will coordinate the navigation of the USV during its seaside missions.

In sum, the integration of different types of sensors, the development of a marine pollution detection algorithm using sensor data, and the use of state-of-the-art intelligent system technologies, including AI, machine learning-based image processing, autonomous navigation, and remote sensing, are presented as scientific and technological objectives of the project. Our understanding of marine pollution monitoring can be enhanced and shaped into a form that is useful for decision makers and sustainable environmental protection with new analytical tools (e.g., AI), multisensor integration, and advanced communication technologies. Within the coverage area, the system will also can improve maritime safety and become a deterrent factor against marine pollution. Moreover, SMARTPOL aims to reuse current European data sources, such as Copernicus satellite products and Copernicus marine services. It is also aimed at providing generated open digital marine pollution monitoring data for reuse in the Copernicus system. Raising awareness of marine pollution and protecting the marine ecosystem are the socio-economic objectives of the project.

3. Consortium Composition

3.1. Yıldız Technical University

Yıldız Technical University (YTU) is one of the seven public universities situated in İstanbul and is the third oldest university in Türkiye. YTU has 11 faculties, 2 institutes, and 25 research centers. YTUs SMARTPOL team consists of academicians that are experts in the fields of Naval Architecture, Marine Engineering and Geomatics Engineering. The project coordinator, Prof. Dr. Nurten Vardar, is a member of the Naval Architecture and Marine Engineering Department. Some of the main research areas of the Geomatic Engineering Department are remote sensing, geographical information systems image processing, artificial intelligence, big data analytics, unmanned aerial/surface vehicles, LIDAR technologies, virtual reality, and multi-criteria decision support systems.

3.2. AquaBioTech

AquaBioTech (ABT) is an independent aquaculture, fisheries, biotechnology, environmental testing/research, engineering, consulting, development, and training company (SME) with its own dedicated biosecure and fully licensed research and marine survey facilities in Malta. These include research laboratories with GLP certification, 31 independent biosecure wet labs containing more than 500 marine and freshwater tanks using precision controllable recirculating aquaculture system technology, and two marine field-testing sites in different marine environments (Natura2000 mixed use site and industrial port). ABT has a strong background in commercial research for aquaculture and the marine environment and has been involved in several EU, regional, and national research projects. ABT Marine™ provides a range of services, including marine surveying and mapping/Geographic Information System.

3.3. The Malta College of Arts, Science and Technology

The Malta College of Arts, Science and Technology (MCAST), established in 2001, is the country's leading Vocational Education and Training Higher Education Institution. With six Institutes in Malta and the Gozo Campus, MCAST offers 180 full-time and over 300 part-time vocational courses ranging from certificates to Master's degrees. MCAST has profound experience participating in and leading various EU funded R&I projects under H2020. EIT Climate-KIC, Interreg Europe and Erasmus + align with the 2030 Agenda for Sustainable Development Goals & Targets and Mediterranean Strategy for Sustainable Development 2025, and the National R&I Strategy 2020 as the main priorities for the College.

3.4. Interactive Software S.R.L

Interactive Software S.R.L is a Romanian company active in the development and integration of voice communication

and data transmission solutions, as well as the development of integrated control-command solutions, especially for defense forces and governmental agencies and institutions. In addition to the suites of Command & Control software with special designations, Interactive Software is also developing special electronic equipment with embedded software.

3.5. University of Cape Town

University of Cape Town (UCT) is South Africa's oldest university and a leading teaching and research institution in Africa. UCT is spread over four main campuses situated in Cape Town, South Africa. UCT has more than 80 specialist research units that provide supervision and support for postgraduate study and research. The Electrical Engineering (EE) department at UCT is part of the Engineering and Built Environment Faculty, which comprises seven departments. The EE department has 11 research groups and 25 academic staff members.

3.6. Sirena Marine

Sirena Marine (SM) is a prominent manufacturer in the yachting and automotive industries. The next step of SM's award-winning sailboats was entering the powerboat market. SM has ISO 9001, IATF 16949, IRIS, ISO 14001, EN 15085, and DIN 6701 certificates.

4. Pilot Studies

4.1. Türkiye Pilot Study

Turkish seas are affected by chronic pollution similar all other marine environments. Typical pollutants consist of household waste, land-based and ship-based pollutants, and oil tankers, which are also one of the most significant sources of this environmental problem. These pollutants can accumulate inside marine organisms and cause their deaths, but they can also harm society and human health through the ingestion of marine life as food, which would create a significant threat and harm biodiversity. The Marmara Sea has been refreshed by the currents of the Bosphorus and the Dardanelles Strait from the Aegean Sea and the Black Sea. Therefore, it is quite urgent and vital to monitor the pollutants flowing from the Aegean and Black Sea regions toward the Marmara Sea to prevent pollution of the Northern Aegean, Black Sea, Marmara Sea, Bosphorus, and Dardanelles. In this pilot study, the multi-scale approach of SMARTPOL will be used instantaneously to detect, monitor, and observe pollution in the Marmara Sea. A new integrated system will be presented to organizations and public institutions to prevent the death of marine life in the Marmara Region.

4.2. Malta Pilot Study

This pilot study will focus on verifying the functionality of the USV and verifying the data that the USV will collect autonomously with ground validation methods that use traditional data collection methods (collecting water samples using boats and analysing them in the laboratory). The USV will cover coastal areas in tandem with the conventional boat approach, and both will collect the same set of data. These two datasets (USV vs. conventional) will be comparatively analyzed. Sea level data collection time will be coordinated in parallel with data collection from satellite imagery. Thus, correlations between both system parameters can be detected. In this project, sensor nodes will be used to monitor pollution and help biologists determine whether it plays a role in habitat destruction.

4.3. South Africa Pilot Study

A boat with a sensor assembly will be used in the South Africa pilot study. It is planned to extract data from both the Indian and Atlantic Oceans off the coast of South Africa. In addition to the above, both ground and satellite-based radar systems will be used to measure and detect pollutants. The data will be fed into an AI-based forecasting system to predict the flow and target of pollutants in the water.

Reviewer List of Volume 11 Issue 3 (2023)

Aşkın Özdağođlu	Dokuz Eylül University	Türkiye
Burak Zincir	İstanbul Technical University	Türkiye
Elif Koç	Bandırma Onyedı Eylül University	Türkiye
Emrah Erginer	Dokuz Eylül University	Türkiye
Emre Akyüz	İstanbul Technical University	Türkiye
Emre Pesman	Karadeniz Technical University	Türkiye
Erdem Kan	Çanakkale Onsekiz Mart University	Türkiye
Fırat Bolat	İstanbul Technical University	Türkiye
Iwan Sudipa	Indonesian Institute of Business And Technology	Indonesia
Ladislav Stazic	University of Split	Croatia
Maria Carrera Arce	World Maritime University	Sweden
Mehmet Kaptan	Recep Tayyip Erdoğan University	Türkiye
Momoko Kitada	World Maritime University	Sweden
Pelin Erdem	University of Strathclyde	United Kingdom
Selçuk Çebi	Yıldız Technical University	Türkiye
Ünal Özdemir	Mersin University	Türkiye
Yiğit Gülmez	İskenderun Technical University	Türkiye
Yusuf Zorba	Dokuz Eylül University	Türkiye

Volume 11 Issue 3 (2023) is indexed in



TRID

the TRIS and ITRD database



TÜBİTAK

ULAKBİM

DOAJ DIRECTORY OF
OPEN ACCESS
JOURNALS



Scopus

JEMS's Sponsors

INCE SHIPPING GROUP



GEMLİK PILOTS



DENİZ ÇALIŞANLARI DAYANIŞMA DERNEĞİ



EGE GAZ INC.



SEFİNE SHIPYARD



GÜRDESAN SHIP MACHINERY CORP.



ER SHIPPING





GEMLIK PILOTS
Gemlik Pilotage and Tugboat Services Inc.

**GEMLIK Pilotage
and Tugboat
Services Inc.,**
provides the highest
level of navigation
and maneuvering
safety, which aims
to continuous
training and
development, in
Gemlik Bay.

GEMLIK PILOTS
GEMLIK Pilotage and Tugboat Services Inc.

Adress : Ata Mh. Sanayi Cd. No:4 İç Kapı No:9
Gemlik / BURSA Phone : 0224 524 77 35 - 0224 524 77 36
Fax : 0224 524 77 64
e-mail : pilotage@geptco.com

